A Predictive Optimal Dispatch and Optimal Sizing Method for a Grid-Connected PV-Diesel-Storage System

Ronald Clark

Supervisor:

Prof. WA Cronje

Co-Supervisor:

Prof. MA van Wyk

A dissertation submitted to the Faculty of Engineering and the Built Environment, University of the Witwatersrand, Johannesburg, in fulfilment of the requirements for the degree of Master of Science in Engineering (by research).

August 2014

Declaration of Authorship

I, Ronald Clark, declare that this dissertation is my own, unaided work. It is being submitted for the Degree of Master of Science (by research only) in the University of the Witwatersrand, Johannesburg. I confirm that:

- This work was done wholly while in candidature for a research degree at this University.
- No part of this thesis has previously been submitted for a degree or any other qualification at this University or any other institution.
- Where I have consulted the published work of others, this is always clearly attributed.
- Where I have quoted from the work of others, the source is always given. With the exception of such quotations, this thesis is entirely my own work.
- I have acknowledged all main sources of help.

Signed: ______________________________

Date: ______________________________

Abstract

Hybrid energy systems are becoming a popular means of exploiting natural sources of energy and increasing electrical efficiency in urban settlements. However, effective implementation of these systems relies on a means of optimally sizing and operating the system to ensure the lifetime costs of the system are minimised.

This dissertation addresses the problem of minimising the lifetime costs of a grid-connected hybrid system with diesel generation, photovoltaic array (PV) and an energy storage component.

To minimise the operational costs a predictive generator-storage scheduling strategy is proposed. The dispatch strategy seeks to minimise the operational costs by scheduling the generator and storage unit to: 1) Minimise the total energy requested from the grid; 2) Minimise the peak energy requested from the grid; 3) Minimise the fuel used by the generator. The dispatch strategy is developed in two papers. In the first paper a demand prediction algorithm is developed which is required by the proposed predictive dispatch strategy. In the second paper, the actual dispatch strategy for the generator and storage unit is formulated. The dispatch strategy takes the form of an integrated convex optimisation model which, when solved, provides the dispatch strategy for the generator and storage.

An optimal sizing method is then developed to take into account the capital costs of the components. The purpose of the optimal sizing method is to balance the trade-off between the increased capital costs incurred by larger PV and storage units and the corresponding decrease in operational costs.

The optimal dispatch strategy and sizing method are then tested on an example case study which investigates the possibility of operating a hybrid on the campus of the University of the Witwatersrand.

Acknowledgements

I would like to acknowledge my supervisor, Prof. Willem Cronje and my co-supervisor Prof. Anton van Wyk for his invaluable support and advice.

Contents

Chapter 1

Introduction

This dissertation presents an optimal dispatch and optimal sizing method for a grid-connected hybrid energy system to reduce the lifetime cost of the system. The goal of the optimal dispatch method is to reduce the operational costs by providing an optimal schedule for the generator and storage unit. The goal of the sizing method is to select the component capacities to balance the initial costs with savings in operational costs to ensure the total cost of the system is in fact minimised over its lifetime.

1.1 Background

Increasing electricity prices, environmental and social pressures are slowly forcing institutions and individuals to find ways of making more efficient use of electrical energy. This has led to a growing interest in optimising urban settlements to make greater use of natural sources of energy and to implement management or control strategies that use available energy more efficiently [1]. This is culminating in a move away from conventional centralised energy generation in favour of more modernised, decentralised energy systems with high levels of renewable energy integration, storage capacity and smarter operation [2, 3]. To improve system reliability, and mitigate downtime risk, such systems utilise storage elements and multiple energy sources. These are known as hybrid energy systems. Such systems may also be referred to hybrid renewable energy systems, grid-tied microgrids or simply smart microgrids but for most purposes these terms can be used interchangeably [3].

Hybrid energy systems integrate a hybrid mix of components which may include conventional and alternative distributed generation such as diesel generators, photovoltaic arrays (PV) as well as a variety of storage options including flow batteries, lead-acid batteries, thermal or small-scale hydro storage [4]. Demand-side hybrid energy systems thus provide a viable means of reducing growing energy needs while at the same time reducing the environmental impact and risk associated with continued reliance on a central utility company.

It is for this reason that many institutions, including the University of the Witwatersrand (Wits), are considering the potential implementation of on-campus hybrid energy systems for academic, practical and financial reasons. However, in order to implement such a system, much is required beyond the hardware itself — operational considerations need to be taken into account which is best achieved through the use of control methods that are able to analyse the technical and financial aspects of the system, and ensure optimal system operation [5]. Specifically, these operational considerations involve scheduling or dispatching the components to ensure cost-effective operation of the system.

The case of Wits provides a concrete example and is the case explicitly addressed in this dissertation.

Like many other institutions [4], Wits has recently begun investigating the possibility of integrating renewable sources on campus.

A hybrid system is a promising prospect for Wits as Wits has high electricity demand and suffers drastically from the unreliability of the national grid. Undergraduate and postgraduate classes have to be postponed and rescheduled and research activities halted. This is why Wits already has high-capacity (total 1 MW) backup diesel generation units to cope with these outages. However, Wits is particularly fortunate – being situated in an area with high solar radiation levels and ample campus-space i.e. "roof-space" to experiment with the integration of renewable energy sources and storage technologies. To this extent, the School of Electrical Engineering is currently busy developing a laboratory-based hardware test-bed that will enable small-scale hardware-in-the-loop testing of new energy technologies which can be used to assess their effectiveness on a small scale before any significant investment is made. The test-bed will be used for evaluating the efficacy and interoperation of a whole range of technologies including inverters, batteries, flywheels, photovoltaics, wind-turbines etc. However, to actually carry out the testing, methods are needed to describe how these devices are intended to operate once they are integrated on campus.

Obviously integrating all these components at once is impractical and Wits's first point-of-call has been to focus on using a storage unit, photovoltaics and the existing 1 MW diesel generator to reduce their monthly electricity bill. In terms of storage, Wits is particularly looking at integrating a new type of storage device - Pumped Heat Electricity

Storage (PHES) for which they have obtained a simulation model from a vendor that looks very promising as the device has a very high nominal capacity and small physical size. This storage technology is thus seen as the enabler for campus-level storage on campus where batteries have proven to be exceeding expensive in the past.

The proposed hybrid energy system for Wits is shown in Figure 1.1.

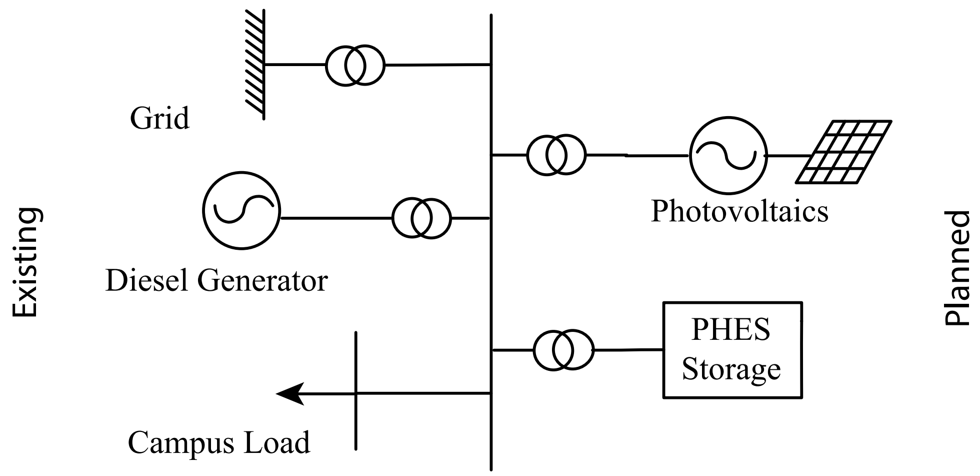

FIGURE 1.1: Single-line diagram of the existing and planned components of the grid-connected hybrid energy system.

The need exists to develop a scheduling method for the generator and storage unit to reduce the energy expenditure of the institution. Furthermore, as no decisions have been made as to the sizing of the PV or storage unit, a guideline is needed as to the selection of the optimal capacities of the units.

The University has a low load factor and can thus benefit substantially from load-levelling as the power utility (Eskom) imposes demand charges (R/kW) in addition to the basic flat-rate tariff (R/kWh) for aggregate energy use. The preferred method of operating and scheduling the storage device is therefore to operate it in such a way that reduces both the demand charge and aggregate energy usage.

The selection of the PV and storage capacity should be done in such a way as to balance the initial costs with the savings that are produced in the operational costs by the inclusion of the PV and storage unit operated under the optimal dispatch strategy.

1.1.1 Framework Formulation

A high-level power flow diagram of the hybrid energy system considered in this dissertation is shown in Figure 1.2. The system consists of the following components: photovoltaic panels, a 1 MW diesel generator, storage unit and the grid supply.

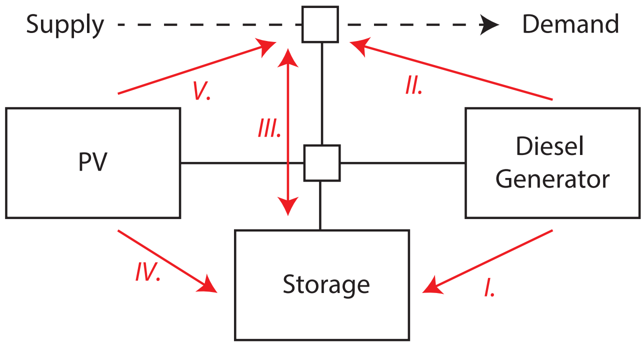

Figure 1.2: Model of the grid-connected hybrid PV-diesel-storage system.

The system is a grid-connected hybrid system which sources the majority of its energy from the utility company through the grid. The photovoltaic panels are to be integrated in such a way that the renewable generation is maximised, while adhering to the available space constraints. Together, the PV panels, the 1 MW diesel generation unit and the grid will meet the campus demand.

The interaction with the grid supply is considered to be uni-directional i.e. there is no feedback tariff and the system does not benefit from supplying energy back into the grid. For the purposes of this dissertation, it is assumed that the components are connected to the distribution system through proper interfaces to a central control unit that can schedule the devices as required.

The schedule of the generator and storage unit defines the power flow in the system. For example, in Figure 1.2, $I.$ represents the transfer of energy from the diesel generator to the storage device – a situation which might occur when the diesel generator is running but the demand is low and adequately covered by the renewable generation thus resulting in the generator "charging" the storage device. The quantity $II.$ represents the energy supplied by the generator to meet the demand. However, in the case of optimal operation this should only occur when the benefit gained from running the generator is greater than the fuel expended – such as in a period of high demand. In such a case, the storage might also assist in meeting the maximum demand ($III.$).

The scheduling of the power flow directly influences the operational cost which is the first component of the lifetime cost.The second component of the lifetime cost of the system is the capital costs of the components which, in this dissertation, is limited to the costs of the PV and storage unit. The diesel generator is not included in the initial costs as it is assumed to be part of the existing system.

Chapter 2

Research Problem

The central research problem addressed in this dissertation is: is it possible to develop an optimal dispatch and optimal sizing method for a grid-connected PV-diesel-storage system to reduce its lifetime costs?

The dispatch method is required to provide a practical method for scheduling the diesel generator and storage to minimise the operational cost by:

1. Minimising the consumption charge incurred by grid energy usage
2. Minimising the maximum demand incurred by grid energy usage
3. Minimising the fuel cost incurred by the generator usage

As the initial costs of the components are the second important factor in the lifetime cost of the system, the optimal sizing method is required to determine the capacities of the PV and storage unit to ensure the reduction in operational cost is not displaced by the initial costs.

2.1 Hypothesis

Firstly it is hypothesised that a predictive dispatch strategy for the generator and storage unit can be developed that will result in a lower overall operational system cost compared to a non-predictive strategy such as the load-following strategy.

Secondly, it is hypothesised that an optimal sizing method can be developed to determine the PV and storage unit capacity that minimises the lifetime cost of the system considering the optimal dispatch strategy.

2.2 Structure of the Dissertation

This dissertation is presented in the "paper-based" format where the main narrative contains short self-contained papers embodying the research process. The rest of the dissertation is structured as follows. In Chapter 3 a review of existing literature on the optimal design and dispatch of hybrid energy systems is presented, along with the rationale for the current work and an outline of the research process followed in this dissertation. In Chapter 4, the first paper is presented in which a demand prediction algorithm is developed and tested. In Chapter 5, the second paper is presented which develops and verifies an optimal dispatch strategy. Chapter 6 presents the third paper addressing the optimal sizing of the PV and storage unit in light of the optimal dispatch strategy. Chapter 7 presents a case study using historical data from Wits to illustrate the operation of the dispatch strategy and sizing method and how the results relate to those obtained using the HOMER package. Finally, in Chapter 8, conclusions are drawn and suggestions are made for future work.

2.3 Publications

The work in this dissertation is based on revised versions of the following manuscripts:

1. Clark, R. and Cronje, WA. Short Term Load Prediction for a Large Institution using Support Vector Regression. In Proceedings of SAUPEC 2013.

2. Clark, R., Van Wyk, MA. and Cronje, WA. Optimal generator and storage dispatch for demand and consumption charge reduction using convex programming. Energy. Elsevier (Submitted)

3. Clark, R., Cronje, WA. and Van Wyk, MA. Design Optimization of a Hybrid Energy System through Convex Programming. In Proceedings of the IEEE International Conference on Intelligent Systems Modelling and Simulation (ISBN 978-1-4799-3857-5).

Paper 1 and 3 appear in this dissertation as published, with minor corrections. Paper 2 has been submitted for publication and is currently under review.

Chapter 3

Literature Review

3.1 Lifetime cost

The lifetime cost of a demand-side hybrid energy system constitutes two components: the initial (or capital) costs (IC) and the operational costs (that depend on usage) (OC). However, assets, as well as prices, typically vary in value over time and thus a factor needs to be introduced to better reflect the present value of the asset or cash flow. The first accounts for the inflation of prices or appreciation and is given by:

$$(1+a)^t, \tag{3.1}$$

where a is the rate of appreciation and t is the current time.

The second is known as the discount factor:

$$\frac{1}{(1+r)^t}, \tag{3.2}$$

where r is the discount rate.

The discount rate can be understood intuitively as the "opportunity cost of capital" – the advantage that is gained in investing in an asset or receiving an income now as opposed to at a later date. The discount rate depends on many factors but in South Africa, the typical discount rate for hybrid energy system projects is around 8% [6]. The discount factor is the basis of net present value analysis (NPV) which is used in this dissertation. The NPV reflects the total present value of the project, including the initial costs and discounted cashflows:

$$\text{Total NPV} = \text{IC} + \sum_{\text{Project life}} \text{OC}. \tag{3.3}$$

The individual costs are calculated as:

$$\text{IC} = \sum_{Components} \text{Cost} \times \text{Capacity}, \tag{3.4}$$

$$\text{OC} = \sum_{Components} \frac{(1+a)^t}{(1+r)^t} \text{Operational cost} \times \text{Usage}. \tag{3.5}$$

For the system under consideration, the operational costs are broken down into three components, the demand charge (DC), consumption charge (CC) and fuel charge (FC):

$$\text{DC} = \sum_{Months} \max\{P_{net}\}, \tag{3.6}$$

$$\text{CC} = \sum_{Months} \sum P_{net}, \tag{3.7}$$

$$\text{FC} = \sum_{Months} \sum P_g. \tag{3.8}$$

Both these tariffs are subject to the yearly price adjustment imposed by Eskom. The annual price adjustment is shown in Figure 3.1. The price adjustment is rather variable, but the mean increase over the period is 11.74%. If this trend continues, and a 8% discount factor is assumed, the present value of the consumption and demand charges at the end of a 20 year period will be 2.87× their current value. However, the National Energy Regulator of South Africa has set the price increase at 8% for the period 2013 - 2018 and thus an inflation rate of 8% is assumed for the demand and consumption charges in this dissertation.

3.1.1 Initial Costs

The initial costs are directly related to the capacity of the generation and storage components. These costs are specified as R/kWp or "Rands per kilowatt of peak power produced". The component capacities themselves are decision variables to be determined by the optimal dimensioning method. Calculation of these optimal quantities relies directly on the operational costs and therefore the control strategies used.

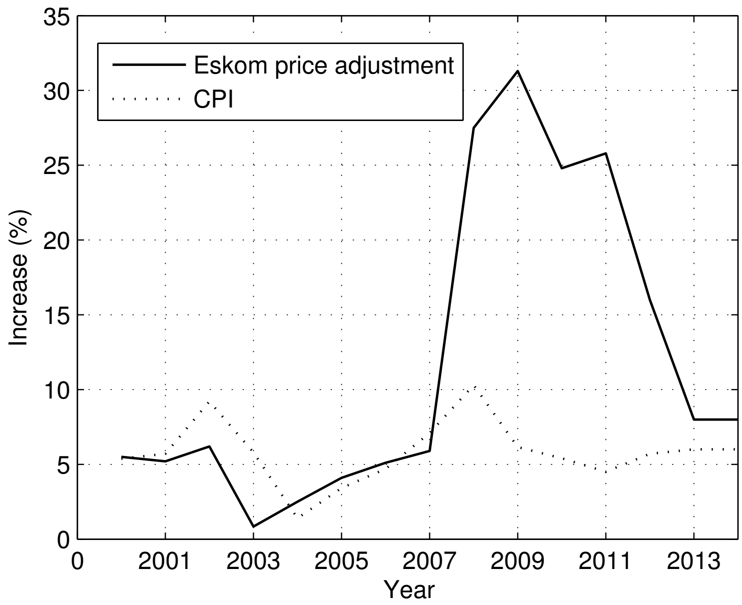

FIGURE 3.1: Electricity price appreciation compared to CPI

3.1.2 Operational Costs

The operational costs of the system are the costs which are directly proportional to the usage of the elements of the system. In the case of the grid-connected PV-diesel-storage system, this constitutes the cost of the fuel used by the generator as well as the charges incurred by using the grid to supply unmet demand.

The grid charges are set by the utility provider which may form part of either a regulated or deregulated electricity market. In a deregulated market, producers of electricity are free to market their electricity to consumers and thus electricity is charged on a real-time pricing scheme characterised by a time-varying buying rate and selling rate. In this dissertation a regulated market is assumed where the utility company is wholly responsible for setting the price to be paid by consumers for electricity. This price is described by the tariff structure.

3.1.3 Tariff Structure

The specific tariff structures imposed by utility companies vary, but generally consist of three components – a consumption (or volumetric) tariff and a maximum demand (demand) tariff. The consumption tariff can be either a flat rate tariff or a time-of-use tariff. A flat-rate tariff is charged at a constant cost per kilowatt hour of energy used. The time-of-use tariff is similar, however, the cost of energy is varied throughout the day to encourage consumers to use less energy during peak periods. The demand tariff is charged based on the highest demand experienced in a month across 30 minute integrating periods.

TABLE 3.1: Summary of the $\geq 500V \& \leq 66kV$ Nightsave Urban Large Tariff [7]

	Active energy charge [c/kWh]	Energy demand charges [R/kVA/m]
High demand [Jun - Aug]	57.00	172.12
Low demand [Sep - May]	44.47	24.03

The specific tariff structure used in this dissertation is the flat-rate Eskom $\geq 500V \& \leq 66kV$ Nightsave Urban Large Tariff for Local Authorities. A summary of the tariff structure is presented in Table 3.1. These values are used for all simulations, and if not specified, the high demand season charges are assumed.

3.2 Existing Dispatch Methods

Dispatch (or scheduling) strategies, as used in this dissertation, refer to the aspect of control that relates to the manipulation of the source and destination of energy flows [8]. The dispatch strategy determines how much energy each source or storage unit should supply during each timestep of the system's operation – a rather complex task – especially considering the integrated operation of the generation and storage elements.

The dispatch strategy is defined and guided by the goal of reducing the operational costs of the system.

The general problem of optimal scheduling of (mainly stand-alone) hybrid systems has been the subject of a number of studies with a variety of different methods being employed to perform the scheduling operations. These can be subdivided into those that consider only storage elements and those that consider both storage and generation.

3.2.1 Storage Only

As mentioned in [9], the problem of maximum demand reduction using a storage reserve finds application in many other areas as well. Two pertinent examples include the smoothing of product production curves whereby a company can increase its production and storage facilities in the early stages of production to prevent shortages when peak demand occurs later on. Similarly, such an algorithm can be used to schedule jobs to minimise workers' load during busy periods.

In [10] the problem of load levelling using a mega battery energy storage system is considered. The storage device is scheduled using a simple load-following simulation which is shown to perform poorly for flat loads and peaks of long duration. In [11], a battery control system is presented with the aim of optimally adding battery energy storage to a grid-connected PV power system to enable the dispatch of the solar energy to the grid at desired times. The main focus here is not on the optimal scheduling of the storage but rather on reducing maintenance requirements, maximising cycle life and operating at optimal state-of-charge (SOC) levels.

In [12], the authors present a method for scheduling a pumped-storage and thermal generator system. Their method is based on a heuristic depth first search to find an optimal operating scheduling for the storage unit over a 24 hour scheduling horizon. The goal of the scheduling is to schedule the pumped-storage in such a way as to reduce the peak load on the thermal generator.

Lee et al. [13] develop a variant of the particle swarm optimisation technique, which they term "multi-pass iteration particle swarm optimisation" to optimally schedule a battery energy storage system to reduce the operating costs for a large organisation with a time-of-use tariff scheme. The presence of wind generation in the system is considered and the authors account for uncertainties in the wind power forecast.

In [14] an analytical procedure is presented for reducing demand using a storage element an in [9] a complex on-line and off-line storage-only scheduling algorithm is presented to reduce maximum demand.

The trade-off between the use of a storage reserve unit and the energy loss due to the inefficiencies of the device, the inaccuracy of forecasts and as a result of under-sizing the storage unit has also been investigated [15]. Gast et al. develop two methods – one for optimally scheduling a storage unit with a large capacity and one for scheduling a unit with small or moderate capacity considering a regulated market with a flat-rate tariff. Although a realistic wind forecast taking into account forecasting errors is used, the authors assume a perfect demand forecast.

Nottrott et al. [16] propose an optimal storage dispatch strategy for demand charge minimisation in a grid-connected PV-battery system. Their dispatch strategy makes use of a load forecast and PV power output forecast to optimally schedule the battery for maximum peak load reduction. The authors test their strategy using "simulated" PV and load forecasts which they generate using a simple moving average over known data and then add random fluctuations to simulate forecast uncertainty. From this simulation, they determine the net present value (NPV) of the system subject to a time-of-use tariff and compare the financial benefits of their optimal dispatch strategy to a basic on-peak charge / off-peak discharge strategy.

Another basic storage dispatch strategy, also described in [16], is the real-time response scheme. This strategy is characterised by a demand threshold value – which can be seen as a charge and discharge threshold. When the demand falls below the threshold, the storage device charges at a constant rate until full. Once the demand rises above the threshold, the storage discharges to reduce demand.

A multitude of research has been conducted on storage scheduling in relation to expected widespread deployment of electric vehicles (EV's). In [17–20] EV's are used as smart storage elements offering a fast and accurate response which can assist in the integration of unpredictable renewable energy sources to assist in frequency regulation.

3.2.2 Storage and Generation

The problem of co-scheduling a storage and generation unit has been studied by a few authors.

Taylor et al. [21] use a dynamic programming approach to derive an optimal control policy for scheduling a generator and storage unit to reduce operational cost in a deregulated market with real-time pricing. They present a game-theory formulation of the interaction between power producers (generators) and storage units and show the Nash Equilibria arising from their inter-dependent scheduling.

In [22] Giuntoli et al. propose an algorithm for day-ahead scheduling of the thermal and electrical generation in a large-scale virtual power plant consisting of many smaller distributed generation sites. They also consider a deregulated market and the generator is scheduled to maximise profit and minimise operational cost considering the real-time electricity purchase rate, electricity selling rate and fuel rate. An accurate day-ahead load and renewable forecast is assumed and mixed integer linear programming is used to determine the optimal schedule.

Jeng et al. [23] investigate the scheduling of pumped-storage units to minimise the fuel costs incurred by thermal generators. The initial scheduling is performed using dynamic programming. The oscillatory behaviour is then analysed using power systems stability analysis software and then the dispatch schedule is refined using a linear programming method to dampen electro-mechanical oscillations.

Barkitzis et al. [24] present a method for solving the generator-scheduling problem to minimise fuel usage in a system consisting of diesel generators, wind turbine generators and photovoltaic panels. The method is able to perform short-term scheduling over a 24 hour scheduling horizon.

For scheduling storage and generation elements, many authors apply basic, heuristic control strategies. Some pertinent examples include the zero-charge strategy which applies in the case of an off-grid system where the generator is only run to meet the demand, never to charge the battery [8] and the full-cycle charge strategy where the batteries are fully charged every time the diesel generator runs [8]. Barley also develops a storage scheduling strategy based on the "frugal use of stored energy" and finds the combination of these methods to be nearly as cost-effective as an ideal predictive strategy [25]. Seeling-Hochmuth proposes a simple state-of-charge (SOC) strategy where the generator is run when the battery's SOC falls below a certain threshold and the storage is dispatched to supply net demand. The threshold is set during the design stage of the system using a genetic algorithm [6].

For grid-connected systems, two popular, basic dispatch strategies are the cycle-charging and the load-following strategy. The two strategies have the same base operating principle. Preference is given to the renewable sources. If the total sum of available renewable energy is sufficient to cover the base load, the dispatchable sources are all "turned off". Each dispatchable source, in turn, is modelled by a fixed cost and operating cost and if the base load cannot be met by the renewables a choice is made depending on the operating cost of the components. If the storage device has available energy, it is discharged. When the storage device has dissipated all its energy, either the generator is run to supply the net load or energy is sourced from the grid depending on which has a lower per-kWh operating cost. In cycle charging, when the generator is run, it is run at full-capacity charging the storage with the excess capacity. In the load following strategy, the generator is run at a level to just meet the net demand.

The cycle-charging and the load-following strategy strategies are implemented in a wide range of hybrid system design and simulation packages (including HOMER and iHOGA) as a means of controlling the dispatchable components. In addition to the considering the dispatch strategy, these packages also include a means of optimising the size of the components to determine what system configuration is best for the particular application and operational strategy employed.

3.3 Optimal Sizing of Hybrid Systems

There are a few studies which focus on sizing a hybrid energy system subjected to a specific dispatch strategy. From these studies a common methodology is evident. The optimisation of the hybrid system always consists of two aspects: the definition of an operational or dispatch strategy and then an optimisation of the lifetime cost of the system [26]. The lifetime cost is based on the total cost of system over its lifetime, or the cost of energy produced by the system which includes initial costs, operational costs and maintenance costs.

3.3.1 Existing Sizing methods

Seeling-Hochsmuth addresses the problem of designing an optimal off-grid hybrid energy system for a rural environment at length in her PhD thesis [27]. Like most of the other studies on optimal system design, she chooses a genetic algorithm to perform the system optimisation. The main motivation given for this choice is the derivative-free nature of the algorithm. This allows for the use of an accurate and complex simulation of the underlying system leaving the optimisation algorithm to cope with a non-smooth objective function. A simple, heuristic control strategy is used to dispatch the battery and diesel generator. A number of other authors have also used genetic algorithms. For example, [28] investigates the impact of a battery energy storage and high RES penetration (wind and PV) on an islanded microgrid, while [29] focuses on the implementation of distributed medium and small scale storage in a smart grid - both authors using genetic algorithms for optimal sizing of components. These heuristic and meta-heuristic methods are favoured mainly because they have the ability to find a global optimum in problems with an arbitrary structure. However, having the ability to find a global optimum does not necessarily mean that they *will* [30]. In fact, these methods are plagued by numerous disadvantages such as the inability to handle large-scale complex problems and their extremely slow convergence. See, for example, Valle [31], Rardin [30] and others [32, 33].

As these solutions are based on general optimisation algorithms that make no assumptions on the nature of the design problem, they have a number of inherent disadvantages [34]

- The stopping criteria used for these algorithms is arbitrary and has to be chosen heuristically
- The algorithms have a poor convergence rate
- The algorithms are subject to a "wandering" solution

To reduce the computational burden, a number of authors have attempted to use the structure of the underlying problem to establish whether the use of less complex optimisation procedures will suffice. Hong et al. present an interesting method that uses a Markov-chain based probabilistic model instead of a time-domain simulation in an effort to reduce computation time [35]. They apply this method to a PV-wind-diesel system - also using a genetic algorithm for optimisation. A similar method is followed by Atwa et al., however, they use a non-linear formulation of the design problem which they solve using mixed integer nonlinear programming [36]. Ter-Gazarian et al. address the problem of optimising the design of a distribution system [37] by modeling each type of component using a generic form they are able to derive a linear programming formulation of the design problem. They include conventional and renewable sources as well as storage elements.

3.3.2 Software Packages

There are some software packages which allow the user to find the optimal sizing of the hybrid system components considering a specific dispatch strategy. These include the Hybrid optimisation Model for Electric Renewables (HOMER) and the improved Hybrid optimisation by Genetic Algorithms (iHOGA) software packages which allow the user to specify a set of possible components and the software then simulates different configurations over the lifetime of the system, using the chosen dispatch strategies and finally returns the optimal, "lowest cost" system. HOMER carries out this optimisation by performing an exhaustive search of the specified system configurations, evaluating each possibility and suggesting the best alternative. Although initially developed for off-grid hybrid systems, HOMER allows for evaluating grid-connected systems as well. HOMER has a number of disadvantages such as slow run-times, inability to take demand tariffs into account and limited support for the use of user defined models in the simulation. iHOGA shares a similar feature-set to that of HOMER, implementing the same dispatch strategies and selection of components. The key difference between iHOGA and HOMER, is iHOGA's means of optimisation. iHOGA allows for the optimisation of multiple simultaneous objectives such as CO_2 emissions, loss-of-supply probability in addition to system cost. In contrast to HOMER, it also uses a genetic algorithm to carry out the optimisation which allows for a larger design space to be used without the combinatorial increase in optimisation time as is the case with HOMER.

3.4 Convex Optimisation: A Fast and Reliable means of Optimisation

Convex optimisation is the field of research concerned with the minimisation of convex functions over convex sets. Convex optimisation has found application in many areas of engineering including telecommunications and circuit design [38–40], but has as of yet not been fully applied to the problem of hybrid energy system design and sizing. For a comprehensive overview of the engineering applications of convex optimisation, see [41].

Convex optimisation problems can be solved more efficiently than general non-linear problems which do not have the convexity property. Thus, in many cases where the objective function is convex or approximately convex, it is advantageous to formulate these problems in convex form.

This allows a solution to the problem to be obtained in very little time with high accuracy (depending on the nature of the approximation) as convex optimisation problems can be solved using one of a wide range of fast and efficient algorithms. These include interior-point methods, bundle methods or sub-gradient projection methods. These algorithms have a number of advantages over non-convex optimisation algorithms which are usually based on heuristics such as genetic algorithms, simulated annealing and sequential quadratic programming. Convex optimisation problems have numerous favourable properties which are based on the following facts: if a convex problem has a minimum, then it is a global minimum and if there is more than one optimal solution, all these solutions share the same minimum and form a convex set. Practically, this has enabled the development of many convex solvers which are guaranteed to find globally optimal solutions to these problems while requiring very little computational time. The specific advantages of using convex optimisation include:

- With convex algorithms convergence is guaranteed
- The solution can be found in a finite (polynomial) time
- The solution is always globally optimal

Therefore, the use of convex optimisation procedures is highly desirable if the problem can be reformulated as a convex problem or even approximately be shown to be of a convex nature.

Convex optimisation problems include all problems that can be formulated as [42]

$$\begin{aligned} &\underset{x}{\text{minimize}} && f(x) \\ &\text{subject to} && g_i(x) \leq 0,\ i \in 1 \ldots n \end{aligned} \tag{3.9}$$

With the restriction that the functions $f(x)$ and $g_i(x)$ are convex functions. Figure 3.2 gives a visual representation of some convex functions and sets.

An extensive list of convex functions are given in [43]. Some pertinent functions include:

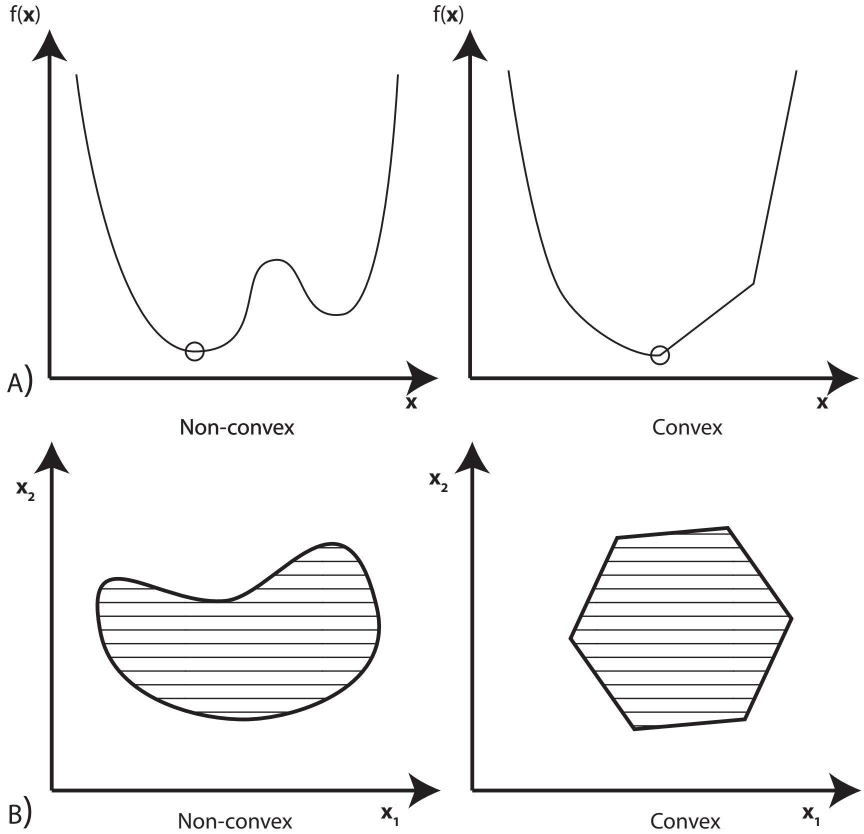

FIGURE 3.2: A) Examples of convex and non-convex objective functions in $\mathbb{R}$ and B) convex and non-convex sets in $\mathbb{R}^2$.

- $f(x_i) = max(x_i)$ (the maximum element of a vector or $||x||_\infty$)
- $f(x_i) = \sum_i c_i x_i$ (a linear combination of elements with $c_i \in \mathcal{R}$)
- $f(x_i) = \text{abs}(x_i)$ (the absolute value of each component or $|x_i|$)
- $f(x_i) = \text{pos}(x_i)$ (the positive part of each component or $(x_i)_+$)

Furthermore, convexity is conserved under a affine combination of functions, i.e. if all $f_j(x_i)$ are convex then so is $f(x_i) = \sum_j a_j f_j(x_i) + b_i$.

Convex sets include [42]:

- (convex) $\leq$ (concave)
- (concave) $\geq$ (convex)
- (affine) $=$ (affine)

Given a definition as general as this it is not surprising that a large number of standard minimisation problems are convex, or can be re-formulated as convex. For example, the following is an incomplete list of a few minimisation problems which can be cast into this form: linear programming problems, geometric programming problems, quadratic programming problems.

This means that if a problem can be formulated as a linear programming problem or geometric program, it can easily be solved using a convex solver.

Many convex solvers exist with similar levels of performance, accuracy and reliability. CVX [44] is a modelling language which can be used to specify convex programs. These can then be solved using the SeDuMi [45] and SDPT3 [46] solvers within the MATLAB environment.

3.5 Rationale

Very little research exists on minimising the lifetime cost of a grid-connected hybrid energy system. Most studies optimise the sizing but not the the operation, consider off-grid systems and do not account for demand charges.

In terms of optimal scheduling, the references discussed in Section 3.2.1 address the problem of scheduling a storage unit only. Although these could possibly be extended to account for a generation unit as well, most are concerned with only a time-of-use tariff and do not account for a maximum demand charge. The method presented in [14] addresses the problem of maximum demand reduction and shows that a scheduled storage unit can, in theory, lead to significant demand charge savings. However, this analytical procedure does not easily lend itself to computational implementation. The literature on scheduling EV's as storage elements [17–20] is interesting, however, these studies address the control object of instantaneous frequency regulation and no consideration is given to the economic dispatch of these storage assets.

Most of the references in Section 3.2.2 for co-scheduling a generator and storage unit [21, 22] are concerned with reducing operating cost in a deregulated electricity market with real-time pricing mechanisms. These methods could be adapted for a flat-rate tariff as real-time pricing can be seen as a time-varying flat-rate tariff but, again, they are not designed for reducing demand charges.

The basic strategies, such as the threshold strategy and load-following strategy, described in Section 3.2.2 are attractive because they are easy to implement and robust. The threshold strategy reliably mitigates demand that exceeds a certain threshold, but performs unreliably when the storage capacity is limited and cannot shave the entire peak [16]. The load-following strategy is more consistent and accounts for the generator operation, but does not perform well in terms of demand charge reduction. They are termed suboptimal because even if given perfect knowledge of future demand, they will not be able to schedule the dispatchable devices to achieve minimum operational cost. The two strategies, while rather simple, are quite effective and therefore provide a good basis of comparison for predictive optimal dispatch strategies.

In terms of optimal sizing, [27, 28] consider off-grid systems. Sizing methods for grid-connected systems subjected to basic dispatch strategies are considered in [35–37] and in software packages such as HOMER and iHOGA. The use of basic dispatch strategies means that although the lifetime cost of the system is optimised, the operational costs could be reduced further by using an optimal dispatch strategy.

3.6 Research process

The central focus of the dissertation is on developing a method for the optimal dispatch and sizing of a grid-connected PV-diesel-storage system to reduce the lifetime cost of the system.

The research process has thus been broken down into the following sequential activities:

1. A load forecasting method is developed and validated. This method establishes that it is possible to achieve a highly accurate forecast for the load data of a large institution. This confirms that it is feasible to develop dispatch strategies for the generator and storage unit that leverage day-ahead knowledge of future demand. It also provides a practical means of acquiring the load forecast that is required by the proposed predictive dispatch strategies to schedule the generator and storage unit.

2. An optimal storage dispatch method is developed. The objective of the dispatch method is to schedule the storage device so that the demand charge of the system is minimised. Simulations of the storage scheduling strategy for various storage capacities are carried out and the results are discussed.

3. A net present value (NPV) optimisation of the PV-diesel-storage system is done to investigate the long-term financial benefits of the predictive dispatch strategy and the optimal sizing of the PV and storage components.

4. The dispatch strategy and sizing method are applied to data from a case study. The results are compared to the basic load-following strategy and discussed.

Chapter 4

Demand Prediction

The dispatch strategy proposed in this dissertation aims to leverage a demand prediction to schedule the storage and generator unit for optimal operational cost reduction. Compared to basic strategies which are based on simple rules defined in terms of the state of other components the optimal predictive strategy requires reasonably accurate prediction of future demand to operate.

The purpose of the following manuscript is thus to develop and validate a practical method for forecasting the load profile using exogenous data. The method is to satisfy the operational requirements of the dispatch strategy. The developed method works by performing a 24 hour rolling window prediction of the load.

Candidate's contribution: The candidate was responsible for identifying the support vector regression method as a viable load forecasting technique as well as implementing and testing it on the sample data.

SHORT TERM LOAD FORECASTING FOR A LARGE INSTITUTION USING SUPPORT VECTOR REGRESSION

R. Clark* **and W. Cronje**†

* *Faculty of Engineering and the Built Environment, Private Bag 3, Wits 2050, South Africa E-mail: ronald.clark@students.wits.ac.za*

† *Faculty of Engineering and the Built Environment, Private Bag 3, Wits 2050, South Africa E-mail: willie.cronje@wits.ac.za*

Abstract: Short term load forecasting is an important aspect of the electricity management process as it allows dispatch strategies to operate using full knowledge of the day's expected load. This paper investigates the use of Support Vector Regression to model the complex non-linear relationship between a number of exogenous variables (temperature, insolation, type of day), the past load data and the current load value. The SVR model is trained using load data from the campuses of the University of the Witwatersrand. The results show that the system is highly accurate with a mean average error of only 3.44% which compares favourably to a number of other techniques. The system can thus be a beneficial component of any dispatch strategy.

Key words: load forecasting, time-series, support vector regression, real-time

1. INTRODUCTION

Dispatch of generators and storage units are essential to the efficient and economical use of electrical power. However, efficient dispatch strategies are often difficult to implement as their efficacy is dependent on knowledge of future demand. For example, a simple strategy to reduce the peak energy usage of a large institution may involve turnining on a diesel generation unit once a ceratin peak demand value is reached. Although simple, this strategy demonstrates the importance of having knowledge the future demand – the operators must know in advance when the generator should be dispatched to meet peak demand .

This paper describes the design and implementation of a load forecasting technique that can be used to aid the load management process. The system is tested using load data from a large academic institution: the University of the Witwatersrand. The report is structured as follows. In Section 2. the Support Vector Regression (SVR) method is explained along with the criteria used to assess the performance of the prediction system. In Section 3., an overview of the forecasting algorithm and its implementation are provided. Then, in Section 4. the the method used to train and test the system is described. Finally, the results are analysed and relevant conclusions are drawn.

2. BACKGROUND

2.1 *Support Vector Regression*

Support Vector Machines (SVMs) are a class of algorithms that are typically used to perform classification in pattern recognition problems [1]. SVMs are very popular for a number of reasons including the absence of local minima, sparseness of the solution and their ability to handle non-linear relationships in the input data [2]. The Support Vector Machine is, however, not limited to classification problems and can be extended to perform regression.

Support Vector Regression (SVR) is characterised by the use of a cost function which ignores errors that are situtated a certain distance ε from the true value [3]. Figure 1 illustrates a one-dimensional linear regression line that has been fitted using an epsilon loss function. The figure also shows the result of applying a mapping to the data points which transforms the non-linear relationship in the one-dimensional feature space to a linear relationship in the two-dimensional space. The quantity ξ represents the cost of the errors of the training data.

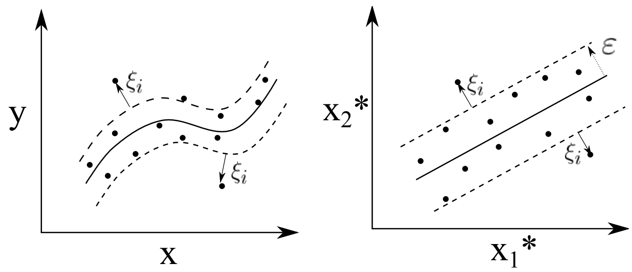

Figure 1: One dimensional non-linear regression [3]. The left axes depicts the original one dimensional input data with a non-linear relationship. The right axes shows the result of applying a non-linear transformation $\Phi()$ to convert the data to a two-dimensional space, allowing a linear regression model to be fitted.

In the case of non-linear regression, the input data is mapped into a higher dimensional space, allowing a linear model to be fitted in the new space [2]. The mapping is denoted by $\phi(\mathbf{x})$ which represents the map to the higher dimensional space where the data are linearly separable.

By using the kernel function $\mathbf{K}(\mathbf{x},\mathbf{x_i}) = \phi(\mathbf{x_i})^\mathbf{T}\phi(\mathbf{x})$, the decision function of the SVM can be represented by:

$$f(\mathbf{x}) = \sum_{\mathbf{i=1}}^{\mathbf{n}} \alpha_{\mathbf{i}} \mathbf{y_i} \mathbf{K}(\mathbf{x}, \mathbf{x_i}) + \mathbf{b} \tag{1}$$

where $f(x)$ is the regression output, y_i is the output corresponding to the training data $\mathbf{x_i}$ and $\mathbf{x}$ is the input data to be processed. The loss function itself is defined by [3,4]:

$$L(y, f(\mathbf{x})) = \begin{cases} 0 & |y - f(\mathbf{x})| \leq \varepsilon \\ |y - f(\mathbf{x})| - \varepsilon & \text{otherwise} \end{cases} \tag{2}$$

The parameters α_i and b in Equation 1 are found during training which is performed by solving the following optimisation problem [3]:

$$\min_{w,b} \frac{1}{2} ||\mathbf{w}||^{\mathbf{2}} + \mathbf{C} \sum_{\mathbf{i=1}}^{\mathbf{n}} (\xi_{\mathbf{i}} + \xi_{\mathbf{i}}^{*}) \tag{3}$$

$$\text{subject to } \begin{cases} |y_i - f(x_i)| \leq \xi_i + \xi_i^* \\ \xi_i, \xi_i^* \geq 0 \end{cases}$$

From Equation 3 it can be seen that SVM regression tries to minimise the loss function as well as keeping the complexity of the model (quantified by $||\mathbf{w}||^{\mathbf{2}}$) as low as possible.

Many kernel functions exist but a well-performing kernel, used in many forecasting systems, is the radial basis function (RBF) [4]:

$$\mathbf{K}(\mathbf{x}, \mathbf{x_i}) = \exp(-\gamma ||\mathbf{x} - \mathbf{x_i}||^{\mathbf{2}}), \gamma > \mathbf{0} \tag{4}$$

The constant C in Equation 3 is the penalty parameter of the error term. It determines the trade off between the complexity of the model and the extent to which deviations larger than ε from the optimal regression function are tolerated.

The constant ε in Equation 2 controls the size of the region outside of which outlying data points are penalised during training. Both of these parameters have a significant effect on the accuracy of the trained system and need to be carefully set prior to the training process. The method used for selecting these parameters is mentioned in Section 2.2.

2.2 Tuning the SVR Parameters

There are two parameters that need to be set when using an RBF kernel: C and γ. The constant C is the penalty parameter of the error term and the constant γ in Equation 4 is a kernel parameter. Both of these values have a significant effect on the accuracy of the trained system and need to be carefully selected prior to the training process. The combination of parameters (C, γ) are chosen which best allow the prediction of new data. To automate this process, the grid-search method described in [3] was implemented as part of the training stage. This method does an exhaustive search using various pairs of (C, γ) values and selects the pair for which the highest cross-validation accuracy is obtained. As suggested in [2], exponentially growing values of C and γ are used during this process. This simple but nave brute force method was chosen in favour of more intelligent procedures for the reasons suggested by Ben-Hur et al. [5]. Firstly, the exhaustive search ensures that globally-optimal parameters are always obtained. Furthermore, the grid-search can be parallelised if needed and, because there are only two parameters, the computational time required by more advanced methods is likely to be similar to that of the grid-search [5].

2.3 Performance Criteria

Numerous criteria exist for quantifying the efficiency of load forecasting techniques. The most popular of these include maximum absolute error and peak error. These quantities are calculated as follows [6]:

1. The accumulated difference between the actual and predicted load values over a 24 hour period

$$MAPE = \frac{100\%}{N} \sum_{k=1}^{N} \left| \frac{e_n}{P(n)} \right| \tag{5}$$

2. The difference between the peak forecasted and predicted value over a 24 hour period

$$PE = max \left\{ \frac{e_n}{P(n)} \right\} \tag{6}$$

where $e_n = P_{forecast} - P_{actual}$, $P_{forecast}$ is the predicted load value and P_{actual} is the actual load.

3. SYSTEM OVERVIEW

As illustrated in Figure 2, the load forecasting algorithm consists of two stages: a training stage and a forecasting stage. During the training stage the SVR model is created and optimised to best allow the prediction of new data during forecasting.

The input data consists of a time series of sampled weather, load and day-type information. These data is preprocessed during normalisation so that all values lie in the $\{0, 1\}$ range.

The prediction module operates on normalised data to produce a single predicted load value. This process is repeated for 48 half-hour time periods to obtain a complete daily forecast.

After the prediction has been obtained, it can be used along with a suitable dispatch strategy to schedule dispatchable devices such as generators or storage units.

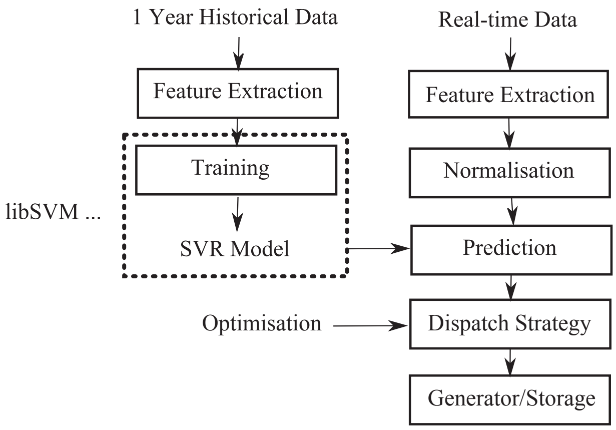

Figure 2: Overview of the load forecasting system

3.1 *Prediction Model*

Load forecasting is performed using SVR. The SVR method was chosen due to the high accuracy obtained for time series forecasting where it was shown to outperform other regression techniques such as Autoregressive Integrated Moving Average (ARIMA), artificial neural networks and self-organising polynomials [4, 7–9]. Although SVR training time is quadratic in the number of samples and thus often slow, the actual regression is very fast, can be performed in realtime and does not depend explicitly on the size of the training set [2, 5]. The libSVM library was used to implement and train the SVM for regression [2].

To implement SVR, a suitable Kernel function has to be selected, along with appropriate parameter values. The Radial Basis Function (RBF) was chosen as the kernel function. This is a well-performing kernel which is used in many forecasting systems.

3.2 *Feature Selection*

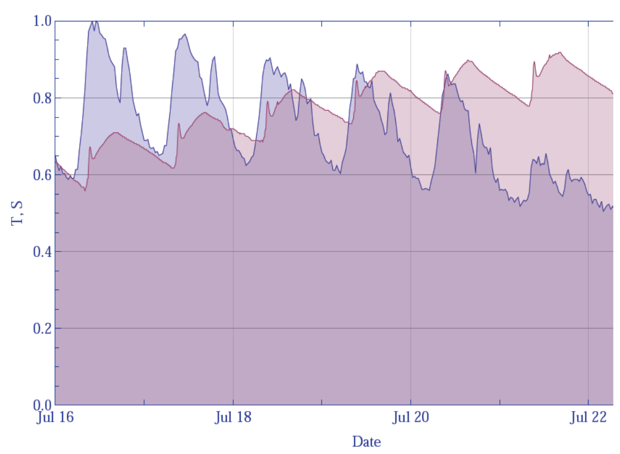

Figure 3: Load and temperature data for the University of the Witwatersrand Raikes road campus between July 16, 2012 and July 22, 2012.

The half-hour load data for the University of the Witwatersrand between 2011 and 2012 is shown in Figure 3. From this Figure, a number of trends are evident. Firstly, the load curve is periodic with a frequency of 1/day, ie. the shape of the load profile is approximately the same for each day. The peak and average load during non-working days, however, are significantly lower than that during the week which suggests that the type of day has a significant effect on the load demand. Furthermore, the load decreases with increasing temperature which, in itself, is directly correlated to the average insolation.

Here it is, however, important to draw a distinction between the short-term (hourly) and medium-term (daily) temperature trend. As the temperature is directly related to the intensity of the solar radiation, there exists a strong short-term correlation between temperature, insolation and load demand. On the other hand, the average daily temperature (with short term variations removed) is inversely related to the load. For example, if the average temperature for a day is low, more heaters will be used and the load demand will increase.

Using the factors mentioned above, the data passed to the SVR for prediction consists of the following features:

$$\mathbf{x_{d,h}} = [\mathbf{L_{d,h}}, \mathbf{L_{d-1}}, \mathbf{L_{d-7}}, \mathbf{W_d}, \mathbf{H_r}, \mathbf{D_T}, \mathbf{\bar{T}}, \mathbf{\bar{I}}, \mathbf{H_m}] \tag{7}$$

where L_{d-1} is the load at the same time during the previous day, L_{d-7} is the load during the same day and hour the previous week, W_d is the day of the week, D_T is the type of day and $\bar{I}$ and $\bar{T}$ are the most recent 24-hour moving averages of insolation and temperature, respectively.

The ouput of the model is the predicted load for the next 30 min interval:

$$y_{d,h+1/2} = L_{d,h+1/2} \tag{8}$$

From Equation 4, it is evident that all the quantities apart from $L_{d,h}$ are available for a 24-hour ahead prediction. Subsequent values of $L_{d,h}$ are obtained by performing a rolling prediction.

4. TESTING METHOD

The SVR model was trained with historical load data from June 20, 2012 to November 3, 2012 obtained from the Raikes Road campus of the University of the Witwatersrand along with the corresponding temperature and insolation information recorded by on-campus data loggers.

5. RESULTS AND DISCUSSION

The results of the grid-search that was run prior to training are shown in Figure 4. In this case the optimal parameter values were found to be $C = 2^{10}$ and $\gamma = 2^{-2}$.

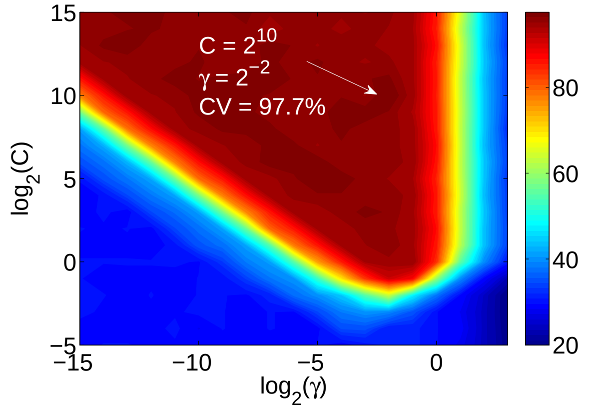

Figure 4: Result of the grid-search procedure carried out prior to training. The contour plot shows the cross validation accuracy obtained using various combinations of parameters. The highest cross validation accuracy is indicated by the arrow.

The contour plot presented in Figure 4 clearly illustrates the importance of selecting the correct training parameters for the SVR. For example, if the parameter values were blindly chosen as $C = 2^{-4}$ and $\gamma = 2^{2}$, then a cross-validation accuracy of only 24.5% would have been achieved, compared to the accuracy of 97.7% obtained using the grid-search method. This parameter search, although paramount to the performance of the system, is by far the most computationally-expensive aspect of the training process as it takes approximately 3m21s to complete a search of 399 points using an Intel 2.8 GHz Core2Quad CPU with 8 GB RAM. However, for the reasons described in Section 2.2, along with the high cross-validation accuracy that was achieved during training, this simple parameter tuning procedure is preferred.

The forecasting result obtained by applying the trained SVR model to unknown load data is shown in Figure 6. From Table 1 it can be seen that the model achieved high forecasting accuracies for the Raikes Road campus.

The maximum peak error that resulted during testing was 0.134 MW or 6.55% which occurred on a Monday. At current electrical tariffs, this corresponds to a R 27 675 underestimate of the peak demand charge. The most likely cause of this error is the use of L_{d-1} as a feature, coupled with the fact that not enough holiday and weekend data was used to allow the SVR model to distinguish between the sharp increase in load from a non-working day (Sunday) to a working day (Monday).

Table 1: Results obtained during testing. The results are for data from the Raikes Road campus of the University of the Witwatersrand from November 4, 2012 to November 14, 2012. All values in MW.

Campus	Error	MAPE	Peak Error	MPE
Raikes Road	0.005	3.44%	0.134	6.55%

A more detailed error analysis is presented in Figure 5 which shows that the errors closely fit a zero-mean normal distribution with a standard deviation of $\sigma = 0.07097$ MW. This means that an error as high as 6.55% is relatively uncommon as an error this large or greater only has a 0.6% chance of occurring. Furthermore, the algorithm is able to predict to an accuracy of 0.125 MW with a confidence of 99%.

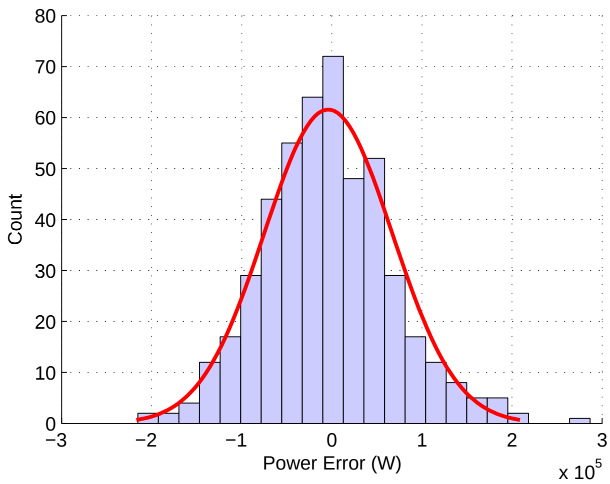

Figure 5: Plot of the error distribution along with an approximate Gaussian fit. The mean and standard deviation estimates are $\mu = -0.0034$ MW and $\sigma = 0.07097$ MW.

The MAE, which relates to the total average energy charge, is significantly less than the peak error. The actual MAE achieved was 3.44%. This value compares favourably to the 9.42% MAE reported by Yuan et al. using the LS-SVM method [9].

6. CRITICISMS AND FUTURE WORK

Future work could also focus on testing the system using data obtained from other institutions and on larger data sets which were not available during the time of publication. A more extensive set of features could also be used as the input to the SVR model, possibly increasing the accuracy. In order to eliminate the inclusion of redundant data in the feature set, dimensionality reduction techniques such as Principle Component Analysis (PCA) or Factor Analysis (FA) could be used to extract the information with the highest correlation to the load.

Finally, the system could be tested in conjunction with a real load management strategy to assess its practical performance.

7. CONCLUSION

This paper presents an SVR-based load forecasting method for predicting load values 24-hours ahead in 30min intervals. The method was implemented and tested using load data from the University of the Witwatersrand. The results are very promising and show that the method has a

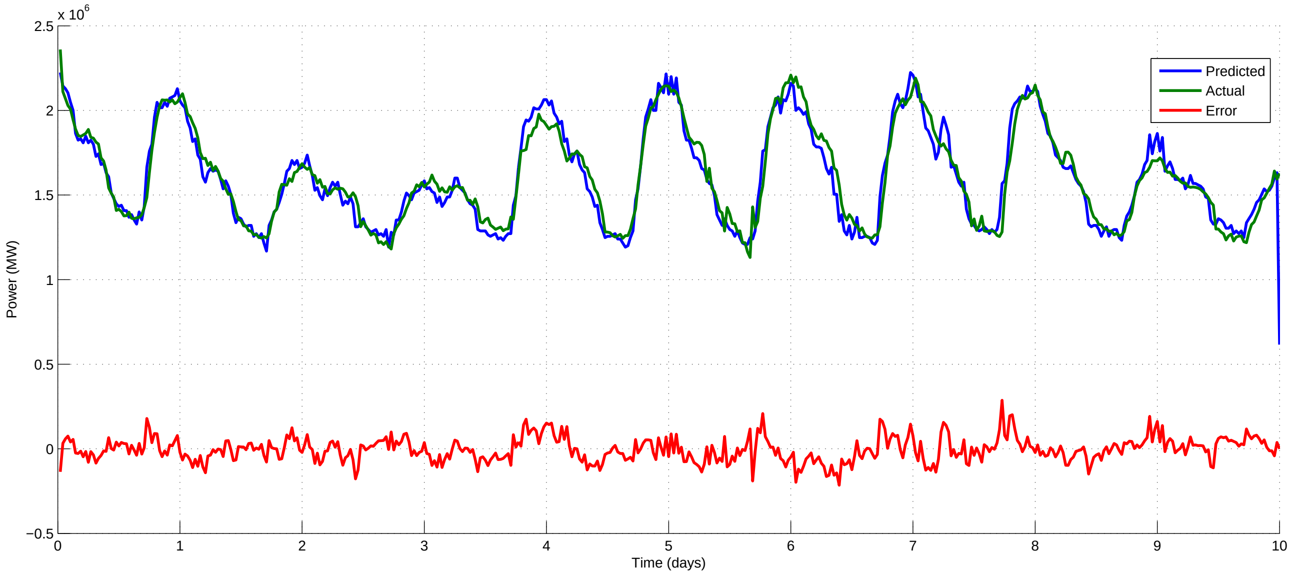

Figure 6: Comparison between the predicted load values and the actual values over a 10-day period. A plot of the error values is also shown. The days with significantly lower load are non-weekdays (Saturday, Sunday).

high prediction accuracy. It is suggested that the system be used with a real dispatch strategy to quantify the benefits that can be obtained by its use.

ACKNOWLEDGEMENTS

The authors would like to thank Ivan Hofsajer from the University of the Witwatersrand for his valuable input and suggestions.

REFERENCES

[1] Xie Feixiang, Huang Mei, Zhang WeiGe, and Li Juan. Research on electric vehicle charging station load forecasting. In *Proceedingsof the 2011 International Conference on Advanced Power System Automation and Protection (APAP)*, 2011.

[2] Chih-Chung Chang and Chih-Jen Lin. Libsvm: A library for support vector machines. *ACM Transactions on Intelligent Systems and Technology*, 2:2701–2707, 2011.

[3] John Shawe-Taylor and Nello Cristianini. *Support Vector Machines*. Cambridge University Press, 2000.

[4] Xueming Yang. Comparison of the ls-svm based load forecasting models. In *Proceedings of the 2011 International Conference on Electronic & Mechanical Engineering and Information Technology*, 2011.

[5] A. Ben-Hur and J. Weston. A users guide to support vector machines. Technical report, Department of Computer Science. Colorado State University, 2010.

[6] Craig Stuart Carlson. Fuzzy logic load forecasting with genetic algorithm parameter adjustment. Master's thesis, University of the Witwatersrand, 2012.

[7] Shu Fan, Yuan-Kang Wu, Wei-Jen Lee, and Ching-Yin Lee. Comparative study on load forecasting technologies for different geographical distributed loads. In *Proceedings of the 2011 Power and Energy Society General Meeting*, 2011.

[8] Yaohui Bai, Jiancheng Sun, Jianguo Luo, and Xiaobin Zhang. Forecasting financial time series with ensemble learning. In *Proceedings of 2010 International Symposium on Intelligent Signal Processing and Communication Systems (ISPACS)*, 2010.

[9] Jinsha Yuan, Yinghui Kong, and Yancui Shi. Online forecasting of time series using incremental wavelet decomposition and least squares support vector machine. In *Proceedings of the 2009 Asia-Pacific Power and Energy Engineering Conference (APPEEC)*, 2009.

Chapter 5

Predictive Dispatch Strategy

In the preceding manuscript an algorithm for obtaining a 24 hour ahead forecast of the demand was developed. This method forms a crucial component of the predictive dispatch strategy for the storage unit and generator considered in this dissertation as the dispatch strategy leverages a load forecast to achieve optimal demand charge reduction. The purpose of the following manuscript is to develop the actual dispatch strategy for scheduling the storage device and generator.

The general operation of the proposed scheduling strategy works in two stages and is based on a type of receding horizon control. In the first stage the demand is predicted for a 24 hour ahead time period. In the second stage, an optimisation algorithm is used to calculate a cost minimising control strategy over the 24 hour prediction horizon that minimises the demand charge and consumption charge for that period.

The scheduling algorithm treats the storage unit as a black box characterised by its specification which includes:

- Storage energy capacity
- Storage power capacity
- Charge and discharge efficiency

The model takes the dynamics of the storage device into account. Technically, this means that the accumulated energy over any period must be greater than zero.

The generator is modelled with a linear fuel-cost curve.

Optimal generator and storage dispatch for demand and consumption charge reduction using convex programming

Ronald Clark[a,b,c], MA van Wyk[a,b,c], WA Cronje[a,b,c]

[a] *Department of Electrical and Information Engineering*
[b] *University of the Witwatersrand*
[c] *Johannesburg, South Africa*

Abstract

In this work, an optimal dispatch strategy is presented for a generator and storage unit in a grid-connected PV-diesel-storage system which minimises the peak power requested from the grid while adhering to the physical constraints of the storage and generator. The dispatch strategy is formulated as a convex minimisation problem and solved efficiently using standard convex programming techniques. By providing a prediction of the load profile, along with the power and energy capacity of the device, the proposed method is able to schedule the storage device to minimise the maximum demand and total grid energy consumed. The proposed method is compared to an existing threshold-based dispatch strategy and it is shown that the proposed method outperforms the threshold strategy in both maximum demand and consumption reduction.

Nomenclature

ΔT	Sample time (assumed to be 3600s in this work)
$\mathbf{P_s^+}(t)$	Electrical power supplied to the storage
$\mathbf{P_s^-}(t)$	Electrical power withdrawn from the storage
$\mathbf{E_s}(t)$	Energy in the storage unit
$\mathbf{P_g}(t)$	Power supplied by the generator
$P_{l,f}(t)$	Load forecast
$P_l(t)$	Actual load
$P_{pv,f}(t)$	PV power forecast
$P_{pv}(t)$	Actual PV power
$P_{out}(t)$	Power supplied by the grid
$P_{net}(t)$	Demand minus available PV power
w_1	Relative value of maximum demand charge
w_2	Relative value of aggregate energy usage
w_3	Relative value of generator fuel usage
$P_{pv,max}$	Photovoltaic array capacity
η_c	Charge efficiency
η_d	Discharge efficiency

Email addresses: `ronald.clark@students.wits.ac.za` (Ronald Clark), `anton.vanwyk@wits.ac.za` (MA van Wyk), `willie.cronje@wits.ac.za` (WA Cronje)

Preprint submitted to Elsevier *July 20, 2014*

1. Introduction

The demand-side deployment of hybrid energy systems has shown great potential in decreasing monthly energy bills as well the reliance of institutions on utility providers for provisioning their daily energy needs. These systems consist of two types of components – those which are dispatchable and those which are non-dispatchable. The renewable sources constituting the system are highly unreliable and therefore "non-dispatchable". This has severe implications on the practicality of employing such sources in companies and organisations where peak availability of the renewable resources may not coincide with peak demand. In worst case, this can lead to a situation where at times of low demand there is more renewable energy (essentially freely available energy) than can be utilised while at times of high demand there may not even be enough to cover the base load.

Storage elements, the first type of dispatchable component considered in this work, can be introduced at the demand side or "behind the meter" to store energy at times of low demand and directly supply the load at times of high demand, thereby reducing the peak demand on the grid and possibly resulting in significant demand charge savings for the customer. As all practical storage devices have a finite capacity it is clear that a careful scheduling algorithm is needed to control the power flow to and from the storage device to ensure the device properly manages its energy for maximum demand charge reduction.

The second type of dispatchable component, the diesel generator, actively supplies energy into the system and can thus be dispatched "at-will" for demand charge reduction. It is not subjected to the stringent charge-discharge dynamics of the storage device. However, unlike a storage unit, the use of the generator incurs an additional financial cost related to the amount of fuel used during its operation. It is therefore only economical to run the diesel generator if the savings resulting from its operation outweigh its running costs.

1.1. Related Work

The problem of reducing maximum demand using a mega battery is considered in [1]. The storage device is scheduled using a simple load-following simulation. This strategy, while simple, is shown to perform poorly for flat loads and peaks of long duration. A battery dispatch strategy is presented in [2], with the aim of optimally scheduling the battery in a grid-connected PV power system to store the PV energy when not required and supply it when the need arises, thereby reducing the total grid energy consumption. This method, like many others, focusses specifically on using a battery as the storage element and thus includes maintenance requirements, depth-of-discharge considerations and operating at optimal state-of-charge (SOC) levels. These considerations are not really applicable to other storage units such as pumped hydro storage, flywheels or the pumped heat electrical storage (PHES) considered in this work.

Nottrott et al. [3] present a storage scheduling strategy for a grid-connected PV-battery system based on linear programming. The objective of their scheduling strategy is specifically to reduce the peak demand on the grid. The system they consider does not include a generator unit and does not account for the consumption charge.

1.2. Threshold-based Dispatch

It is clear that ideal load-levelling corresponds to the mean of the net demand curve (i.e. the actual demand minus the current PV output). A basic demand charge reduction method therefore involves taking the mean of the demand and using the result as a threshold for scheduling the storage. This method, although simple, has a number of disadvantages:

- A mean filter is non-causal but can be implemented by making use of the demand prediction data which is assumed to be available.
- The mean filter will not take into account the storage limitations.
- It will also not take into account the system losses

For these reasons the schedule produced by the threshold method will result in non-optimal operational cost reduction when used on a real system. However, due to its robustness and simplicity, it will be used in this work as a baseline for comparison.

It is clear that in order to achieve optimal demand charge reduction, a dynamic optimisation needs to be carried out to schedule the charging and discharging of the storage elements to ensure that enough stored energy is available during times of high demand. The work presented in this work is perhaps most similar to that of [4] and [5] with a number of key differences. In [4] an analytical procedure is presented which does not easily lend itself to computational implementation. In [5] a complex on-line and off-line algorithm is presented for optimally scheduling a storage element to reduce demand charges, however, this method does not address the integrated scheduling of a generator and storage unit.

Therefore, what is sought in this work is a practical method that can schedule the storage unit and generator to perform optimal demand charge reduction.

1.3. Current Work

This work considers a simplified PV-diesel-storage system shown in Figure 1 where the PV array, storage unit and diesel generator are connected to the grid and together supply the load. The goal of the work is to develop a method for determining the optimal dispatch schedule for the storage and generator that achieves the maximum possible demand charge as well as consumption charge reduction. The problem is formulated as a convex optimisation model which makes use of a 24 hour prediction of the load demand and the expected solar radiation to determine the optimal supply schedule for the generator and the charge-discharge schedule for storage unit.

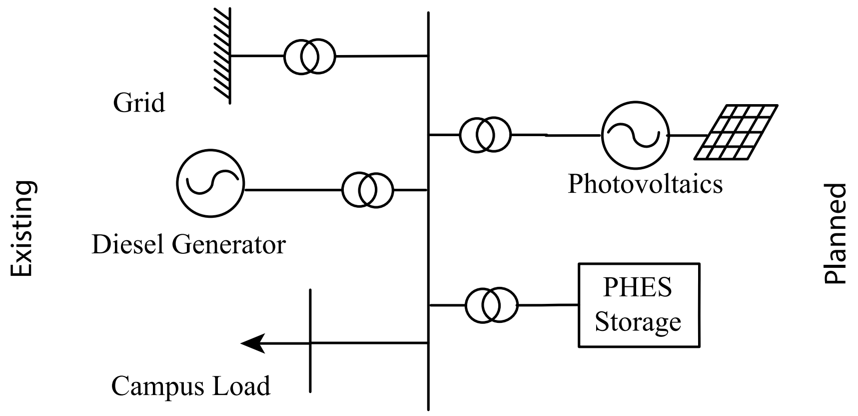

Figure 1: The PV-Diesel Storage system considered in this work.

2. Method

2.1. Convex Optimisation

The optimal dispatch method presented in this work is solved using convex programming. In general, a convex problem can be specified by

$$\begin{aligned} \underset{x}{\text{minimize}} \quad & f(x) \\ \text{subject to} \quad & g_i(x) \leq 0,\ i \in 1 \ldots n \end{aligned} \tag{1}$$

With the restriction that the functions $f(x)$ and $g_i(x)$ are convex functions.

Should the nature of the problem allow it, there are many advantages to formulating an optimisation problem in convex form:

- The convex optimisation problem is one of the most well-studied problems in the field of optimisation and therefore many fast, efficient and accurate algorithms exist to solve this type of problem.
- Many convex algorithms inherently handle equality and inequality constraints which makes it easy to add constraints on the problem domain
- The convex solution is guaranteed to converge and will converge in finite time
- The solution will be a globally optimal solution

2.2. Optimisation Model

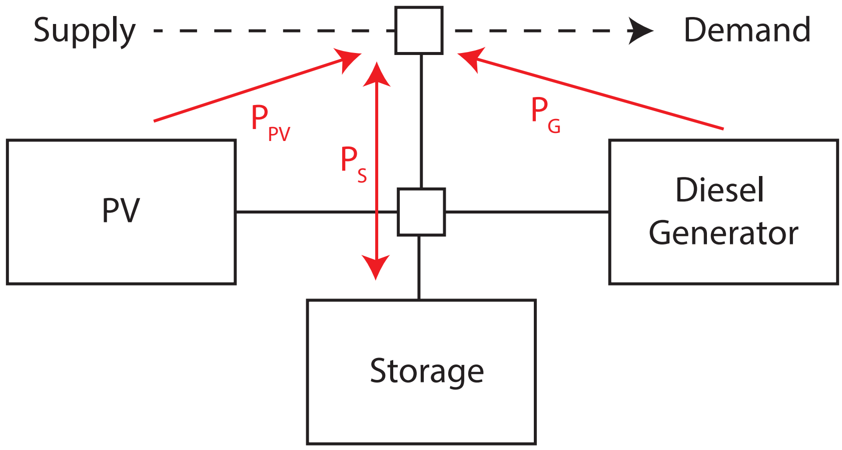

Figure 2: Illustration of the type of hybrid energy system considered in this work.

The system under consideration is shown in Figure 2 which comprises a storage unit, diesel generator, PV array and load connected to the electric utility grid. The dispatchable components are assumed to be controllable through a centralised control unit and the inverters, switches and lines are assumed to be lossless. The response time of the PHES unit and the generator is assumed to be much faster than the timestep of the scheduling method used in this work which is 30-min intervals. The power supplied by the utility company, $P_{net}(t)$ is assumed to be unbounded. The power drawn by the load cannot be controlled by the system (i.e. there is no demand side management) and it is assumed that an accurate 24-hour prediction of the load is available, denoted by $P_{l,f}(t)$. The optimisation model uses a general model of the storage device, characterised by its charge and discharge efficiencies. The electrical power supplied, $\mathbf{P}_\mathbf{s}^+(t)$, and withdrawn, $\mathbf{P}_\mathbf{s}^-(t)$, from the storage device is limited by the units's specifications. The total energy available in storage, $\mathbf{E}_\mathbf{s}(t)$ is determined by an integration, or equivalently, a summation as discrete samples are used.

The dispatch strategy is considered a finite-horizon convex optimisation problem. The convex model is defined as follows.

$$\min_{\mathbf{P_g},\mathbf{P_s^+},\mathbf{P_s^-}} \quad w_1 \max\{P_{net}(t)\}\} + w_2 \sum_{h=1}^{24} \{P_{net}(t)\} + w_3 \sum_{h=1}^{24} \mathbf{P_g}(t), \tag{2}$$

$$\text{subject to} \quad P_{net}(t) = P_{l,f}(t) - n_1 P_{pv,f}(t) - \mathbf{P_g}(t) - \mathbf{P_s^-}(t) + \mathbf{P_s^+}(t), \tag{3}$$

$$\mathbf{E_s}(t) = \mathbf{E_s}(t-1) + \eta_c \mathbf{P_s^+}(t-1) - \eta_d \mathbf{P_s^-}(t-1), \tag{4}$$

$$\mathbf{E_s}(t) \leq E_{s,max} \tag{5}$$

$$\mathbf{E_s}(t) \geq E_{s,min} \tag{6}$$

$$\mathbf{E_s}(0) = E_{s,init} \tag{7}$$

$$\mathbf{P_s^+}(t) \leq P_{s,max} \tag{8}$$

$$\mathbf{P_s^-}(t) \leq P_{s,max} \tag{9}$$

$$\mathbf{P_s^+}(t) \geq 0 \tag{10}$$

$$\mathbf{P_s^-}(t) \geq 0 \tag{11}$$

$$\mathbf{P_g}(t) \leq P_{g,max}, \tag{12}$$

$$\mathbf{P_g}(t) \geq 0. \tag{13}$$

The objective function in Equation 2 minimises the expected demand charge, the aggregate energy charge and the fuel expense incurred by the use of the diesel generator. The three constants, w_1, w_2, w_3, are included in the objective to represent the relative weights of the different operational costs. These factors are included so that the optimisation model properly balances the value of a reduction in the demand charge (which is billed per month) with the aggregate energy charge and the aggregate fuel usage (which is calculated here over a 24-hour optimization horizon). The decision variables, $\mathbf{P_s^+}(t)$ and $\mathbf{P_s^-}(t)$ represent the electrical power supplied and withdrawn from the storage device respectively. The decision variable $\mathbf{P_g}(t)$ represents the generator scheduling. The net demand is defined through the energy balance equation which is represented by the equality constraint in Equation 3. The storage dynamics (i.e. the requirement that energy has to be accumulated before it can be supplied) of the physical device are modelled through the equality constraint in Equation 4. Because the storage element is modelled as a first-order system, its initial state needs to be specified. The initial energy in the storage device is specified in Equation 7. As the scheduling is carried out in a rolling-horizon manner, the initial condition is set to the state of the storage device during the previous optimisation. During the first run of the system, the energy stored in the device is likely to be limited to zero by practical considerations. Equation 5 and 6 specify the storage capacity constraints. Equation 8 and 9 defines the maximum rate at which the storage device can charge and discharge. Equation 12 specifies the maximum generator output.

This model is clearly convex in the decision variables – the objective function includes only a linear combination of the decision variables and the max function (or infinity norm) is a convex function. Furthermore, the constraints are also convex, being made up of affine quantities compared to constants. The storage efficiency is modelled as an effective charge and discharge efficiency, η_c and η_d, which play a major role in the performance of the storage device. The optimisation model takes into account these inefficiencies (i.e. the storage losses) that occur when energy is to the storage device and the back to electrical energy. This needs to be achieved while still adhering to the general convex programming form which is difficult as the energy lost is a non-conservative quantity (the round-trip efficiency depends on the absolute value $|\mathbf{P_s}(i)|$ of the energy flow to the storage). By separating the the energy supplied and withdrawn from the device into two quantities this problem is still convex. Equation 10 and 11 are therefore necessary to enforce a proper sign convention for energy flow to and from the storage. The convex programming problem can be solved using any convex programming technique. In this work CVX is used to parse the problem and then it is solved using SeDuMi.

2.3. Running the Scheduling

A flow-chart showing the operation of the scheduling method is given in Figure 3. Before the scheduling is started, the storage specifications, generator specifications and tariff parameters are supplied to the optimisation model. These include the storage energy capacity, power capacity and the generator peak power output. During each timestep, the 24 hour load and PV forecasts are supplied to the optimisation model. In this work, it is assumed the forecasts are updated hourly on a receding horizon basis and thus at each timestep, a new 24 hour load and PV predictions are available. The gray box in Figure 3 represents the main scheduling procedure. The scheduling is also carried out in a receding horizon manner. Initially, at say t = 0h, an optimal schedule is computed for the storage unit and generator which minimises the objective function in Equation 2 over the next 24 hours. These values are used to schedule the generator and storage unit at t = 0.5h. To account for the inevitable inaccuracies in the forecasts, the storage unit is dispatched to meet the actual demand during the intra-hour period. This ensures that any unforeseen spikes in demand are accounted for by the storage unit, not the utility grid, which mitigates their effect on the demand charge. During the next timestep, the actual energy stored in the storage unit is measured and used as the initial condition for the optimisation model. The forecasts are updated, and the procedure is repeated for the next timestep. This results in a continuous optimal receding horizon schedule for the generator and storage unit.

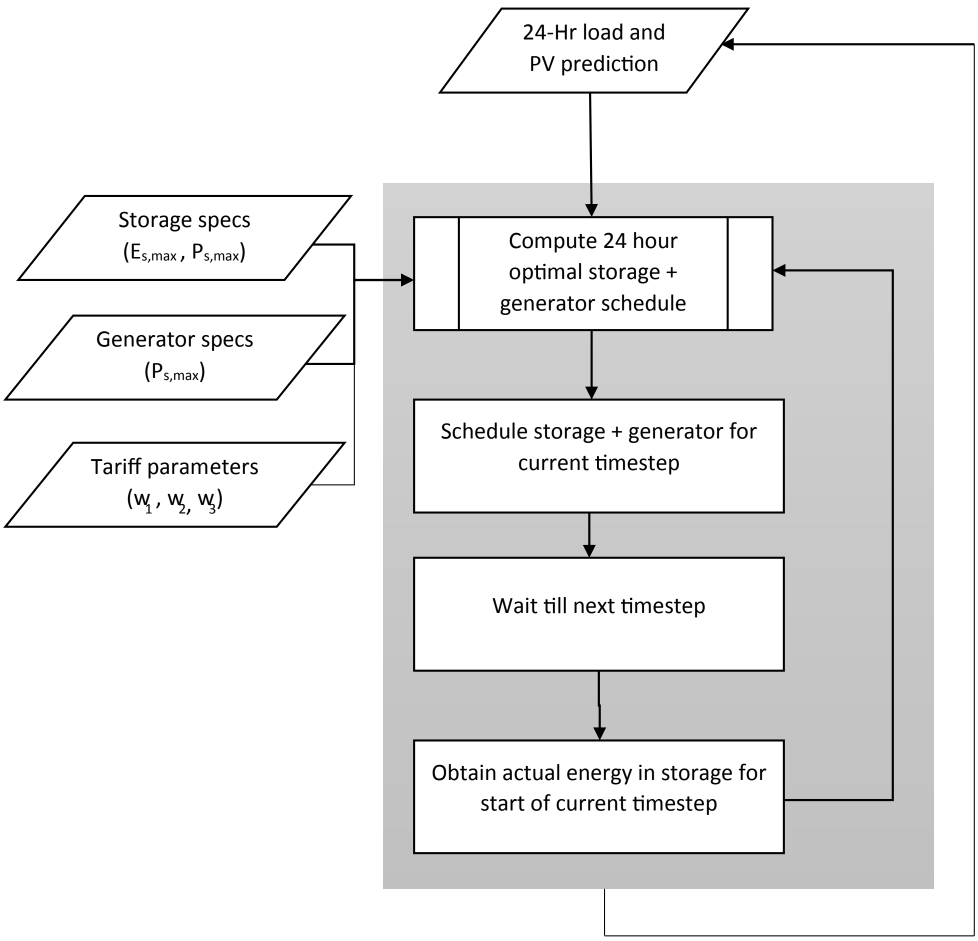

Figure 3: Flow chart of the scheduling method.

2.4. Load and Solar Radiation Data

The load forecast is obtained using a Support Vector Regression based short term load forecasting method [6]. The horizon of the load forecast is 24 hours and the forecast has a time resolution of 30 min. The forecasting method uses as its input various previous load data up until the current time period, as well as historical temperature data and calendar data (i.e. weekday, weekend, holiday). For the application considered in this work, the mean absolute percentage error is 3.44% and the errors of the load forecast method are approximately normally distributed with a standard deviation of 70.9 kW.

The PV forecast is obtained using the free meteoblue pointSOLAR system which provides an online API for obtaining localised short term forecasts of the output of PV systems. The system uses the solar radiation forecast of the numerical mesoscale model (NMM) combined with the PV system specifications to produce the PV power output forecast. The system has a mean absolute error of $20 - 35\%$. The horizon of the forecast is 144 hours with a time resolution of 1 hour. In this work, the PV forecast data are interpolated to fit the 30 min timestep used in the dispatch method.

2.5. Dealing with Prediction Errors

Prediction errors are accounted for in the scheduling method through a simple real-time response procedure. The dispatch model itself does not accommodate for this response. For example, the difference between the actual load during a certain timestep might exceed the available energy in storage, resulting in a spike in the grid utilisation. The scheduling algorithm can be modified to be more robust in the presence of errors. This can be achieved by keeping some reserve energy in the storage to restrict the probability that the uncovered prediction error will exceed a certain value. As the distribution of the prediction errors is known, this approach is readily adopted. The prediction errors follow a standard normal distribution with mean $\mu = 0$, variance σ and CDF

$$F(P_{FE}) = \frac{1}{2}\left[1 + erf\left(\frac{P_{FE} - \mu}{\sqrt{2\sigma^2}}\right)\right] = p \tag{14}$$

For a given confidence level p, the associated error threshold can be determined using the inverse CDF

$$E_{RES} = F^{-1}(p) \tag{15}$$

The minimum energy in the storage unit is set to ensure the reserve energy in storage remains above this value.

$$E_{s,min}(t) = E_{RES} \tag{16}$$

3. Results and discussion

The performance of the proposed predictive dispatch method was tested on its ability to achieve optimal peak shaving for a large institution, using a PHES unit to store purchased energy for later use. The load data are sourced from energy meters on the campus of the University of the Witwatersrand. The particular hybrid energy system configuration considered in the case study constitutes a 1 MW diesel generator and a 100 kW PV array. The storage device used in the case study is a Pumped Heat Electrical Storage (PHES) device. The device has a nominal energy capacity of 4 MWh and a maximum power capacity of 1 MW.

The electricity tariff under consideration consists of two components, the aggregate energy usage and a maximum demand charge. The demand charge is determined using discrete timeslots comprised of 30 minute moving averages. For simplicity of analysis, peak values within fixed 30 minute slots have been used in this work. As in many other countries, the per-unit peak demand charge is significantly greater than the total usage charge, thus there is great interest in reducing the peak consumption by storing utility-supplied energy for times of peak demand. The specific tariff structure considered is the Eskom Nightsave Urban Large Tariff for the Johannesburg, South Africa region which is given in Table 1. The price of diesel fuel is assumed to be R13/L and the diesel generator fuel usage is 0.4 L/h/kW.

Table 1: Summary of the $\geq 500V \& \leq 66kV$ Nightsave Urban Large Tariff

	Active energy charge [c/kWh]	Energy demand charges [R/kVA/m]
High demand [Jun - Aug]	57.00	172.12
Low demand [Sep - May]	44.47	24.03

3.1. Low-Demand Season [Sep - May]

This section investigates the scheduling strategy obtained for a low-demand season where the demand charge is R 24.03/kVA and the active energy charge is R 0.44/kWh. The values assigned to the relative tariff weights are therefore:

- Demand charge: $w_1 = 24.03$
- Energy charge: $w_2 = 0.44 \times 31$. The expected energy charge for the month if the 24 hour period is representative of the entire month.
- Fuel cost: $w_3 = 13 \times 0.4 \times 31$. The expected fuel charge for the month if the 24 hour period is representative of the entire month.

An example schedule obtained by running the dispatch strategy over a 48 hour period during the low demand season is shown in Figure 4. The storage unit is initialised to full capacity (4 MWh). From the Figure it is evident that during the low-demand season where the demand charge is rather low, it is never economical to run the generator to reduce the demand charge. The storage unit is charged and discharged to optimally shave the peaks of the net load, as is evidenced, for example, in 14h - 20h.

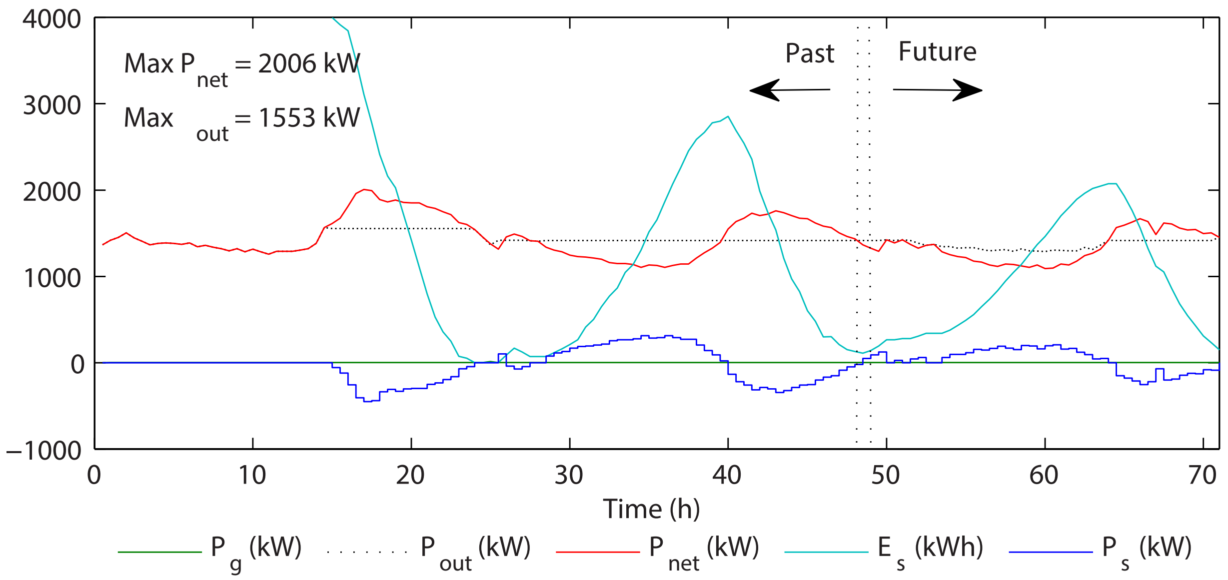

Figure 4: Generator and storage schedule for low demand season.

A comparison between the basic threshold dispatch strategy and the optimal strategy presented in this work is shown in Figure 5. Subfigures 1a,b,c show the threshold strategy and 2a,b,c show the optimal strategy. The simple strategy accumulates energy in 1h - 10h while the predicted demand is lower than the rolling mean. The storage then discharges to significantly shave the peak demand in 10h - 17h. However, at around 18h - 20h, the energy in the storage has depleted and a spike in output demand occurs. This results in the maximum demand for the period being 1912 kW, while the optimal dispatch strategy properly

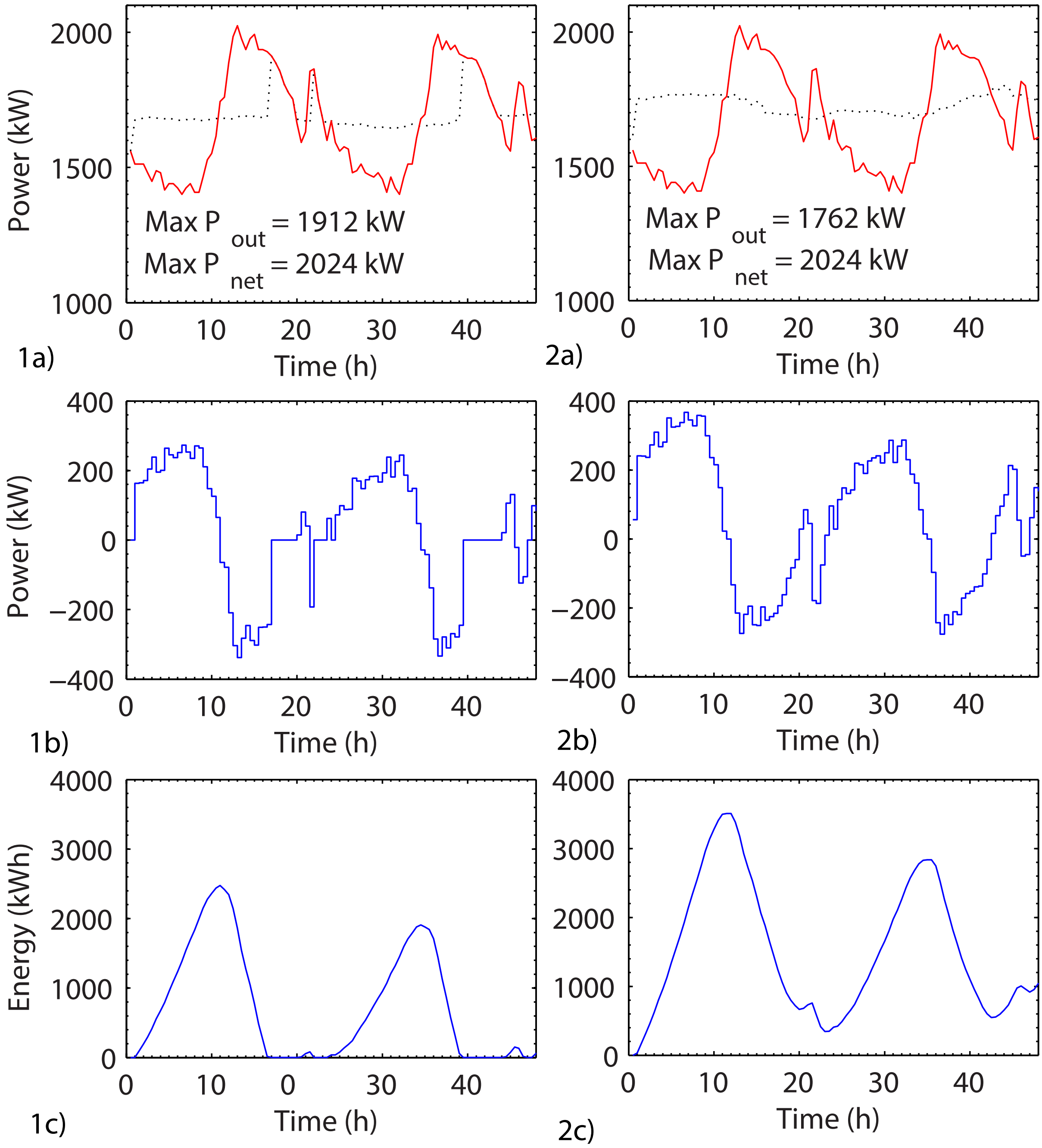

Figure 5: Comparison between the basic threshold strategy and the optimal dispatch strategy developed in this work for a 4 MWh storage capacity.

manages the storage to reduce the peak demand to 1762 kW. The performance of the optimal strategy is therefore clearly better than the basic strategy in this case.

Figure 6 shows the maximum demand for 1 month using both scheduling methods for various PV and storage capacities. The advantage of the optimal strategy is again evident. The optimal strategy gives a lower peak demand for nearly every configuration.

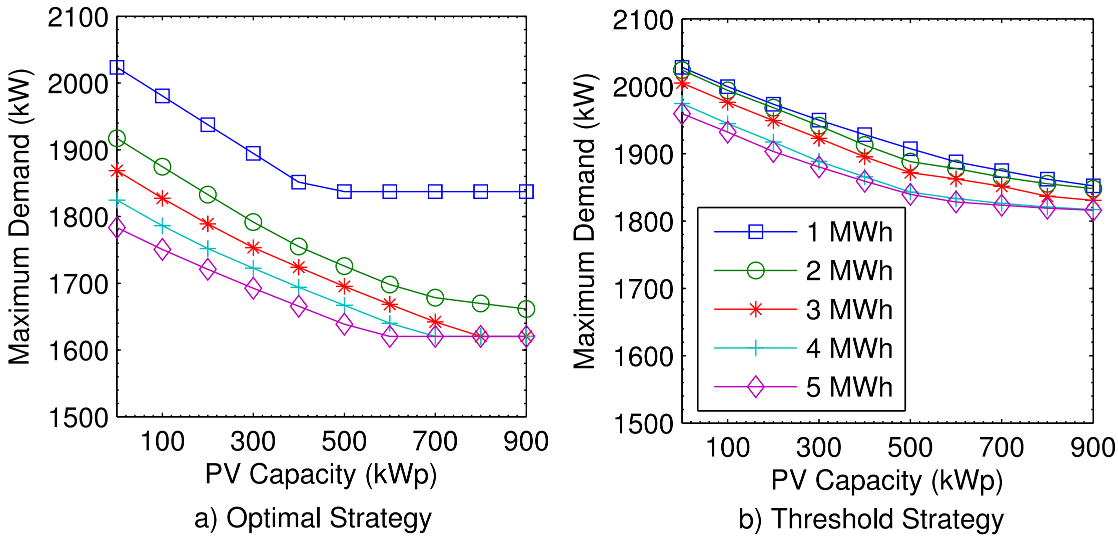

Figure 6: Maximum demand for 1 month using threshold and optimal dispatch strategy.

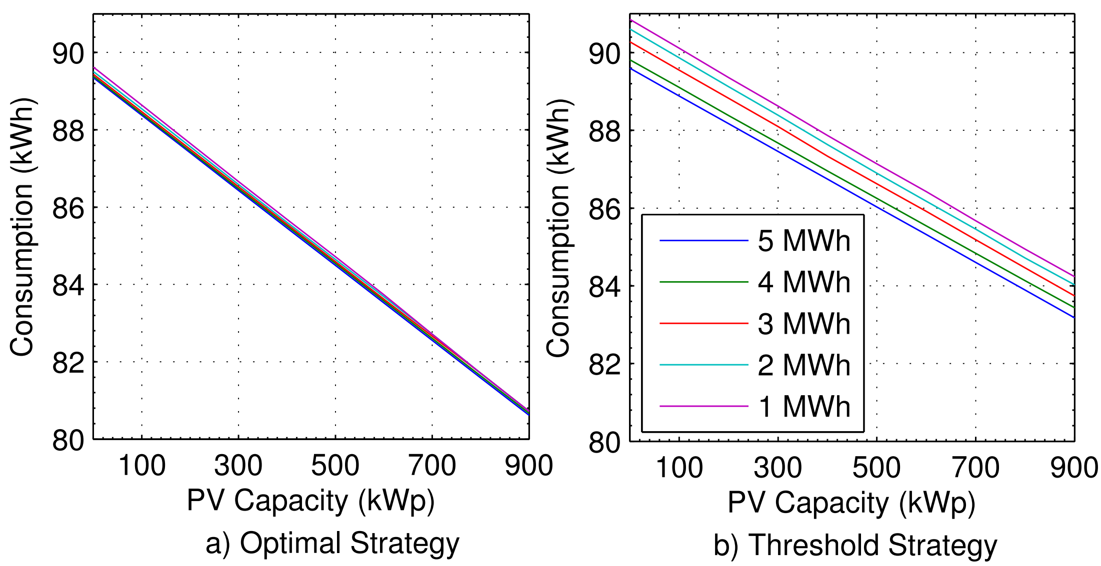

Figure 7: Total consumption for 1 month using threshold and optimal dispatch strategy.

The total consumption for 1 month using the optimal strategy and the basic threshold strategy are shown in Figure 7. The optimal strategy also outperforms the threshold strategy in terms of total consumption.

The main difference in the consumption charge is accounted for by the inclusion of the consumption charge in the objective function. This results in the optimal strategy not allowing the storage to charge and discharge excessively, thereby saving losses. The basic threshold strategy, however, charges and discharges whenever the demand is below the mean even if this energy will not help in reducing the maximum demand.

3.2. Sizing the storage

The results from Figure 4 show that the 1 MW storage device only achieves ≈ 500 kW reduction in peak demand. This suggests that half its power capacity is wasted and the same demand reduction might be achieved with a storage device of lower specification. The proposed scheduling algorithm can be used to give a basic guideline as to the best capacity specifications of the storage device. For example, Figure 8 was generated by explicitly varying the power and energy capacity values used in the simulation. The achieved peak reduction was then plotted against these values. By inspecting the graph, it is evident that for a energy capacity less than 200 kWh, little or no peak reduction can be achieved regardless of the power capacity of the device. Similarly, maximum power capacity of less than 1 MW leads to very little peak reduction for all capacities. The graph also shows that a rather large storage device is required to achieve significant peak reduction. This suggests that battery-based energy storage might not be financially viable for achieving the peak shaving. However, PHES systems have an estimated price in the region of R 720/kWh with single unit sizes in the range of 2-5 MW, making them a viable option [7].

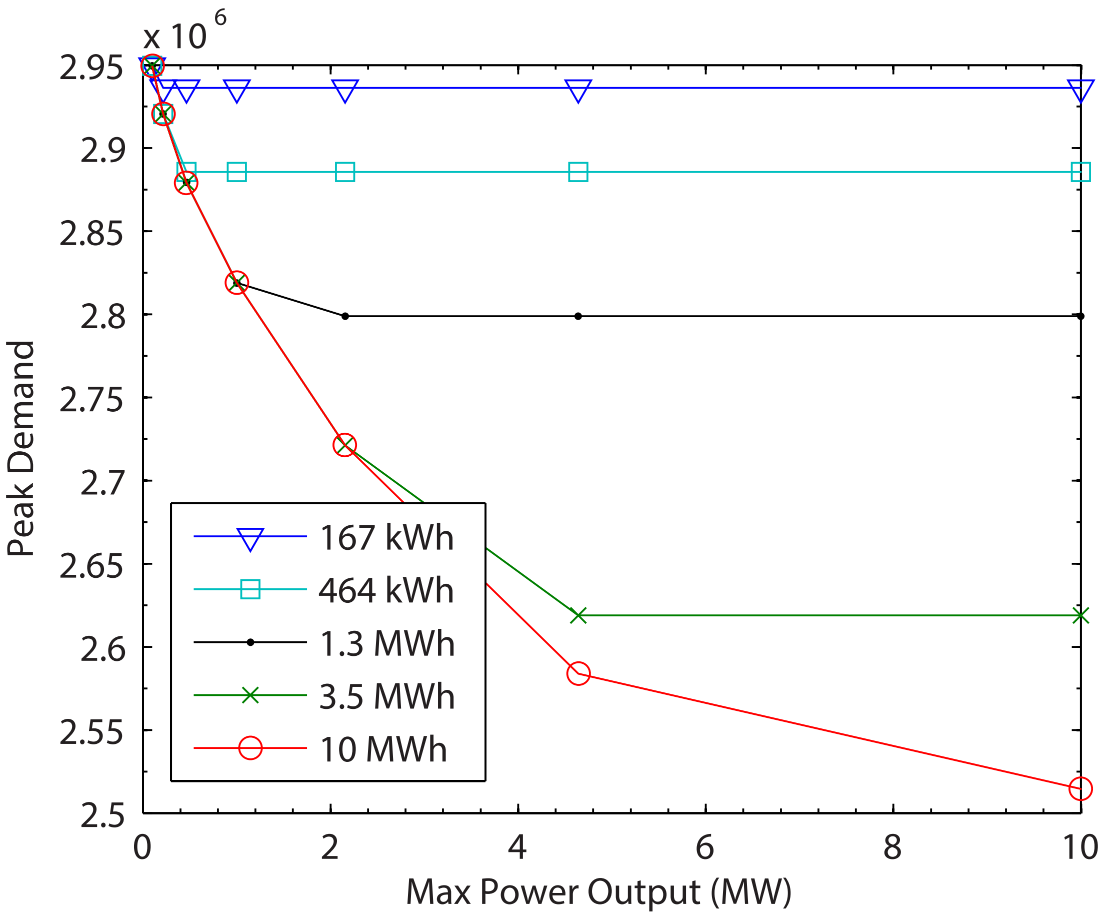

Figure 8: Peak reduction achieved for various PHES capacities and maximum power outputs.

3.3. High-Demand Season [Jun - Aug]

This section investigates the scheduling strategy obtained for a high-demand season where the demand charge is R 172.2/kVA and the active energy charge is R 0.57/kWh. The values assigned to the relative tariff weights are therefore:

- Demand charge: $w_1 = 172.12$
- Energy charge: $w_2 = 0.57 \times 31$. The expected energy charge for the month if the 24 hour period is representative of the entire month.
- Fuel cost: $w_3 = 13 \times 0.4 \times 31$. The expected fuel charge for the month if the 24 hour period is representative of the entire month.

Figure 9 shows the schedule for a 1 MW generator and 4 MWh storage unit two days during the high demand period. The key difference between the low demand results of Figure 4 and the high demand period is that the diesel generator is now used to assist in lowering the peak demand. The storage device is now also more fully utilised, being charge between its energy capacity limits around once per day. A significant trend to note is that the optimal scheduling always runs the generator while the storage is discharging. This suggests that although it is economical to run the generator to shave peaks during a high demand season, it is still not economical to use it to charge the storage device i.e run it at times of low demand. A 20% (603 kW) reduction in peak demand is achieved which results in demand charge savings of R 103790 per month for the high demand tariff.

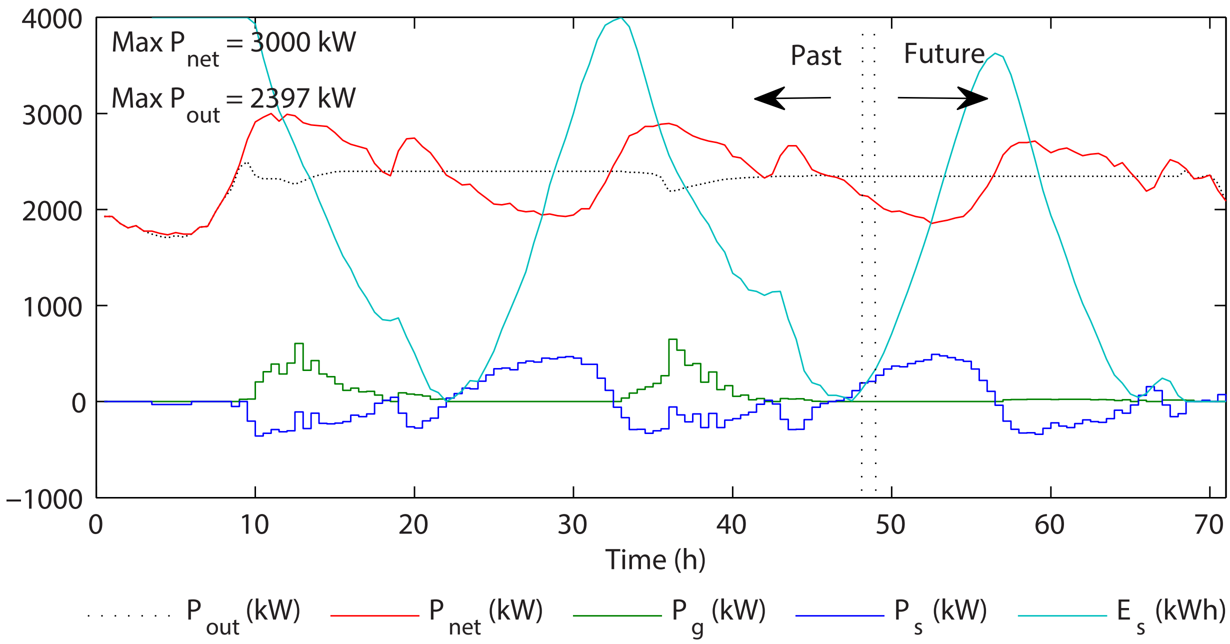

Figure 9: Generator and storage schedule for high demand season.

The impact that the prediction error has on the optimal scheduling is demonstrated in Figure 10 which shows the schedules obtained for a badly forecasted day (a) and assuming perfect knowledge of the demand is known (b). The value of having an accurate forecast is clearly evident as the peak demand in Figure 10 (b) is around 4% lower than the peak demand using the realistic forecast.

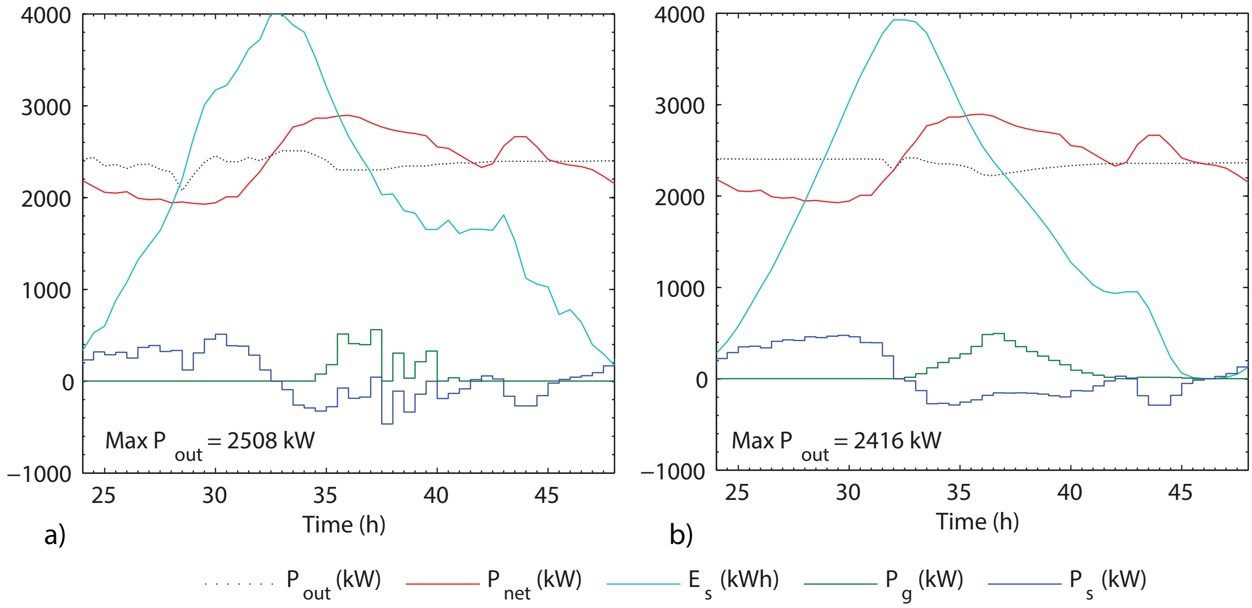

Figure 10: Comparison between the use of the actual prediction (a) and perfect knowledge of future demand (b).

4. Conclusion

Grid-connected hybrid energy systems implemented at the demand side are a viable means of reducing energy bills for consumers. In this work, a dispatch strategy was presented that optimally schedules a storage unit and generator to achieve maximum demand and consumption charge reduction in a PV-diesel-Storage hybrid system. The algorithm was extended to take both storage losses and uncertainties in demand into account. The algorithm was tested using a model simulating a realistic PHES system. It was illustrated that the optimal scheduling strategy performs better than a basic threshold strategy at reducing both consumption and maximum demand. It is concluded that the algorithm can be successfully used to schedule a storage unit to achieve significant reductions in operational costs for a grid-connected PV-diesel-Storage system.

References

[1] G. Dupont, P. Baltus, Dimensioning and grid integration of mega battery energy storage system for system load leveling, in: PowerTech, 2009 IEEE Bucharest, 2009, pp. 1–6.

[2] E. Palomino, J. Stevens, J. Wiles, A control system for improved battery utilization in a pv-powered peak-shaving system, in: Photovoltaic Specialists Conference, 1996., Conference Record of the Twenty Fifth IEEE, 1996, pp. 1525–1528.

[3] A. Nottrott, J. Kleissl, B. Washom, Energy dispatch schedule optimization and cost benefit analysis for a grid-connected, photovoltaic-battery storage systems, Renewable Energy 55 (0) (2013) 230 – 240.

[4] Y. Levron, D. Shmilovitz, Power systems' optimal peak-shaving applying secondary storage, Electric Power Systems Research 89 (0) (2012) 80 – 84.

[5] M. P. Johnson, A. Bar-Noy, O. Liu, Y. Feng, Energy peak shaving with local storage, Sustainable Computing: Informatics and Systems 1 (3) (2011) 177 – 188.

[6] R. Clark, W. Cronje, Short term load forecasting for a large institution using support vector regression, in: SAUPEC 2013, 2013.

[7] T. U. of Crete, A five minute guide to electricity storage (2013).
URL `http://publications.arup.com/`

Appendix A. Physical storage unit simulation model

This appendix provides the storage simulation model that is used in the results as a substitute for the real storage device. The model simulates the efficiencies, storage dynamics and constraints. The input to the model is the storage schedule and the output is the actual power supplied or drawn by the device. This is a simplified version of the Alstom PHES model.

Algorithm 1 Program used for simulating the physical storage device.

$charge \leftarrow 1$
$discharge \leftarrow 0$
for $t \leftarrow 1$ **to** $length(Pin) - 1$
  do if $Pin(t) >= 0$
  then $charge$
  else if $Pin(t) < 0$
  then $discharge$
$POut(t) \leftarrow Pin(t)$
if $(charge)$

$$\textbf{then} \begin{cases} \textbf{if } Pin(t) < Pmin \\ \quad \textbf{then } POut(t) \leftarrow 0 \\ \quad \textbf{else if } Pin(t) > Pmax \\ \quad \textbf{then } POut(t) \leftarrow Pmax \\ \textbf{if } (abs(POut(t)) > 0) \\ \quad \textbf{then } \begin{cases} Pth = (POut(t) \times effCharge) \\ E_s(t+1) \leftarrow E_s(t) + Pth * T \end{cases} \\ \textbf{if } E_s(t) > Emax \\ \quad \textbf{then } \begin{cases} POut(t) \leftarrow 0 \\ E_s(t+1) \leftarrow E_s(t) \end{cases} \end{cases}$$

  else if $(discharge)$

$$\textbf{then} \begin{cases} \textbf{if } abs(Pin(t)) < Pmin \\ \quad \textbf{then } POut(t) \leftarrow 0 \\ \quad \textbf{else if } abs(Pin(t)) > Pmax \\ \quad \textbf{then } POut(t) \leftarrow -Pmax \\ \textbf{if } abs(POut(t)) > 0 \\ \quad \textbf{then } \begin{cases} Pth \leftarrow -POut(t)/effDischarge \\ E_s(t+1) \leftarrow E_s(t) - Pth * T \end{cases} \\ \textbf{if } E_s(t) < Emin \\ \quad \textbf{then } \begin{cases} POut(t) \leftarrow 0 \\ E_s(t+1) \leftarrow E_s(t) \end{cases} \end{cases}$$

Chapter 6

Optimal PV and Storage Sizing

In the preceding manuscript a functional method for optimally dispatching the storage and generator was developed. Combined with the prediction algorithm, it forms a practical method to reduce the operational costs of the system. It was shown that the dispatch strategy is very effective at reducing the operational charges. It was also shown that the reduction in operational charges is highly dependent on the size of the PV array and storage capacity, with a strong negative correlation between these variables. This means that increasing the PV and storage unit sizes will result in lower total demand and consumption charges over the lifetime of the system. However, the savings produced by the demand and consumption charge reduction can easily be displaced by the initial costs of the units, negating the benefits of including these components.

The following manuscript presents a method for determining the optimal PV and storage sizes with respect to the optimal dispatch strategy. As opposed to the functional dispatch strategy in the previous chapter which uses a 24 hour prediction of the load, year-length historical load data are now used in the sizing method to determine the total cost of the system over its lifetime. The purpose of the optimal sizing is to answer the question what PV and storage capacity will lead to the lowest system cost over a 20 year period considering the optimal dispatch strategy is used for the generator and storage?

Candidate's contribution: The candidate was responsible for devising the integrated optimal sizing and optimal dispatch method based on convex optimisation.

Design Optimization of a Hybrid Energy System through Convex Programming

Ronald Clark
School of Electrical and Information Engineering
University of the Witwatersrand
Johannesburg, South Africa
ron.clark@live.com

Willem Cronje
School of Electrical and Information Engineering
University of the Witwatersrand
Johannesburg, South Africa
willie.cronje@wits.ac.za

Michael Antonie van Wyk
School of Electrical and Information Engineering
University of the Witwatersrand
Johannesburg, South Africa
anton.vanwyk@wits.ac.za

Abstract

In this work, a methodology for the optimal sizing of the PV and storage capacity in a grid-connected PV-Diesel-Storage hybrid energy system is presented subjected to demand and consumption charges. A convex objective function is formulated based on the NPV of the system which includes both the consumption charge and demand charge. The generator and storage schedule is optimised for optimal demand charge reduction. The method is used to size the storage and PV capacity to obtain lowest overall cost (capital+running costs) for a small university campus over a 20 year project lifetime.

Keywords

convex programming; optimization; hybrid energy; design; simulation

I. Introduction

When designing a hybrid energy system for a large building or institution, the sizing of the generation and storage units is generally an under-constrained problem - various combinations of component sizes can be chosen to satisfy the given demand. In order to find an optimal solution to this design problem, a cost function can be defined and the “minimum cost’’configuration used to size the components. The specific hybrid energy system addressed in this work is a PV-Diesel-Storage system shown in Figure 1.

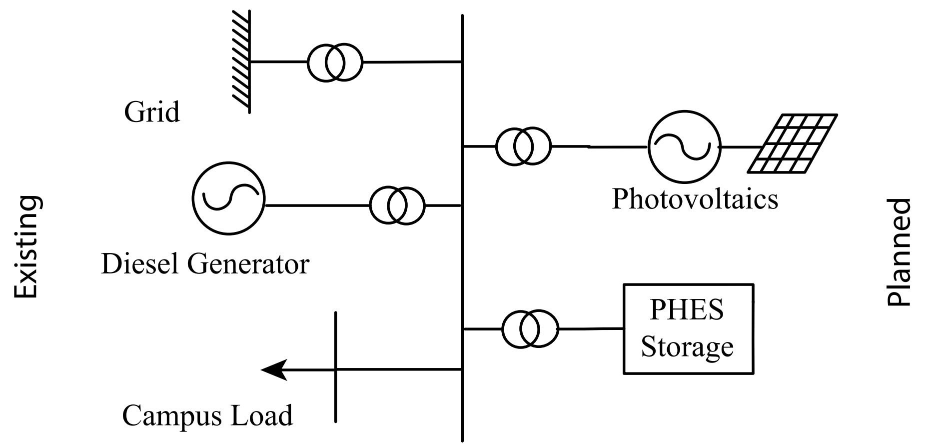

Figure 1: An overview of the hybrid energy system configuration. The input variables include a year’s worth of time domain load data, along with solar radiation time data. The sizes of the PV and storage components are to be determined.

The optimal design problem for alternative energy systems has been well studied in the literature. Borowy et al. [1] address the problem of sizing an off-grid PV-wind-battery system. To do this, hourly wind speed and solar insolation data over a 30 year period is used to calculate the average energy generated by various PV and WECS capacities for the region. A simple paper based method is then used to size the battery bank and PV to limit the loss-of-supply probability. Tina et al. developed a probabilistic approach for sizing a PV-wind system that eliminates the need for time-series analysis [2], however this model does not accommodate for storage devices and is restricted to expected-energy-not-supplied as its measure of merit. To cope with more complicated cost functions, system components and to simultaneously optimise the dispatch strategy, most authors turn to heuristic, non-linear optimisation methods with the genetic algorithm being by far the most popular. Kornelakis et al. [3] consider a grid-connected PV system and employ a genetic algorithm to find the optimal number of PV modules, their tilt angle and optimal arrangement. Yang et al. also use a genetic algorithm to find the optimal number of PV panels, wind turbines and batteries in a grid-connected PV-wind-battery system [4]. In [5], Seeling-Hochmuth presents a method for the combined optimisation of the sizing of the PV-Wind and dispatch of the generator and storage. The optimisation is carried out using a genetic algorithm. The operational strategy is collected in a 5-element vector which specifies the decision variables of the strategy for every hour of the year. The elements of the vector are found during the optimisation procedure using the genetic algorithm. Application of genetic algorithms to other variations of hybrid energy system configurations include those presented in [6], [7], [8], [9], [10], [11], [12]. A multitude of design methods based on particle swarm optimisation (PSO) have also been proposed [13], [14], [15], [16]. The technique of simulated annealing, although notably less widespread, has also been applied to the hybrid energy system design problem [17], [18].

A. Hybrid Energy System Metrics

In order to optimally size components, a measure needs to be chosen that can quantify its benefits as a single value. This value, known as the measure-of-merit of the system may take into account a range of factors depending on the needs of the particular hybrid energy system application. For example, the measure-of-merit for an off-grid hybrid energy system may be defined as the average percentage of demand met during its lifetime, or the reduction in CO_2 emissions it achieves. For grid-connected applications benefits might include the reduction in maximum demand that is achieved or the reduction in net energy needing to be purchased form the grid each month. Standalone or islanded systems do not have any backup supply of power. They are therefore optimised on aspects related to the cost of or probability of losing power which include Loss of Power Supply Probability (LPSP), Expected Energy Not Supplied (EENS), Level of Autonomy (LOA) and battery State of Charge (SOC). For grid-connected systems, however, “losing supply” typically means having to buy energy from the grid which has a direct monetary value determined by the utility company. Therefore, for grid-connected systems the benefits are quantified by the savings produced in the energy bill i.e. the system’s ability to reduce consumption charges and demand charges. These are eveluated over the expected lifetime of the system by calculating either the Levelized Cost of Energy (LCOE), Annualised System Cost (ASC) or Net Present Value (NPV) which all produce a single value by which different system configurations can be compared.

II. Convex optimization

This section discusses the particular type of optimization problem addressed in this work, namely, convex optimization. Convex optimization problem considered is a specific form of the more general non-linear optimization problems. Non-linear optimization problems take the form [19]

$$\begin{aligned} &\text{minimize } f(x) \\ &\text{subject to } g_i(x) \leq 0 \end{aligned} \tag{1}$$

Such an optimisation problem is convex when the objective function, $f(x)$, and constraints, $g_i(x)$ are all convex ie. they satisfy the constraint

$$f(ax + by) \leq af(x) + bf(y)$$

Convex optimization problems can be solved more efficiently than general non-linear problems which do not have the convexity property. Thus, in many cases where the objective function is convex or approximately convex, it is advantageous to approximate these non-convex problems as a suitable convex problem. This allows an approximate solution to the original problem to be obtained in very little time with high accuracy (depending on the nature of the approximation) as convex optimization problems can be solved using one of a wide range of fast and efficient algorithms. These include interior-point methods, bundle methods or sub-gradient projection methods. These algorithms have a number of advantages over non-convex optimization algorithms which are usually based on heuristics such as genetic algorithms, simulated annealing and sequential quadratic programming. These advantages include:

- With convex algorithms convergence is guaranteed
- The solution can be found in a finite (polynomial) time
- The solution is always globally optimal

Therefore, the use of convex optimization procedures is highly desirable if the problem can be reformulated as a convex problem or even approximately be shown to be of a convex nature. A large number of commonly-encountered functions are known to be convex. Of particular interest in this case are the following [19] :

- Every function that is a norm on $\mathcal{R}^N$ is convex
- The max function $f(\mathbf{x}) = \max\{x_1, x_2, \ldots, x_N\}$ is convex on $\mathcal{R}^N$

A number of operations exist that preserve convexity. These operations allow the construction of new functions which are themselves convex. One such operation which will be used in this work is the non-negative weighted sum of convex functions [19].

Proposition 1: If the functions $f_i, i = 1 \dots n$ are convex then [19]

$$f(x) = w_1 f_1(x) + \cdots + w_n f_n(x)$$

is also convex where each $w_i \geq 0$.

III. Component Models

A. PV Model

The PV array is characterised by its nominal capacity, measured in kWp and relative efficiency. The losses due to the relative efficiency (temperature and low irradiance effects) is assumed to be a constant 15.8%, the losses due to reflectance are assumed to be 3.1% and other losses in the system (inverters) are taken as 14%. This results in combined losses of 29.9%, or an overall efficiency of 70.1%. The global irradiance data are then multiplied by the nominal capacity and the overall efficiency to determine the actual PV output for each timestep.

B. Grid

The grid is modeled as an infinite supply of power carrying a maximum demand and aggregate usage charge. As the grid impedance losses are negligible compared to those of the other elements of the system.

C. Diesel Generator

A linear cost model for the diesel generator is used. The model assumes the generator need 0.4 L/kWh of diesel for generation throughout its operating range. This is a really simple but realistic model. If desired it can easily be replaced by a quadratic fuel consumption model, but in our experiences this is not required as the results produced are nearly identical to those of the linear model. The schedule of the generator is included as a decision variable in the objective function.

D. Cost Model

The total cost constitutes three components: the initial (or capital) costs (IC), the operational costs (that depend on usage) (OC) and the fixed monthly costs (which occur at regular time intervals) (FC). However, assets, as well as prices, typically vary in value over time and thus a factor needs to be introduced to better reflect the present value of the asset or cash flow. The first accounts for the inflation of prices or appreciation and is given by:

$$(1 + a)^t, \tag{2}$$

where a is the rate of appreciation and t is the current time.

The second is known as the discount factor:

$$\frac{1}{(1 + r)^t}, \tag{3}$$

where r is the discount rate.

The discount rate can be understood intuitively as the "opportunity cost of capital" – the advantage that is gained in investing in an asset or receiving an income now as opposed to at a later date. The discount rate depends on many factors but in South Africa, the typical discount rate for hybrid energy system projects is around 8% [**?**] and thus a discount rate of 8% is used throughout this work. The discount factor is the basis of net present value analysis (NPV) which is used in this dissertation. The NPV reflects the total present value of the project, including the initial costs and discounted cashflows:

$$\text{Total NPV} = \text{IC} + \sum_{\text{Project life}} \text{OC}. \tag{4}$$

The individual costs are calculated as:

$$\text{IC} = \sum_{Components} \text{Cost} \ \times \text{Capacity}, \tag{5}$$

$$\text{OC} = \sum_{Components} \frac{(1+a)^t}{(1+r)^t} \text{operational cost} \ \times \text{Usage}. \tag{6}$$

For the system under consideration, the operational costs are broken down into three components, the demand charge (DC), consumption charge (CC) and fuel charge (FC):

$$\text{DC} = \sum_{Months} \max\{P_{net}\}, \tag{7}$$

$$\text{CC} = \sum_{Months} \sum P_{net}, \tag{8}$$

$$\text{FC} = \sum_{Months} \sum P_{g}. \tag{9}$$

Both these tariffs are subject to the yearly price adjustment imposed by Eskom. The annual price adjustment is shown in Figure 2. The price adjustment is rather variable, but the mean increase over the period is 11.74%. If this trend continues, and a 8% discount factor is assumed, the present value of the consumption and demand charges at the end of a 20 year period will be $2.87\times$ their current value. However, the National Energy Regulator of South Africa has set the annual price increase at 8% for the next five years and thus an 8% increase in assumed in this work.

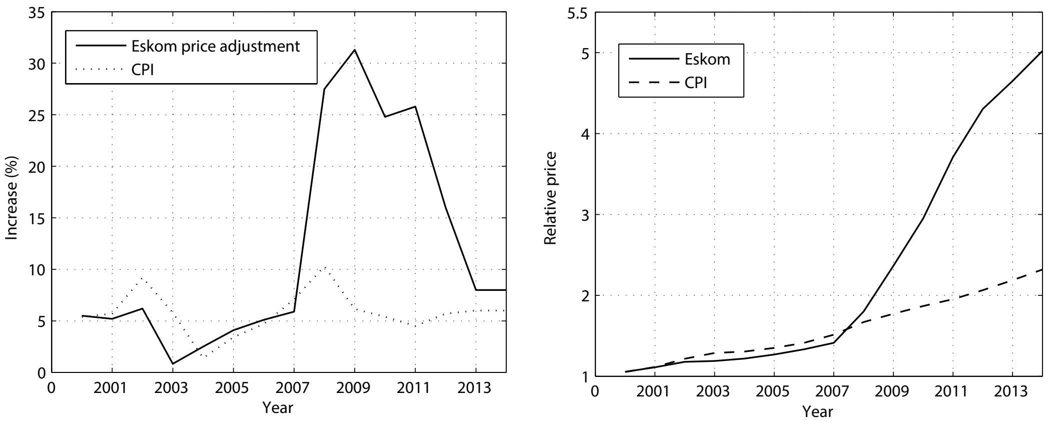

Figure 2: Electricity price appreciation compared to CPI

E. Initial Costs

The initial costs are directly related to the capacity of the generation and storage components. These costs are specified as R/kWp or "Rands per kilowatt of peak power produced". The component capacities themselves are decision variables to be determined by the optimal dimensioning method. Calculation of these optimal quantities relies directly on the operational costs and therefore the control strategies used.

IV. Objective Function

The convex optimisation model used to carry out the optimal sizing considering an optimal dispatch strategy for the generator and sotrage unit is show in Equation 6 to 18. The economic model forms the basis of the objective function of the model which is used to find the optimal storage and PV capacity. The objective function is given in Equation 6 and 7. The objective includes the consumption charge, maximum demand charge, PV initial costs and storage unit initial costs. The maximum demand charge is calculated as the sum of the maximum demand value achieved each month over the 12 months of the year and then extrapolated over a 20 year period using the discount factor. Similarly, the consumption charge is calculated as the sum of the consumption each month over the 12 months of the year and extended over 20 years. The discount factor described in Section III-D is used with a discount rate of r_t percent and an appreciation rate of a_t for the tariffs and r_d and a_d for the diesel fuel.

The net demand supplied by the grid is specified in Equation 8 which is the total demand less the PV power, generator output and storage output. The dynamics of the storage device are represented Equation 9 to 12. The storage capacity is included as a decision variable, along with the nominal PV capacity. The storage power capacity is specified in Equation 13 to 16. Equation 17 and 18 specify the generator power constraints.

The objective function is clearly convex. All three quantities in the running costs are norms. The consumption charge is a 1-norm, maximum demand is an infinity-norm and the diesel consumption is again a 1-norm. Obviously these are not direct norms of the argument (i.e. the component sizes) but rather norms of the net demand which is itself a function of the decision variables and constants. As such, the overall functionis convex.

$$\min_{\mathbf{x_w},\mathbf{x_{pv}},\mathbf{P_g},\mathbf{x_s}} \quad \sum_{n=1}^{20}\{\frac{(1+a)^n}{(1+r)^n}\sum_{m=1}^{12}\sum_{h=1}^{31\times24}\{P_{net}(h))\}+\sum_{m=1}^{12}\max\{P_{net}(h)\}\} \tag{6}$$

$$+p_d\sum_{n=1}^{20}\{\frac{(1+a)^n}{(1+r)^n}\sum_{m=1}^{12}\sum_{h=1}^{31\times24}\mathbf{P_g}(h)+\mathbf{x_{pv}}p_{pv}+\mathbf{E_{s,max}}p_s, \tag{7}$$

subject to

$$P_{net}(h) = P_{demand}(h) - \mathbf{x_{pv}}P_{pv}(h) - \mathbf{P_g}(h) - \mathbf{P_s^-}(h) + \mathbf{P_s^+}(h) \tag{8}$$

$$\mathbf{E_s}(i) = \mathbf{E_s}(h-1) + \eta_c\mathbf{P_s^+}(h-1) - \eta_d\mathbf{P_s^-}(h-1), \tag{9}$$

$$\mathbf{E_s}(h) \le \mathbf{E_{s,max}} \tag{10}$$

$$\mathbf{E_s}(h) \ge E_{s,min} \tag{11}$$

$$\mathbf{E_s}(0) = E_{s,initial} \tag{12}$$

$$\mathbf{P_s^+}(h) \le P_{max} \tag{13}$$

$$\mathbf{P_s^-}(h) \le P_{max} \tag{14}$$

$$\mathbf{P_s^+}(h) \ge 0 \tag{15}$$

$$\mathbf{P_s^-}(h) \ge 0 \tag{16}$$

$$\mathbf{P_g}(h) \le P_{g,max}, \tag{17}$$

$$\mathbf{P_g}(h) \ge 0. \tag{18}$$

Symbol	**Units**	**Description**
$\mathbf{x_{pv}}$	kWp	Decision variable representing the optimal PV capacity.
$\mathbf{P_g}(h)$	kW	Decision variable representing the generation dispatch schedule.
$\mathbf{P_s^+}(h)$	kW	Decision variable representing the energy supplied to the storage.
$\mathbf{P_s^-}(h)$	kW	Decision variable representing the energy removed from the storage.
$\mathbf{E_s}(h)$	kW	Decision variable representing the storage state of charge.
$\mathbf{E_{s,max}}$	kWh	Energy capacity of the storage device.
$P_{demand}(h)$	kW	Input variable representing the power demand.
$P_{pv}(h)$	kW/kWp	Input variable representing the available solar power.
r	%	The discount rate p.a.
a	%	The inflation rate p.a.
p_{pv}	R/kWp	Price of the PV
p_d	R/kWh	Price of running the generator
η_c	-	Charge efficiency of the storage device
η_d	-	Discharge efficiency of the storage device

The design optimisation problem involves finding the decision variables which minimise the objective function. Usually, the sizing of the components is considered a non-linear, discrete optimization problem that seeks to find the component sizes that give the lowest total cost. For example, the prospective PV arrays might consist of a number of 1kW panels strung together, in either series or parallel, to achieve the desired output capacity. A naive solution to this problem is to enumerate all possible combinations of components and evaluate the objective function for each combination. However, this becomes computationally intractable for even a small number of possible configurations. For these reasons, this work focuses on using convex optimsation to obtain a fast and reliable solution. The convex optimisation is carried out using the free MATLAB toolbox for disciplined convex optimisation CVX [20]. CVX requires the problem to be specified in much the same way as analysis presented here – building up the objective using smaller convex functions through the rules of convex analysis. Equation (2) and (3) can thus be directly used as the objective.

V. Case Study

In order to test the optimsation model, the prices shown in Table I have been used. These prices are realistic at the time of publication but are meant to demonstrate the main results, not to provide an accurate sizing for a particular application. Solar radiation data for the University of the Witwatersrand, Johannesburg, South Africa have also been used.

Table I: Table showing the prices for various expenses used during testing

Cost	Price	Unit
PV unit	R51077	per kW
Storage capacity	R720	per kWh
Diesel Generator	R5735	per kW
Fuel (diesel)	R13	per liter
Consumption charge (Utility)	R0.55	per kWh
Demand charge (Utility)	R172.12	per kVA

VI. Results

The first set of results presented in this section explicitly investigate the relationship between the PV and storage sizing and the total cost of the system subjected to the optimal dispatch strategy to demonstrate the impact these quantities have on the total cost of the system. This is done by fixing the capacities at specific values in the optimisation model and obtaining the appropriate cost components.

In Figure 3, the consumption charge component of the total system cost is plotted for a system with various PV and energy storage capacities. From the graph a strong trend is evident. At low PV capacities, the ability of the system to reduce the demand charge depends strongly on the size of the storage unit as through the optimal dispatch strategy, the storage shaves the demand charge even if the peaks of the PV and demand do not exactly coincide. At higher PV capacities, the size of the storage matters less in terms of demand charge as the main peak is adequately shaved by the PV alone (or by the PV and a small storage unit).

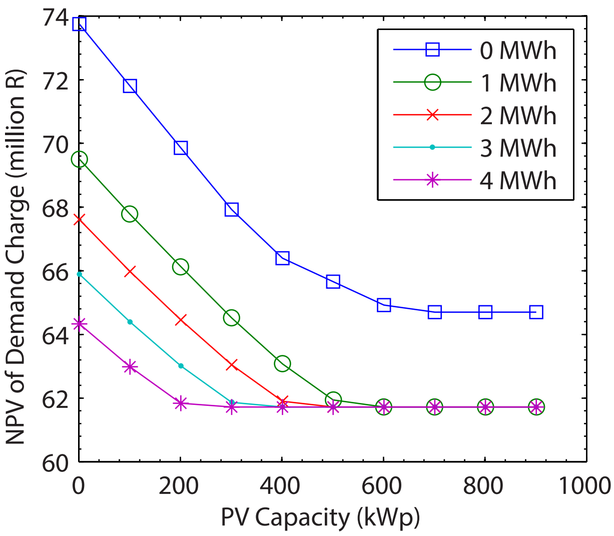

Figure 3: Demand charges over a 20 year period.

In Figure 4a, the consumption charge component of the total system cost is plotted for a system with various PV (0-1000 kWp) and energy storage capacities to investigate the effect that the storage size has on the total cost of the system. From the Figure, it is clear that the PV size has a significant effect on the total consumption charge over the period. The size of the storage does not significantly affect the consumption charge. However, at low PV capacities, the consumption charge increases with the storage size. This is most likely due to the storage losses in the system. As mentioned before, using the optimal dispatch strategy, the storage shaves the demand charge even if the peaks of the PV and demand do not exactly coincide, however, as it charges and discharges to do so, it loses energy due to its inefficiencies, thereby incurring additional consumption charges. In Figure 4b, the consumption charge component of the total system cost is plotted for a range of larger PV array sizes (0-10 MWp) to investigate the effect the storage has for large scale PV integration. The results agree with those for the small-scale PV arrays. There is little advantage to be gained from a larger storage size for PV arrays greater than 600 kWp

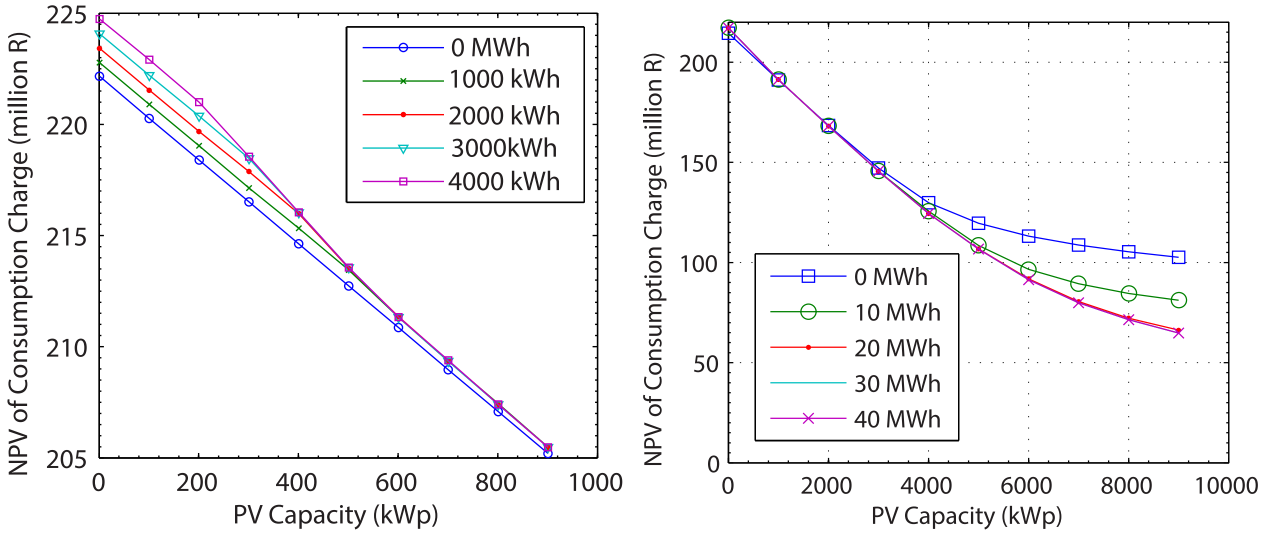

(a) Consumption charges for small PV array size range. (b) Consumption charges for large PV array size range.

and smaller than 4 MWp. However, for installations larger than 4 MWp it becomes advantageous to use a larger storage unit. This can be attributed to the fact that at these large capacities the peak PV power exceeds the total demand even during peak period thus a larger storage unit allows for the system to make better use of the PV energy – storing the energy at times when available PV power exceeds demand and supplying energy when demand exceeds the available PV power.

The total cost of the system (demand charge + consumption charge + initial costs) of the system using the proposed dispatch method is shown in Figure 4. The optimal PV and storage capacity (in terms of the NPV) can be determined from this plot at the point giving the lowest NPV. This occurs at a storage size of 1 MWh and PV capacity of 550 kWp. However, it should be noted that at the current prices, the difference in 20 year NPV for the optimal system and a system without any storage or PV is rather small – the optimal system is only 1.35% cheaper (R 5m) than the system without these components. However, this saving will increase as the capital prices of the PV and storage unit decrease, making the consideration of optimal sizing of the system even more important in the future as technology prices continue to decline.

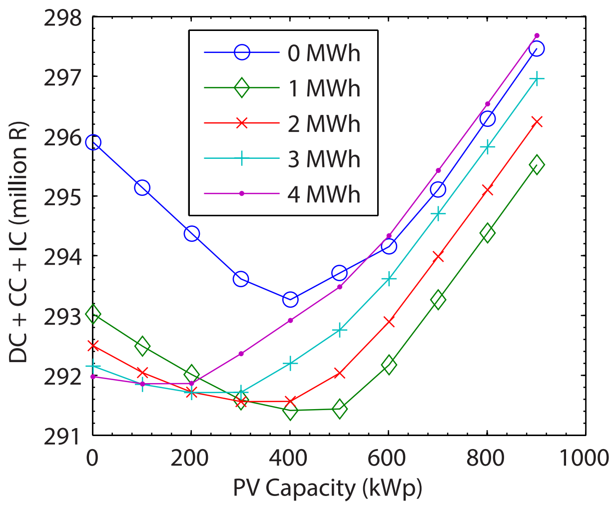

Figure 4: Total cost over a 20 year period.

In the next section, the full optimisation is carried out to investigate the optimal PV and storage sizings. The effect of a decrease in the PV capital cost and the savings produced by the optimal system configuration are also investigated.

A. *Optimisation of PV and storage size*

This section investigates the nature of the optimal storage and PV sizes obtained for the Wits load which minimise the 20 year NPV of the system. First, the optimal storage size is determined assuming various fixed PV capacities. This result is shown in Figure 5. At low PV capacities, it is optimal to include a large storage device in the system to help reduce the maximum demand charge. At PV capacities greater than 4 MWp, it is again optimal to use a larger storage capacity to store energy when the PV supply exceeds demand and release it at times of lower PV availability. This agrees with the trend observed in Figure 4b where it was seen that at PV capacities greater than 4 MWp, the demand charge is reduced through the use of a larger storage unit. As the price of the storage increases, the optimal storage size decreases over all PV capacities. However, even at R2880/kWh, it is still optimal to include some storage (0.1 MWh) in the system.

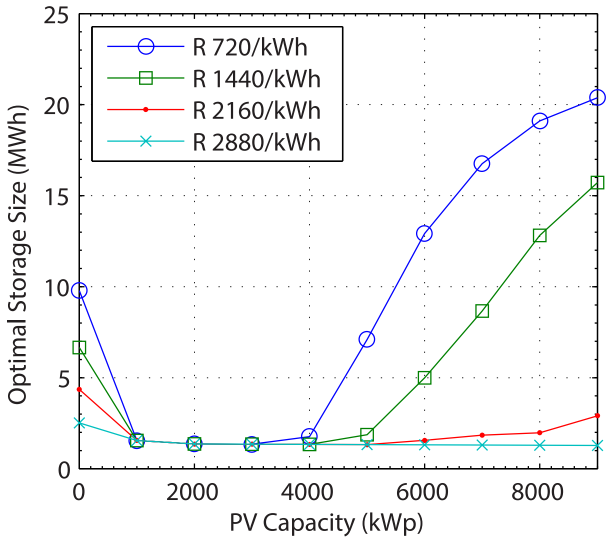

Figure 5: Optimal storage size for various PV capacities.

In Figure 4 it was seen that the cost of the optimal system at current PV prices (R 51077/kWp) is not significantly less than using the grid-only to supply the demand. However, PV prices are likely to continue their drastic decline in the future and the PV price has a significant effect on the savings produced by the optimal system. Table II shows the savings produced by the optimal system configurations for various PV prices. The table also shows the saving that would be produced using the optimal PV capacity but with no storage unit and using the optimal storage capacity but with no PV. For each configuration, the savings obtained using no storage unit are significantly less than those using the optimal capacities. It should be noted that these results were calculated using a storage price of R 720/kWh, which is rather low compared to batteries but is the expected market price for pumped heat electricity storage units. Because the optimal scheduling of the devices take into account the demand charge as well as the consumption charge, savings are still achieved using a storage unit only. However, these are again significantly less than using both PV and storage.

Table II: Cost of the optimal system compared to a system with no storage and a system using the grid only.

PV Price (R/kWp)	PV (kWp)	Storage (MWh)	Saving compared to grid only (%)	Saving with no storage (%)	Saving with no PV (%)
51077.00	0	9.800	4.94	0	4.94
45969.30	0	9.800	4.94	0	4.94
40861.60	0	9.800	4.94	0	4.94
35753.90	114	8.593	4.97	0.53	4.75
30646.20	751	2.300	5.57	1.99	2.69
25538.50	810	1.837	6.74	3.05	2.39
20430.80	3250	1.349	9.26	5.24	2.07
15323.10	4128	2.364	14.62	10.13	2.73
10215.40	6313	14.387	22.10	14.53	3.99
5107.70	9115	20.522	32.83	22.31	2.73

VII. Conclusions

In this work a optimisation model was described to find the optimal storage and PV sizing in a grid-connected PV-diesel-storage system. A general tariff structure consisting of a consumption charge and a demand charge was considered and the optimisation carried out in terms of the 20 year NPV of the system. The storage and generator schedules were included in the objective function, allowing the optimal sizing to be studied with respect to an optimal dispatch strategy.

It has been shown that larger PV and storage sizes typically lead to reduced demand and consumption charges over the lifetime of the system and, when combined with the initial costs of these units it becomes important to find the optimal capacities. From the simulations, it is clear that the size of the storage unit has a greater effect on the demand charge at low PV capacities, and has a larger effect on the consumption charge at high PV capacities.

Thus, in terms of optimal sizing, the results indicate that the demand charge justifies the installation of a larger storage size for low PV capacities ($\leq$ 400 kWp) to allow the system to effectively shave the peak demand. Similarly, at large PV capacities ($\geq$ 4 MWp) a larger storage size is again favoured –this time to help reduce the consumption charge. At medium PV capacities, the storage size does not significantly influence the optimality of the system, however, some storage is still needed to effectively reduce the maximum demand.

In terms of PV capacity, it has been shown that the optimal configuration only includes PV at a nominal PV price less than R 35753.90 per kWp. Due to the storage unit's ability to reduce maximum demand and shift load and the low PHES unit price of R 720/kWh, some storage capacity is an essential component in the optimal system.

VIII. Future Work and Improvements

Future work should focus on further investigation on the optimal storage and PV size for other load profiles and tariff rates.

References

[1] B. Borowy and Z. Salameh, "Methodology for optimally sizing the combination of a battery bank and PV array in a wind/PV hybrid system," *IEEE Transactions on Energy Conversion*, vol. 11, no. 2, pp. 367–375, 1996.

[2] G. Tina, S. Gagliano, and S. Raiti, "Hybrid solar/wind power system probabilistic modelling for long-term performance assessment," *Solar Energy*, vol. 80, no. 5, pp. 578–588, 2006.

[3] A. Kornelakis and E. Koutroulis, "Methodology for the design optimisation and the economic analysis of grid-connected photovoltaic systems," *IET Renewable Power Generation*, vol. 3, no. 4, pp. 476–492, 2009.

[4] H. Yang, W. Zhou, L. Lu, and Z. Fang, "Optimal sizing method for stand-alone hybrid solar–wind system with lpsp technology by using genetic algorithm," *Solar energy*, vol. 82, no. 4, pp. 354–367, 2008.

[5] G. Seeling-Hochmuth, "Optimisation of Hybrid Energy Systems Sizing and Control," Ph.D. dissertation, University of Kassel, 1998.

[6] A. Al-Shamma'a and K. Addoweesh, "Optimum sizing of hybrid PV/wind/battery/diesel system considering wind turbine parameters using genetic algorithm," in *Power and Energy (PECon), 2012 IEEE International Conference on*, 2012, pp. 121–126.

[7] R. Atia and N. Yamada, "Optimization of a PV-wind-diesel system using a hybrid genetic algorithm," in *Electrical Power and Energy Conference (EPEC), 2012 IEEE*, 2012, pp. 80–85.

[8] B. Bilal, V. Sambou, P. Ndiaye, C. Kebe, and M. Ndongo, "Multi-objective design of PV-wind-batteries hybrid systems by minimizing the annualized cost system and the loss of power supply probability (lpsp)," in *Industrial Technology (ICIT), 2013 IEEE International Conference on*, 2013, pp. 861–868.

[9] A. Shahirinia, S. Tafreshi, A. Gastaj, and A. Moghaddomjoo, "Optimal sizing of hybrid power system using genetic algorithm," in *Future Power Systems, 2005 International Conference on*, 2005.

[10] I. Tegani, A. Aboubou, M. Becherif, M. Ayad, O. Kraa, M. Bahri, and O. Akhrif, "Optimal sizing study of hybrid wind/PV/diesel power generation unit using genetic algorithm," in *Power Engineering, Energy and Electrical Drives (POWERENG), 2013 Fourth International Conference on*, 2013, pp. 134–140.

[11] N. Tutkun and E. San, "Optimal power scheduling of an off-grid renewable hybrid system used for heating and lighting in a typical residential house," in *Environment and Electrical Engineering (EEEIC), 2013 13th International Conference on*, 2013, pp. 352–355.

[12] H. Xiaoyu, S. Qiuye, Z. Huaguang, and W. Zhan, "Multi-objective optimal design of wind/PV/pumped-storage system based on ga," in *Power and Energy Engineering Conference (APPEEC), 2012 Asia-Pacific*, 2012, pp. 1–4.

[13] S. Pourmousavi, M. Nehrir, C. Colson, and C. Wang, "Real-time energy management of a stand-alone hybrid wind-microturbine energy system using particle swarm optimization," *Sustainable Energy, IEEE Transactions on*, vol. 1, no. 3, pp. 193–201, Oct 2010.

[14] J. Wang and F. Yang, "Optimal capacity allocation of standalone wind/solar/battery hybrid power system based on improved particle swarm optimisation algorithm," *Renewable Power Generation, IET*, vol. 7, no. 5, pp. 443–448, Sept 2013.

[15] W. S. Tan, M. Hassan, H. Rahman, M. Abdullah, and F. Hussin, "Multi-distributed generation planning using hybrid particle swarm optimisation-gravitational search algorithm including voltage rise issue," *Generation, Transmission Distribution, IET*, vol. 7, no. 9, pp. 929–942, Sept 2013.

[16] S. Kahrobaee, S. Asgarpoor, and W. Qiao, "Optimum sizing of distributed generation and storage capacity in smart households," *Smart Grid, IEEE Transactions on*, vol. 4, no. 4, pp. 1791–1801, Dec 2013.

[17] C. Fung, S. Ho, and C. Nayar, "Optimisation of a hybrid energy system using simulated annealing technique," in *TENCON '93. Proceedings. Computer, Communication, Control and Power Engineering.1993 IEEE Region 10 Conference on*, no. 0, 1993, pp. 235–238.

[18] Y. Katsigiannis, P. Georgilakis, and E. Karapidakis, "Hybrid simulated annealing–tabu search method for optimal sizing of autonomous power systems with renewables," *IEEE Transactions on Sustainable Energy*, vol. 3, no. 3, pp. 330–338, 2012.

[19] S. Boyd, *Convex Optimization*. Cambridge University Press, 2004.

[20] M. Grant and S. Boyd, "CVX: Matlab software for disciplined convex programming, version 2.1," http://cvxr.com/cvx, Mar. 2014.

Chapter 7

Case Study

A functional method for optimally scheduling the storage and generator of a grid-connected PV-diesel-storage hybrid energy system taking into consideration demand and consumption charges has been developed in the preceding chapters. A method to optimally size the PV and storage unit was also developed. In this chapter, the presented dispatch and sizing method is applied to a simple case study to demonstrate how it assists in the optimal integration of the hybrid components by minimising the total energy drawn from the grid, the fuel used by the generator and the peak energy requested from the grid on a day-to-day basis. To demonstrate how the model addresses some of the shortcomings of existing approaches, comparisons are drawn to what can be achieved with the load-following dispatch strategy (as implemented in the HOMER package) and the advantages (and need) for the developed dispatch strategy and sizing method are demonstrated.

The case study describes a typical urban application with the user being a institution situated on a large campus – in particular, the West Campus of the University of the Witwatersrand. The campus is situated in an area that receives high solar radiation. The load data are sourced from meters on the campus.

The case study uses the costs in Table 7.1 as estimates of current component prices and specifications as a baseline for the results obtained.

The West campus (see Figure 7.1) has about $65000m^2$ of rooftop area available, which, for the purposes of this demonstration, is assumed to be able to support the renewable capacity installed on top of it. The renewable capacity is assumed to be limited by the energy density of the wind turbines and PV panels which is given in Table 7.2. The capacity of the diesel generator is assumed to be fixed at 1 MW.

The specific type of storage unit used for the case study is a PHES unit.

Table 7.1: Prices used for the Hybrid Energy System Components in the case study

Photovoltaic panels Capital cost: R 51077.00 per kWp, Maintenance cost: R 0, Energy Density: 175 W/m^2
Storage (PHES Unit) Capacity: R366 per MWh
Diesel generator Capacity: 1 MW (fixed), Fuel: 0.4 L/kWh (R 13 per L)

Table 7.2: Additional details for the case study

Project details Interest rate: 8% pa, Component lifetime: 20 years Active energy charge: R 0.55 per kWh, maximum demand charge: R 172.12 per kW
Solar radiation data Mean: 248 W/m^2

Figure 7.1: Map of the Wits campus with the potential hybrid energy system components. [Adapted from: OpenStreetmap.org]

7.1 PHES Model

The specific storage device considered in this dissertation is a Pumped Thermal Energy Storage system. A simple description is provided here for the reader who is not familiar with such a device.

PHES is a relatively new type of storage based on mature and well-known heat transfer technology. The operation of a Rankine-cycle based PHES system is illustrated in Figure 7.2. The discharge process follows the forward Rankine cycle. The fluid, as a liquid, is

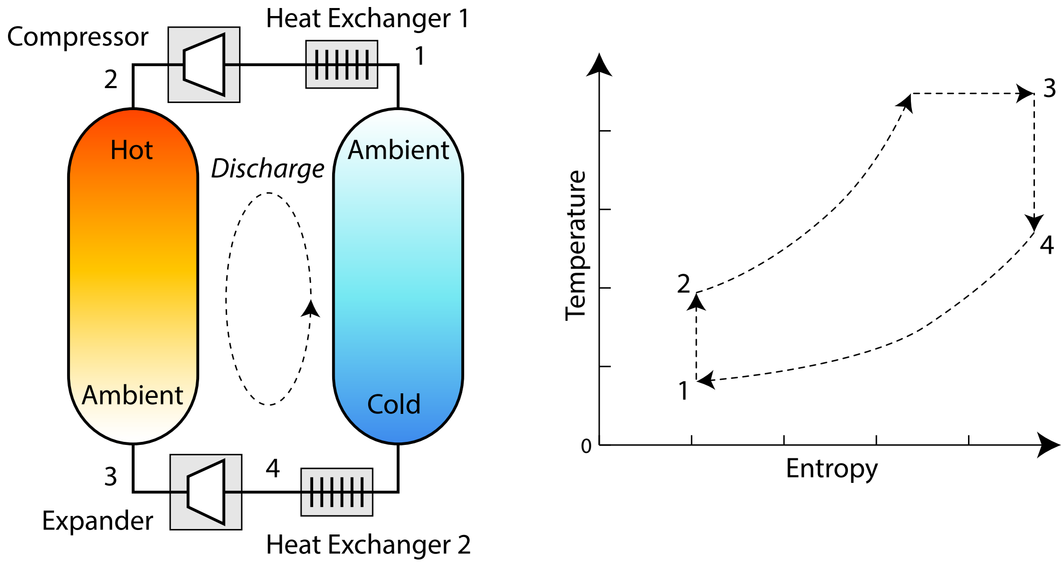

FIGURE 7.2: Diagram illustrating the operation of a PTES based on the Rankine cycle. Adapted from [47]

pumped from low to high pressure (1 to 2 - an isentropic process). It then enters a hot storage tank where it is heated under constant pressure until it vaporises (2 to 3 - an isobaric process). The fluid then undergoes expansion by being passed through a turbine (3 to 4 - another isentropic process) and finally enters the cold storage tank where it is cooled to form a liquid (4 to 1 - again an isobaric process). During charging, this process is reversed. It has been shown that a Brayton-cycle PHES with a high temperature ratio in each storage reservoir can achieve theoretical round-trip efficiencies in excess of 90% [47]. Practical units have round-trip efficiencies of $72 - 80\%$.

An approximate model is used for the simulation. This model has been derived empirically, but its derivation is beyond the scope of this dissertation. For details on modelling of a PHES unit see [47]. The model takes into account the round trip efficiency of the actual device as well as the non-linearities associated with its physical operation.

The effective thermal energy stored during charging (η_c) of the device by $P_{In}(t)$ kW of electrical power is given by

$$\eta_c = 0.0143 \times \ln(\mathbf{P_s^+}(t)) + 0.87, \tag{7.1}$$

and the total thermal energy stored is

$$\Delta E_{tes} = \eta_c \mathbf{P_s^+}(t) \Delta t, \tag{7.2}$$

and during discharging, the effective thermal energy removed to supply (η_d) is given by

$$\eta_d = 0.0026 \times \ln(abs(\mathbf{P}_\mathbf{s}^-(t))) + 0.697, \tag{7.3}$$

and the total thermal energy removed is

$$\Delta E_{tes} = \frac{\mathbf{P}_\mathbf{s}^-(t)}{\eta_d}\Delta t. \tag{7.4}$$

From these equations, it is evident that the PHES system has a highly non-linear behaviour in terms of energy storage efficiency which depends on the power being supplied or withdrawn from the system. However, as the system will be operated at rather high power levels, the input-output characteristics behave approximately linearly. This phenomenon is shown in Figure 7.3 which shows the thermal energy stored during charge (green) and the thermal energy released during discharge (red).

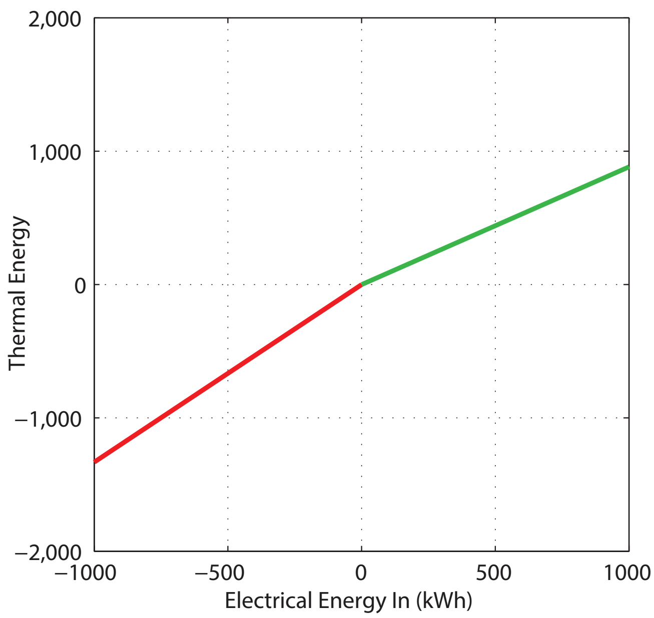

FIGURE 7.3: Thermal energy stored for electrical power supplied.

A linear fit can be used to give the following approximate storage efficiencies:

$$\eta_c \approx 0.9 \tag{7.5}$$

and

$$\eta_d \approx 0.71. \tag{7.6}$$

Algorithm 1 Simulation model of the Alstom PHES storage device.

Algorithm 7.1.1: PHES(Pin)

$charge \leftarrow 1$
$discharge \leftarrow 0$
for $t \leftarrow 1$ **to** $length(Pin) - 1$
  do if $Pin(t) >= 0$
  then $charge$
  else if $Pin(t) < 0$
  then $discharge$
$POut(t) \leftarrow Pin(t)$
if $(charge)$

$$\textbf{then} \begin{cases} \textbf{if } Pin(t) < Pmin \\ \quad \textbf{then } POut(t) \leftarrow 0 \\ \quad \textbf{else if } Pin(t) > Pmax \\ \quad \textbf{then } POut(t) \leftarrow Pmax \textbf{if } (abs(POut(t)) > 0) \\ \quad \textbf{then } \begin{cases} effCharge \leftarrow 0.0143 \times log(POut(t)) + 0.87 \\ Pth = (POut(t) \times effCharge) \\ Etes(t+1) \leftarrow Etes(t) + Pth \times deltat \end{cases} \\ \textbf{if } Etes(t) > Emax \\ \quad \textbf{then } \begin{cases} POut(t) \leftarrow 0 \\ Etes(t+1) \leftarrow Etes(t) \end{cases} \end{cases}$$

else if $(discharge)$

$$\textbf{then} \begin{cases} \textbf{if } abs(Pin(t)) < Pmin \\ \quad \textbf{then } POut(t) \leftarrow 0 \\ \quad \textbf{else if } abs(Pin(t)) > Pmax \\ \quad \textbf{then } POut(t) \leftarrow -Pmax \textbf{if } abs(POut(t)) > 0 \\ \quad \textbf{then } \begin{cases} effDischarge \leftarrow 0.0026 \times log(abs(POut(t))) + 0.697 \\ Pth \leftarrow (-POut(t)/effDischarge) \\ Etes(t+1) \leftarrow Etes(t) - Pth \times deltat \end{cases} \\ \textbf{if } Etes(t) < Emin \\ \quad \textbf{then } \begin{cases} POut(t) \leftarrow 0 \\ Etes(t+1) \leftarrow Etes(t) \end{cases} \end{cases}$$

7.2 Testing methodology

The methodology used to apply the developed method to the case study is now presented. The methodology gives a more detailed overview of what data are used with the design method and how it functions as a design tool to aid in the design process for PV-Diesel-Storage hybrid energy system where maximum demand plays a significant role.

Firstly, the appropriate data are collected, this includes:

1. A 365 day load profile

2. A 365 day solar radiation time series for the area under consideration

As mentioned, the dispatch strategy can be used to investigate the maximum demand reduction capabilities of the storage device. This is done as follows:

1. The storage device is scheduled using the algorithm in Chapter 5. This produces the desired storage dispatch signal.
2. The dispatch signal is applied to the storage model which gives an indication of the actual power supplied by the device.
3. The peak reduction achieved is recorded.
4. The process is repeated for all storage capacities and powers being considered.

This gives an idea as to the maximum demand reduction that can realistically be achieved for various storage capacities and peak power outputs.

To investigate the full optimal storage and generator dispatch and component sizing:

1. The unified objective function in Chapter 6 is solved using SeDuMi or equivalent convex solver.
2. The solution produces the optimal renewable capacities, the storage and generator schedule

In the next section, the results obtained by applying this methodology to the simplified design case for the West Campus of the University of the Witwatersrand are given.

7.2.1 HOMER: A basis for comparison

HOMER is a software package designed at the National Renewable Energy Laboratory to facilitate the design of hybrid renewable energy systems [48]. The package allows the user to simulate various dispatch strategies and optimise the sizing of renewable components [48]. Due to its similarity with the methods developed in this dissertation, it is chosen as a basis for comparison.

HOMER's simulation model is based on a time-domain simulation run at the energy-flow level with discrete time-steps of 1 hour to determine the NPV for a chosen configuration over a specified project lifetime. HOMER uses a discrete combinatorial optimization approach to select the optimal system configuration. This means that it searches every possible combination and chooses the one with lowest cost as optimal. An advantage of this approach is that it will give a globally optimal solution (in terms of the simulated

Table 7.3: Table comparing the optimization model presented in this paper to HOMER

Feature	HOMER	Proposed method
Optimisation method	Combinatorial	Convex optimisation
Costs	No maximum demand	Includes maximum demand
Storage dispatch	Load-following	Predictive
Generator dispatch	Load-following	Predictive

configurations) and thus provides a good basis for comparison to the convex optimisation method proposed in this dissertation (which also finds a globally optimal solution).

However, there are a number of key differences between the HOMER model and that developed in this dissertation which makes the comparison somewhat more complicated and some assumptions have to be made.

These differences, as well as how they are addressed to give a fair means of comparison are addressed as follows:

- First, the component sizes have to be specified in discrete values and thus have been chosen carefully (i.e. with high enough granularity) so the HOMER solution is not restricted
- The selection of storage devices in HOMER does not include the type addressed in the case study (pumped thermal storage). However, one of the existing types may be used as a substitute and thus as a means of comparison the PHES is substituted for a battery model in the HOMER results. To this extent HOMER models a battery as a device with a fixed round trip efficiency, bounded peak charge/discharge capacity and bounded total storage capacity. To do this it uses the "kinetic energy model" which is specified by the aforementioned three parameters. However, these parameters cannot be set explicitly. To determine them, it finds a best-fit-curve for a specific battery's (Ah-A) capacity curve and derives the model parameters from this fit. The PHES unit has a very long life-span and thus negligible operating cost.
- maximum demand cannot be included in HOMER's cost model. Therefore, all cost comparisons here have been done by extracting the relevant data from HOMER and using the same costing model as that for the developed method.

7.3 Simulation Results

7.3.1 Storage-Only

This section investigates the effect that the sizing of the storage device can have on reducing the maximum demand, independently of the other components.

The proposed scheduling algorithm can also be used as a design tool to give a basic guideline as to the capacity and peak power output specifications. Figure 7.4 was generated by explicitly varying the maximum power and capacity values used in the simulation. The achieved peak reduction was then plotted against these values. The result of performing such an analysis is shown in Figure 7.4 which gives the fraction of fraction of peak reduction achieved for the Wits demand profile (in terms of ideal load levelling). By inspecting the graph, it is evident that for a storage capacity less than 100 kWh, little or no peak reduction can be achieved. Similarly, maximum power outputs of less than 10 kW leads to very little peak reduction. On the other end of the spectrum, at capacities greater than 1 MWh, the graph begins to taper off suggesting that capacities greater than this value are never worth the investment. From the figure it can be concluded that, in terms of peak reduction, power output is more important than storage capacity, however capacity also has an effect on the efficacy of the storage device. At capacities greater than 1.75 MWh, and storage powers greater than 2.4 MW, severe diminishing returns are experienced and thus there is no need for such high storage specifications.

Figure 7.5 shows a sample predictive dispatch strategy over a 14 day period determined by the unified convex optimisation model where the diesel fuel price has been adjusted to 0.4× the nominal price to illustrate the detailed, interdependent operation of the generator and storage device. The top sub-figure shows that the dispatch strategy functions as expected and achieves the first objective of the hybrid energy system – to minimise the maximum demand as seen by the grid. To this the net demand is levelled in a (near) ideal manner by the combined operation of the generator and storage. From the bottom sub-figure it is clear that the second objective of the system is also adhered to which is to reduce the aggregate costs of the system. For example, the diesel generator is used in a very frugal manner, operating at only peak periods in order to reduce the total quantity of fuel consumed. What is interesting to note is that in most cases the storage device discharges fully and then starts to peak capacity immediately before the next peak. In periods when a peak is not close by (such as in hours 0-25, 175-200 and 310-350 in Figure 7.5), it remains at around 50% of its capacity – increasing its power draw only when a peak in demand is imminent.

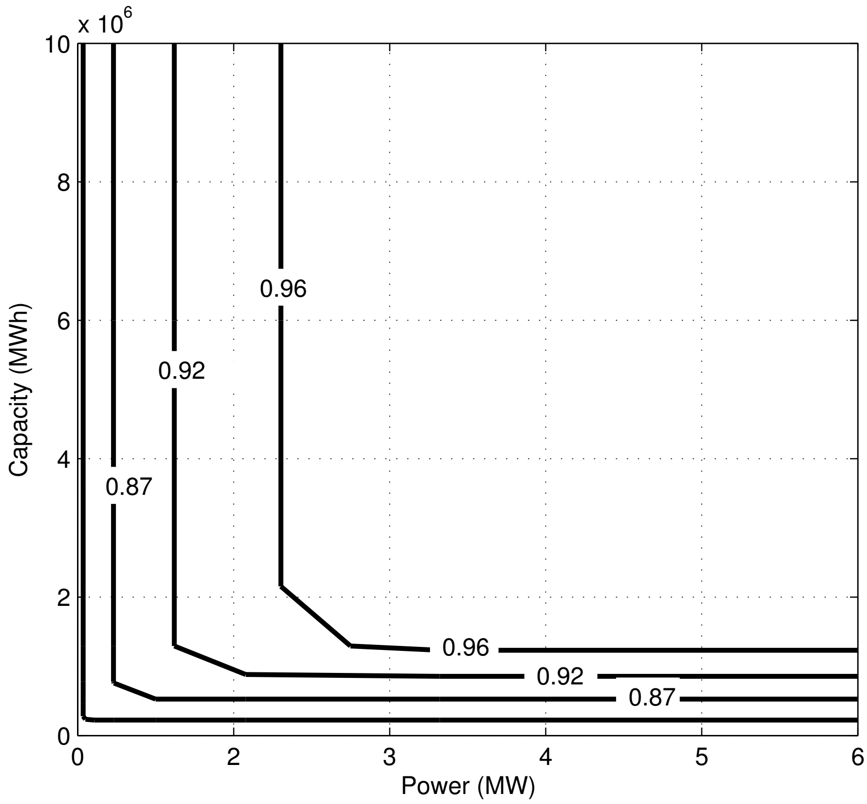

FIGURE 7.4: Net peak grid usage as a function of storage capacity and power.

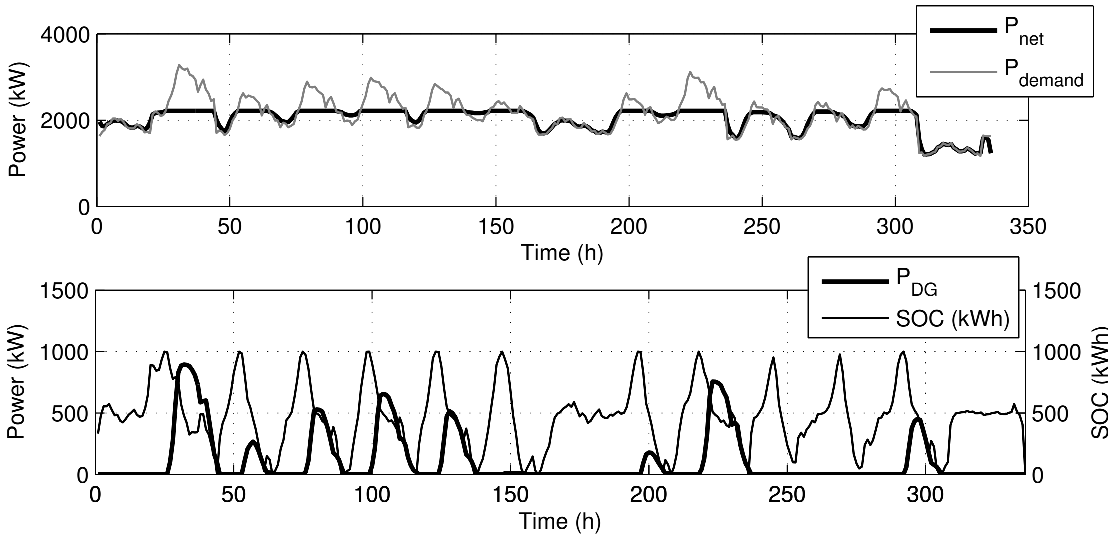

FIGURE 7.5: Example of the results for the predictive dispatch strategy obtained using the unified convex method. Storage capacity = 1000 kWh, Storage power = 1000 kW, Diesel generator = 1000 kW, fuel price = 0.4× nominal

Next, the effect of a smaller storage capacity is investigated. This case is shown in Figure 7.6 where the storage capacity has been reduced to 200 kWh while keeping the peak storage power at 1000 kW. As expected, the diesel generator utilisation remains the same but becomes noticeably less "smooth" due to the decreased storage capacity.

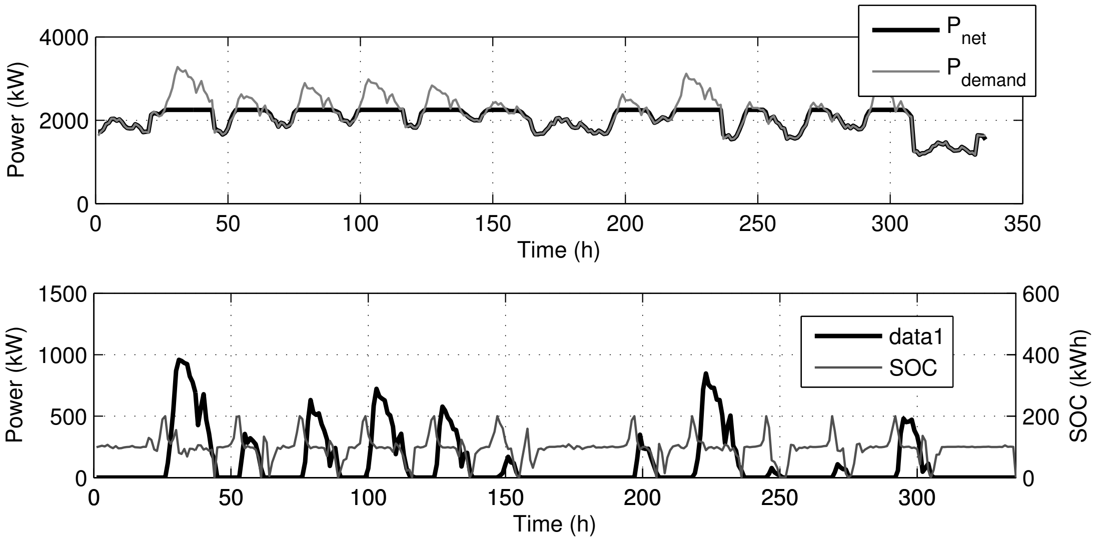

FIGURE 7.6: Example of the results for the predictive dispatch strategy obtained using the unified convex method. Storage capacity = 200 kWh, Storage power = 1000 kW, Diesel generator = 1000 kW, fuel price = 0.4× nominal.

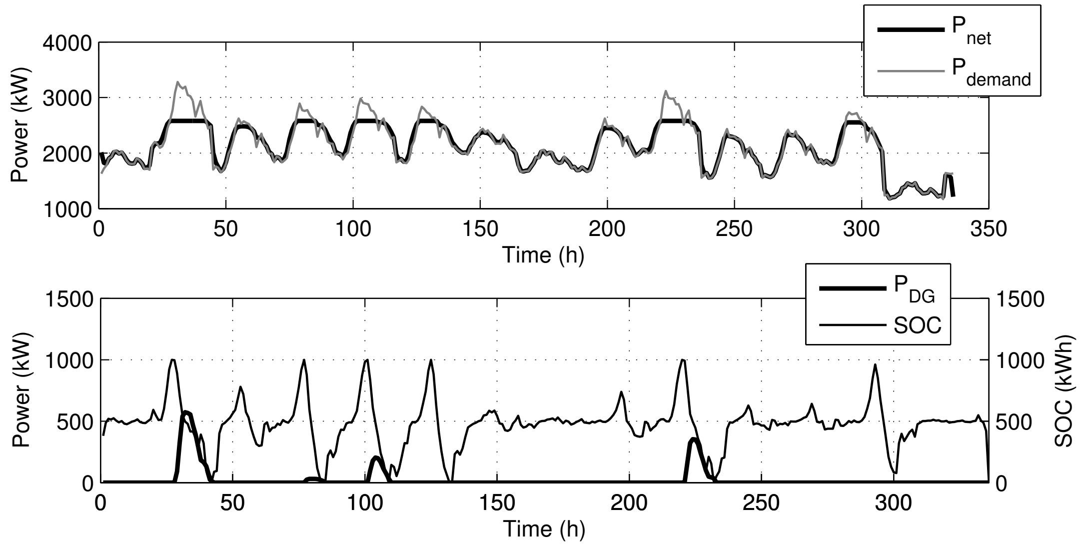

FIGURE 7.7: Example of the results for the predictive dispatch strategy obtained using the unified convex method. Storage capacity = 1000 kWh, Storage power = 1000 kW, Diesel generator = 1000 kW, fuel price = 0.8× nominal

Likewise, the storage schedule becomes more peaked with the storage charging and discharging over a shorter period during times of maximum demand.The peak reduction capability of the system is not hampered to any great extent – mainly due to the generator still being able to cover the maximum demand at an economical rate.

Figure 7.7 shows what happens when the fuel price is increased to 0.8× the reference value, again with a storage capacity of 1000 kWh. The generator utilisation drops as it is no longer as economical to cover peaks with the diesel fuel. The storage also exhibits interesting behaviour. Compare, for example, what happens with the storage at around day 7 in Figure 7.5 with that which happens at the same time in Figure 7.7. In Figure 7.5 the storage discharges which successfully reduces the maximum demand of the day. In Figure 7.7, however, the storage as doing so would have no benefit – the generator did not assist in reducing the peak the previous day and thus the storage (with its limited peak power output) cannot reduce the peak during this day and thus it remains inactive.

For all the previous configurations, no PV was present in the optimal solution. This is understandable, as from Figure 7.12, PV only becomes cost effective at around 0.6× the current price. To investigate the system operation when a renewable source is included, the PV price is lowered to 0.5× the reference. This result is shown in Figure 7.8. The optimal PV capacity suggested by the system is 2098 kWp and the effect of the PV integration on the net demand can clearly be seen in the upper sub-figure. The storage is now utilised to a much smaller extent – assisting in peak reduction only before the PV power output peaks.

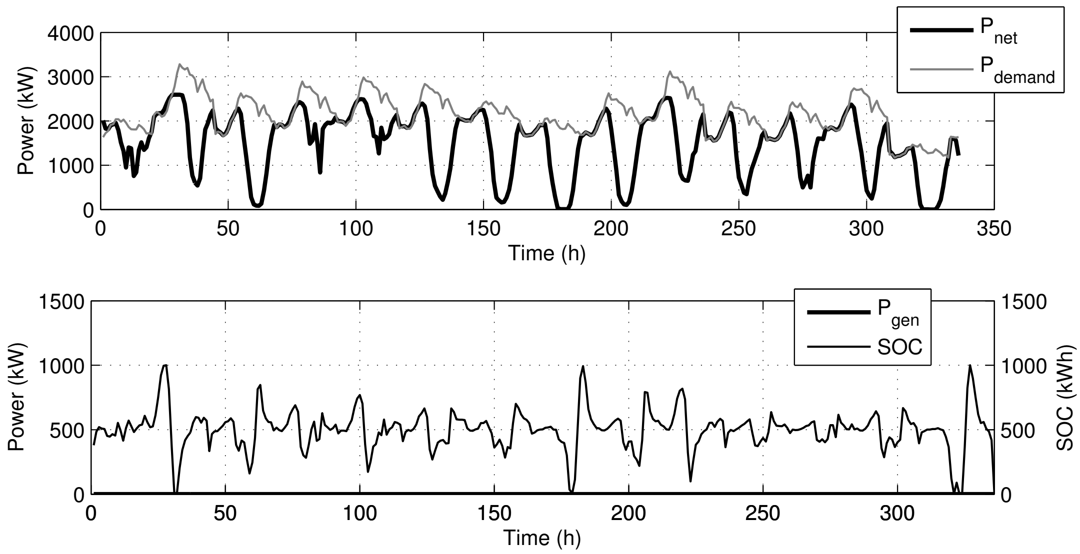

FIGURE 7.8: Example of the results for the predictive dispatch strategy obtained using the unified convex method. Storage capacity = 1000 kWh, Storage power = 1000 kW, Diesel generator = 1000 kW, PV price = 0.5× reference

The monthly variation in the stored energy as determined by the predictive dispatch is shown in Figure 7.9, along with the variation in the power supplied by the diesel generator. The diesel generation generally peaks following a complete discharge of the storage device. Not surprisingly, this occurs around the time of maximum demand (around 12h00). The highly dependent behaviour of the storage and generator is clearly evident – the generator's power output only peaks after the storage has fully discharged. This indicates how they are working together to flatten a peak of longer duration than could be handled by the storage alone.

Furthermore, the storage discharge is perfectly scheduled so that it discharges at a rate to allow it to cover the entire peak. This is especially important when the capacity of the device is limited. Notice also how the generator is never active when the storage device is accumulating energy (around 14h00 to 20h00). This shows that using the grid energy to charge is cheaper than running the generator for this case. The storage device is also not really utilised during the evening (18h00 to 24h00).

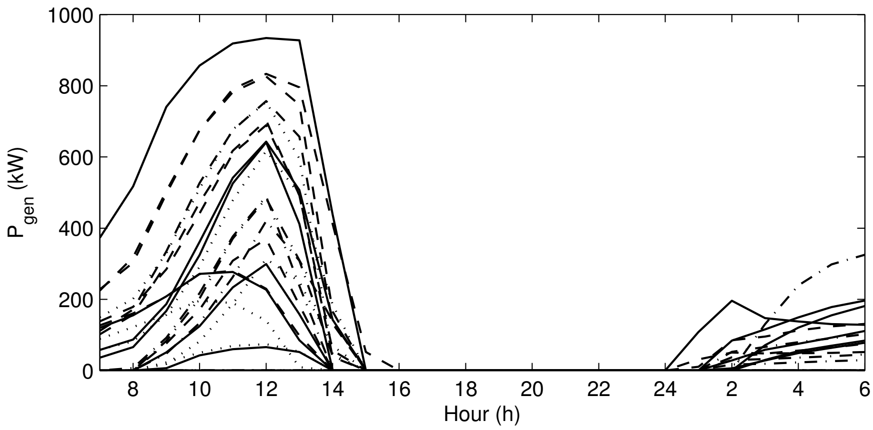

(a) Diesel generator

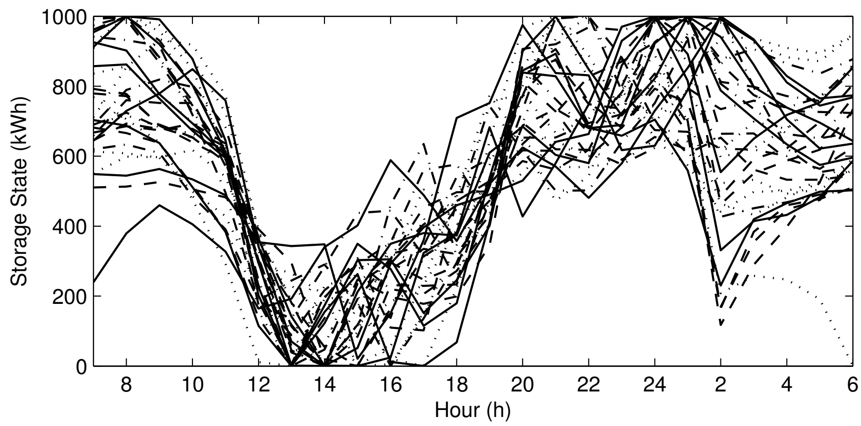

(b) Storage

Figure 7.9: Annual variation in the stored energy and the diesel generation, as determined by the predictive dispatch strategy.

Figure 7.10 provides a comparison between the load-following dispatch strategy (obtained using HOMER) and the predictive dispatch method developed in this dissertation. From the figure it is clear that the predictive dispatch strategy results in much greater utilisation of the storage unit than the load-following dispatch strategy. The load-following strategy only charges when there is excess energy available from the PV and discharges as soon as the renewable energy drops as it sees the storage energy as "cheaper" than sourcing energy from the grid. The proposed predictive dispatch strategy carefully manages the charge and discharge of the storage device throughout the day to level the net load. Pumped heat electricity storage, the preferred storage means in the Wits case, does not have any depth-of-discharge or cycling limits and therefore the optimal strategy is the better choice in this respect.

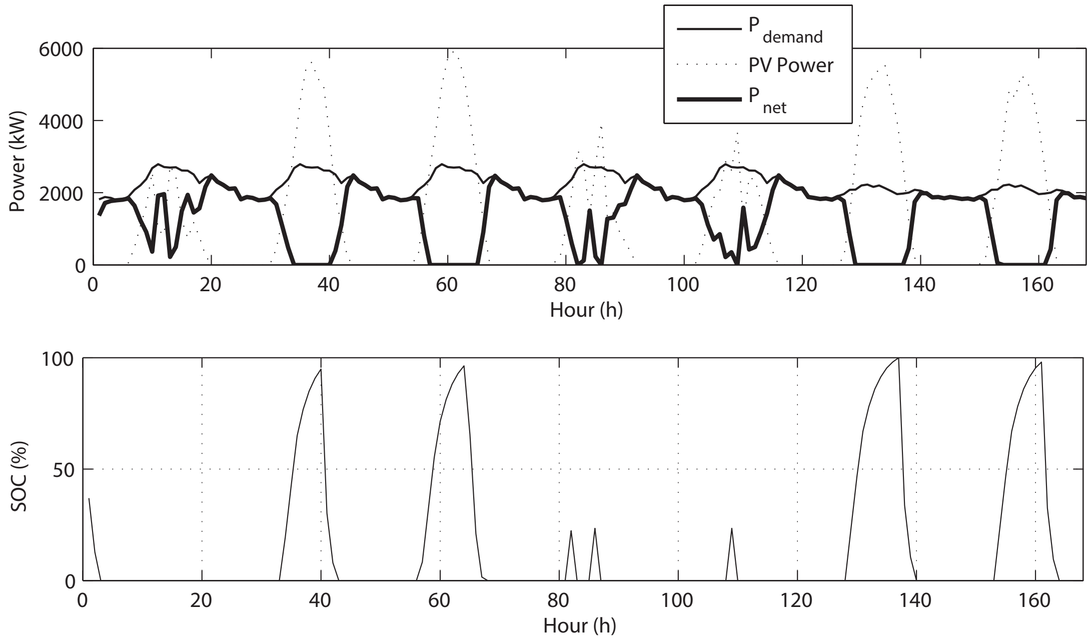

(a) The load-following dispatch strategy in HOMER

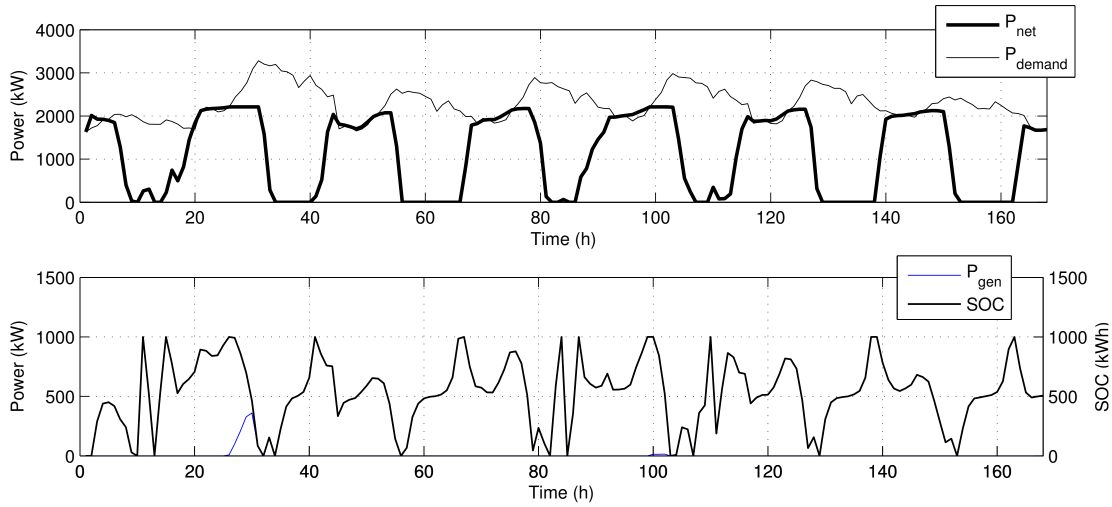

(b) Optimal Strategy presented in this dissertation

FIGURE 7.10: Comparison between the load-following dispatch strategy (as implemented in HOMER) and the optimal strategy proposed in this dissertation.

7.3.2 System Cost Comparison

Table 7.4 compares the monthly maximum demand of 3 different optimal configurations, using the the method proposed in this dissertation and the load-following dispatch

Table 7.4: Monthly maximum demand of system using load-following dispatch vs. the predictive dispatch developed in this dissertation.

PV capacity	100	500	900
Predictive Dispatch Method	R 34114.02	R 33136.54	R 32248.92
Load-Following Dispatch (HOMER)	R 34516.16	R 34516.16	R 34516.16
No storage	R 38648.62	R 38648.62	R 38648.62

method. The maximum demand using the predictive dispatch is significantly less than a system run using the load-following dispatch for all the tested PV prices as it is able to better manage the energy to reduce maximum demand.

This is shown more clearly in Figure 7.11 which gives a 48 hour comparison of the two systems. Note how the optimal strategy uses the load prediction to intelligently level the load – at hour 28 it charges by drawing energy from the grid and 35 discharges to level the peak before the PV supply peaks.

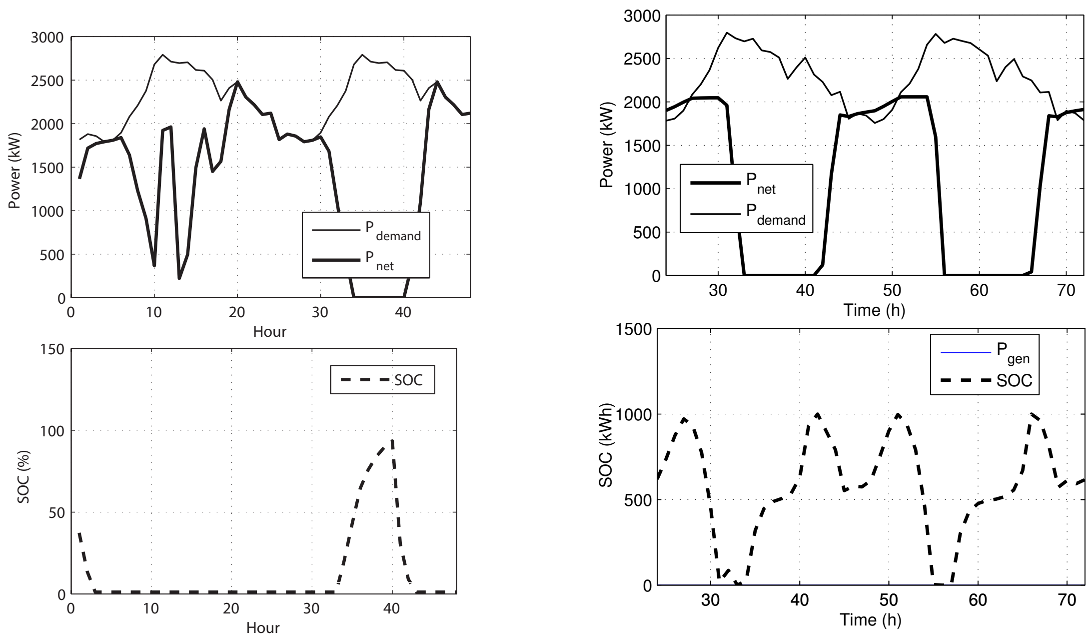

(a) Load-following dispatch strategy (HOMER) (b) Optimal Strategy

Figure 7.11: Two-day comparison between the load-following dispatch strategy (as implemented in HOMER) and the optimal strategy proposed in this dissertation.

7.3.3 PV Sizing Comparison

Figure 7.12 shows the optimal PV configurations suggested by the HOMER software package and those obtained for the optimal sizing using the integrated predictive dispatch strategy developed in this dissertation. As the HOMER model does not take into

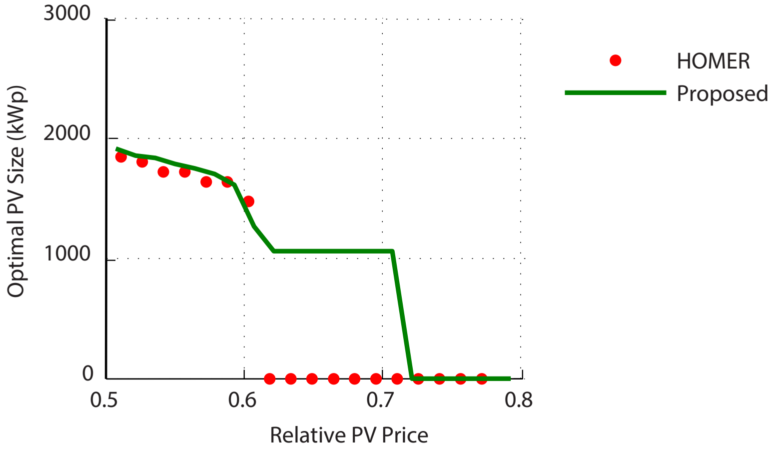

Figure 7.12: Comparison between optimal PV configuration obtained using HOMER and using the sizing method presented in this dissertation. The PV price is relative to the current price of R 51077 per kWp.

account maximum demand, results are also reported for a modified convex objective function with the maximum demand removed.

The optimal configurations differ slightly. The key difference is that the HOMER solution uses the simple load-following strategy for dispatching the generator and storage which (as has been shown) results in higher operational costs. The HOMER solution, using the load-following method to dispatch the components, suggests that a PV solution becomes feasible at around 0.6× the current price (R 51077 per kWp) at an interest rate of 8% p.a. and a project lifetime of 20 years. The sizing for the proposed optimal dispatch method shows that PV becomes feasible at a slightly higher price point (0.7× current) as this extra investment is justified by the reduction in operational charge that is achieved.

Chapter 8

Conclusion

In this dissertation a a predictive optimal dispatch and optimal sizing method for a grid-connected PV-diesel-storage system was developed to reduce the lifetime cost of the system. The required demand prediction algorithm to enable the practical implementation of the dispatch strategy was also presented.

In terms of the dispatch, a convex optimisation model was proposed which simultaneously determines the optimal dispatch strategy for the generator and storage device. It has been shown that, using this strategy, the storage device and generator can be scheduled to reliably reduce maximum demand and consumption charges. Furthermore, the simulations using the Wits load data illustrate that the proposed dispatch method achieves greater reductions in consumption and demand charges compared to a basic threshold dispatch strategy.

It has also been shown that larger storage and PV capacities allow for a greater overall reduction in the operational costs of the system. However, increasing the capacities of these components leads to higher initial costs which can easily offset the savings achieved in operational costs. The proposed optimal sizing method seeks to balance the savings in operational costs with the initial costs of the components, thereby ensuring the operational strategy is economically beneficial over the lifetime of the system. The simulations show that larger storage unit capacities are justified for small PV capacities to assist in peak shaving for demand charge reduction and for large PV capacities to assist in load-shifting for consumption charge reduction.

In the case study using the Wits load data and Eskom Nightsave Urban Large tariff proposed sizing and dispatch method was compared to the HOMER software package and its basic load following dispatch strategy. It is concluded that the developed optimal dispatch strategy outperforms HOMER's load-following strategy for operational cost reduction. This results in a lower lifetime cost and larger optimal PV capacity.

It is concluded that the predictive optimal dispatch method and the corresponding optimal sizing method developed in this dissertation can greatly assist in not only the decision making process for investing in hybrid energy systems, but also in optimising the operation of the components once they are implemented.

Furthermore, it is concluded that convex optimisation is a useful tool in the optimal design and dispatch of hybrid energy systems.

8.1 Scope of Future Work

Future work should focus on the physical implementation and testing of the optimal dispatch strategy for the generator and storage unit. These can then be compared to the real-world performance of the simpler strategies in actual operating conditions. The possibility of extending the convex formulation to include more complicated models of the current components as well as additional components can be investigated.

The tariff structures used in the optimization of the hybrid energy system consist of only a flat-rate charge and a maximum demand charge. The optimisation model could be extended to also consider a more general time-of-use tariff which will be important for some organisations.

In terms of the optimal sizing where historical load data is used, it is often difficult to obtain demand profiles as these datasets are usually incomplete. HOMER solves this problem by providing simple options for synthesizing the required hourly data. As additional variables are available that influence the load (past temperature and solar radiation data, University term dates, calender days), the SVR method could be used as a state-of-the-art method to fill in the missing data.

The proposed control method takes into account the first-order dynamics of the storage device, however, it does not take into account some other dynamic restrictions that might be placed on the system. These included the start-up delay for the generator and the second-order dynamics of the storage device i.e. how long the storage device takes to reach a specified power output. However, as a demand prediction is available it should not be difficult to correct for these factors in advance.

Appendix A

MATLAB Code

This Appendix provides a short listing of the most significant portions of code used for the various papers. Trivial and/or self-explanatory functions have been omitted.

A.1 SVR Load Forecast

This code is used to find the best SVR model parameters for the load data. It is currently hard-coded for the paramters of an exponential kernel.

```
%**************** Type of SVR training/kernel function *************
s = 3; % Epsilon SVR
t = 2; % Exponential Kernel
%*******************************************************************

%*******************************************************************
n_fold = 5;
gamma_range = 2.^[-15, 5];
C_range = 2^[-5, 15];
epsilon = 0.2;
%*******************************************************************

for i=1:n_fold

%************* Split into training/validation **********************
    data = [train_data.x, train_data.y];
    [learning, validation] = n_fold_split(data,5,1);
%*******************************************************************

    for i=1:size(gamma_range,1)
```

```
        for j=1:size(C_range,1)

%***************** Setup the parameters ***************************
          param_string = ['-s ', num2str(s), ' -t ', num2str(t), ...
                          ' -c ', num2str(C), ' -g ', num2str(gamma), ...
                          ' -p ', num2str(epsilon)];
%********************************************************************

%*************** Train using current parameters ********************
          model = svmtrain(learning.y, learning.x, param_string);
%********************************************************************

%**************** Test the current model **************************
          [y_hat, accuracy, ~] = svmpredict(validation.y, ...
                                   validation.x, param_string);

%**************** Store the test results **************************
          cv(i,j) = cv(i,j) + sum((validation.y - y_hat).^2).^0.5;
%********************************************************************

        end
    end
end

%************* Extract the results (best CV parameters) *************
[val1, idx1] = min(cv);
[val2, idx2] = min(val1);

gamma = gamma_range(idx1);
C = C_range(idx2);
%********************************************************************
```

This is the helper function used during cross-validation to split the training data into learning/validation sets.

```
function [learning, validation] = n_fold_split(data,n,i)
%********************************************************************
% 'n_fold_split' splits the training data into n groups to be used
% for cross-validation of the model during training.
%
%*******************************************************************
%
% ********************** Parameters *******************************
% [learning, validation] = n_fold_split(data,n,i)
% The input arguments are the following:
% data  -> The training data, stored as [trn.x, trn.y]
```

```
% n      -> The number of groups to spli the data into
% i      -> Starting index of validation data
%
% The output contains:
% learning   -> The sub-set used to train the model
% validation -> The sub-set used for testing the accuracy of the
%               current model (during training).
%
%*******************************************************************
%
%*******************************************************************
% Adapted from libSVM documentation.
%
%*******************************************************************

  end_idx = size(data,1);
  validation = data(i:n:end,:);
  learning = removerows(data,'ind',i:n:end_idx);

end
```

The function used to perform the SVR load forecasting in **Paper 1**. This function can only be run after the cross-validation has been performed.

```
%****************** Setup the parameters ***************************
param_string = ['-s ', num2str(s), ' -t ', num2str(t), ...
                          ' -c ', num2str(C), ' -g ', num2str(gamma), ...
                          ' -p ', num2str(epsilon)];
%********************************************************************

%*************** Train using current parameters ********************
model = svmtrain(test.y, test.x, param_string);
%********************************************************************

%**************** Perform the prediction ***************************
[y_hat, ~, ~] = svmpredict([], test.x, param_string);
%********************************************************************
```

The following code gives a MATLAB implementation of support vector regression. It was initially developed to perform the load forecasting presented in **Paper 1** but turned out to be too slow for practical use. As such, *libSVM* was used as an alternative. It is presented here as it gives insight into the details behind the SVR model.

```
function [y, alpha_out, b_out] = svr(xdata,ydata,x,alpha, b, c, epsilon)
```

```
%**********************************************************************
% SVR  Utilises Support Vector Regression to approximate
%           the functional relationship from which the
%           the training data was generated.
%**********************************************************************
%  Function call:
%
%    [y, alpha0,b0] = SVR(xdata,ydata,x,alpha,b,c,epsilon);
%    [~,alpha0,b0] = SVR(xdata,ydata,[],[],[],c,epsilon);
%    y = SVR(xdata,ydata,x,[],[],[],[]);
%    y = SVR(xdata,[],x,alpha,b,[],[]);
%
%  Example usage:
%
%   [X, Y] = meshgrid(linspace(-10,10,15),linspace(-10,10,15)); z = (X.^2 -
%   Y.^2).*sin(0.5*X) + randn(15).*10;
%
%   xdata = [reshape(X,15,1) reshape(Y,15,1)]';
%   ydata = [reshape(z,15,1)]';
%
%   [~, alpha0] = svr(xdata,ydata,[],[]);
%   for x=1:15
%        for y=1:15
%            z_approx(x,y) = svr(xdata,[],[X(1,x) Y(y,1)]',alpha0);
%       end
%   end
%**********************************************************************
%  Date: 09/09/2013
%
%  References:
%  This code is based on the description given in the following paper:
%    [1] B. Palanczi, L. volgyesi and Gy. Popper "Support Vector Regression
%        via Mathematica", Retrieved from
%        http://www.agt.bme.hu/volgyesi/kiegyen/pp_vecto.pdf
%**********************************************************************

ntrain = size(xdata,2);

M = zeros(ntrain);

y = inf;

if size(alpha,1) == 0
    svr_train()
end

if size(x,1) ~= 0
    y = svr_eval(x);
```

```
end

alpha_out = alpha;
b_out = b;

function svr_train()

%************* Set up constraints (Paper 2, Eqn. 3 ) ******************
    Aeq = sparse([ones(1,ntrain); zeros(ntrain-1,ntrain)]);
    beq = sparse(zeros(ntrain,1));
    lb = -c*ones(ntrain,1);
    ub = c*ones(ntrain,1);
    alpha0 = zeros(ntrain,1);
    M = zeros(ntrain);
%***********************************************************************

%******************** Precompute the kernel ***************************
    for l=1:ntrain
        for m=1:ntrain
            M(l,m) = K(xdata(:,l),xdata(:,m));
        end
    end
%***********************************************************************

%*********Set up the optimization problem (Paper 2, Eqn. 3 ) **********
    M = M + 1/c*eye(ntrain);
    options = optimoptions('fmincon','Algorithm','sqp','MaxFunEvals',...
            100000,'TolX',1e-10,'Display','iter');
    %options = gaoptimset('TolFun',1e-10);
    alpha = fmincon(@W, alpha0, [],[],Aeq, beq, lb, ub,[],options);

    for m=1:ntrain
        bmat(m) = ydata(m);
        for n = 1:ntrain
            bmat(m) = bmat(m) - alpha(n)*M(m,n);
        end
        bmat(m) = bmat(m) - epsilon - alpha(m)/c;
    end
    b = mean(bmat);
end
%***********************************************************************

%*********************************************************************
% Function to evaluate the SVR model at a point (Paper 2, Eqn. 1 )
%********************************************************************
function f = svr_eval(x)
    f = 0;
```

```
    for i=1:ntrain
        f = f + alpha(i)*K(x,xdata(:,i));
    end
    f = f + b;
end
%********************************************************************

%**********************************************************************
% Cost function used during training (Paper 2, Eqn. 3 )
%*********************************************************************
function cost = W(alpha)
    cost = 0;

    for i=1:ntrain
        cost = cost + alpha(i)*ydata(i) - epsilon*abs(alpha(i));
        for j = 1:ntrain
            cost = cost - 0.5*alpha(i)*alpha(j)*M(i,j);
        end
    end
    cost = -cost;
end
%**********************************************************************

%**********************************************************************
% Function to evaluate the kernel (Paper 2, Eqn. 4 )
%*********************************************************************
function uv = K(u,v)
a = 4;
n = size(u);
uv = 1;
    for k=1:n
        uv = exp(-gamma*abs(u-v).^2);
    end
end
%**********************************************************************

end
```

A.2 Generator and Storage Dispatch

This section provides the MATLAB code used in **Paper 2**.

A.2.1 Optimal Dispatch

This is the MATLAB code for the optimal dispatch strategy of the generator and storage unit. The convex optimsation is carried out using the CVX convex optimisation modelling language.

```
function [P_s P_g E_s] = optimal_dispatch(...
                P_load_forecast, P_solar_forecast, P_solar_nom,...
                P_s_max, P_g_max, E_max, E_s_init, P_out_init, ...
                P_in_init)
%*******************************************************************
% 'optimal_dispatch' calculates the storage control signal (schedule)
% of the generator and storage unit required to minimize the peak demand.
% The algorithm makes use of a predicted (or known) load value
% 'P_load_forecast'.
%******************************************************************
%
% ********************** Parameters ******************************
% [P_in P_out P_g E_s] = optimal_dispatch(...
%               P_load_forecast, P_solar_forecast, P_solar_nom,...
%               P_s_max, P_g_max, E_max, E_s_init, P_out_init, ...
%               P_in_init)
% The input arguments are the following:
% P_load_forecast   -> The 24hr predicted load demand values
% P_solar_forecast  -> The 24hr predicted solar energy (normalised)
% P_solar_nom       -> The capacity of the PV
% P_s_max           -> The storage power capacity
% P_g_max           -> The generator power capacity
% E_max             -> The storage energy capacity
% E_s_init          -> The initial energy stored
% P_out_init
% P_in_init
% The output contains:
% P_s -> The storage schedule (the power to be supplied/drawn
%        from the storage.
% P_g -> The generator schedule
%
%******************************************************************
%
% ********************** Info *************************************
% $Author: R Clark $    $Date: 2014/02/15 15:11:00 $    $Revision: 1.0 $
% Wits EIE
%*******************************************************************

%********************** Constants *********************************
    eta_c = 1.185;
```

```
    eta_d = 1.88;
    deltat = 0.5;
%*****************************************************************
%**************** Convex Optimisation model **********************
    cvx_begin
    cvx_precision low
        variable P_out(48) nonnegative;
        variable P_in(48) nonnegative;
        variable P_g(48) nonnegative;
        variable E_s(48);
        variable P_net(48);
%**************** Cost component weights ************************
        w_1 = 172.12*10;
        w_2 = 0.55*30*0.5;
        w_3 = 0.4*13*30*0.5;
%*****************************************************************

        minimize( w_1*max(P_net) + ...
                  w_2*sum(P_net) + ...
                  w_3*sum(P_g) ...
                 );
%************************ Constraints ***************************
        subject to
            P_net == P_load_forecast - P_solar_nom*P_solar_forecast ...
                    - P_out + P_in - P_g;
            P_out <= P_s_max;
            P_in <= P_s_max;
            P_g <= P_g_max;

            for i=2:48
              E_s(i) == E_s(i-1) + eta_c*P_in(i-1)*deltat ...
                        -eta_d*P_out(i-1)*deltat;
            end
            E_s(2:end) <= E_max ;
            E_s(2:end) >= 0;
            E_s(1) == E_s_init;
            P_out(1) == P_out_init;
            P_in(1) == P_in_init;
    cvx_end
%********************** Output variables ************************
    P_g = P_g(2:48);
    P_out = P_out(2:48);
    P_in = P_in(2:48);
    E_s = E_s(2:48);
end
% *****************************************************************
```

A.2.2 Threshold Dispatch

This is the MATLAB code for threshold dispatch strategy which is used as a baseline for comparison of the optimal dispatch method.

```
E_s = 0;
P_out = 0;
P_s = 0;
P_g = 0;
P_out_actual = 0;

for i=2:96
    idx1 = i;
    idx2 = i+48-1;
    P_solar = 0;
    P_s_max = 1000;
    P_g_max = 1000;
    P_solar_nom = 0;
    E_max = 4000;
    P_load_forecast = P_demand_forecast(idx1-1:idx2-1);
    P_load = P_demand_low(idx1-1:idx2-1);
    P_solar_forecast = 0;

    % Determine the threshold for the current horizon
    threshold = mean(P_load_forecast);

    % Determine the threshold schedule
    P_s(idx1:idx2-1) = -(P_load_forecast(2:end) - threshold);
    P_g(idx1:idx2-1) = 0;
    %E_s(idx1:idx2-1) = E_s(idx1-1)+cumsum(P_s(idx1:idx2-1));

    P_forecast_error = P_load(1:end)' - P_load_forecast(1:end)' ;

    [P_out_actual(idx1-1:idx2-1),Es_actual] = Storage_Unit(...
                            P_s(idx1-1:idx2-1)-P_forecast_error,..
                            1000, 4000,E_s(idx1-1));

    P_out_actual(idx1-1:idx2-1);
    P_needed = P_s(idx1-1:idx2-1)-P_forecast_error;
    sprintf('Actual: %4.3f Needed: %4.3f ',P_out_actual(idx1-1),P_needed(1))

    E_s(idx1:idx2-1) = Es_actual(2:end);

    sprintf('Hour: %4.0f',i)

end
```

A.3 Optimal Sizing of PV and Storage

This is the MATLAB code for the optimal sizing of the PV and storage capacity. The convex optimsation is carried out using the CVX convex optimisation modelling language.

```
function [Consumption, Demand, IC, Total, SOC_max,...
P_demand, P_net, soc, P_out, P_in, P_g, x] = ...
        convex_hes(storage_price_multiplier, pv_price_multiplier)

cvx_begin quiet
cvx_precision low
    variable P_out(365) nonnegative;
    variable P_in(365) nonnegative;
    variable P_g(365) nonnegative;
    variable P_net(365);
    variable soc(365);
    variable x(1) nonnegative;
    variable SOC_max nonnegative;

    storage_price = 720*storage_price_multiplier;
    p_pv = 51077*pv_price_multiplier;
    x = pv_capacity;
    Pgen_max = 1000;

    p_d = 0.4*13;
    P_demand = Loadrand(24:365+23);
    Solar = Solar(1:365);

   minimize(  20*172.12*12*max(P_net) ...
            + 365/14*20*0.57*sum(pos(P_net)) ...
            + 365/14*20*p_d*sum(P_g) ...
            + p_pv*x(1) + storage_price*SOC_max );

       subject to
        P_net == P_demand - x(1)*Solar/1.4 - P_g - P_out + P_in;

        P_g <= Pgen_max;
        P_out <= Ps_max;
        P_in <= Ps_max;

        for hour=2:365
            soc(hour) == soc(hour-1) + 1.185*P_in(hour-1) -...
                             1.88*P_out(hour-1);
        end
```

```
        soc <= SOC_max ;
        soc >= 0;
        soc(1) == 0;

    cvx_end

    Consumption = 20*0.57*sum(pos(P_net));
    IC = p_pv*x(1) + 720*SOC_max;
    Demand = 20*172.12*12*max(P_net);
    Total = Consumption + Demand + IC;
    savings = (349773269.04 - Total)/349773269.04*100;
    P_net = P_net;
    opt = cvx_optval;

end
```

Appendix B

Kernel Selection for Demand Prediction

In this dissertation a demand forecasting algorithm that can be used in conjunction with hybrid energy system dispatch methods was developed and verified. The technique is based on a type of kernel method known as Support Vector Regression and a gaussian kernel was used. Although this is adequate for most cases, it may be possible to improve the method by tailoring the kernel specifically for the load prediction purpose.

For the interested reader, the manuscript in this Appendix presents an initial note considering the application of kernel design methods for use in the non-parametric modelling of the load-temperature relationship. It is shown that the kernel can be designed, rather than chosen, for a specific problem and trained in an on-line manner.

,,

Application of an RKHS approach to the Prediction of Energy Demand from Temperature data

Abstract

Kernel methods have become very popular in a wide range of applications, however, attention is seldom paid to the design or choice of the kernel itself. The focus of this paper is to investigate the problem of designing the kernel for a specific application. To do so, recent results in the field of Reproducing Kernel Hilbert Spaces, which the authors believe show great promise for combining the generalization ability of non-parametric kernel-based methods with the explicability of parametric models, are applied to the problem of designing a kernel for modelling the relationship between temperature and energy demand. The test model is trained using an online gradient descent procedure. The results indicate that the interpolator trained using the designed kernel has a number of distinct advantages — including faster convergence and lower testing error compared to a conventional exponential kernel. The novelty of the research lies in the the application of the kernel design procedure to the temperature-load modelling problem and the demonstration of the advantages to be gained thereby.

1. Introduction

Current load-forecasting methods can be divided into two categories — parametric and non-parametric. Parametric function estimation methods have the advantage of being explanatory. The designer can use apriori knowledge to increase the accuracy of the model and they are based on clear, observable trends in the data that can be explained through physical reasoning. Furthermore, the sensitivity of the predictions to each of the explanatory variables is known. Non-parametric methods, on the other hand, are far more popular as they are often more accurate. The most popular non-parametric models are kernel methods.

In much of the literature where kernel methods are used (both in load forecasting and the machine learning field in general), the need arises to determine a suitable kernel to capture the non-linear relationships in the underlying data. To this extent, authors often speak of simply "choosing" or "selecting" a kernel. However, we feel that this approach is rather naive because, as has been shown in context of RKHS theory, the kernel is uniquely related not only to the feature map but also the form of the regularisation term and the set of functions that can be approximated [1].

In fact, it is astonishing how there seems to exist an ignorance with regards to kernel methods in the machine learning and mathematical modelling community in general where kernel based techniques are applied with little or no regard for observed trends in the underlying data.

The reader might argue that this entirely non-parametric approach has the advantages of being more generalisable and more easily implementable than trying to derive a suitable model from the data and to this extent, the disadvantages of purely parametric models are readily apparent. These disadvantages, however, stem from the fact that parametric models are not universal approximators — they can only model functions that lie within the bounds of their parameters. Therefore, in this paper an argument is made for a more thoughtful application of kernel methods — one which allows for the inclusion of the structure of the observed data while still being universal approximators. For example, by deriving a suitable reproducing kernel, van Wyk et al. were able to devise an approximator to solve the problem of graph matching[4].

Although the general method followed is well known [5, 6], its application to modelling the load-temperature relationship and its use as a kernel design method for given, explicit parametric model are novel.

This paper describes the problem of kernel de-

,,

sign for the implementation of a nonparametric interpolator which approximates the functional relationship between the energy demand of an institution and a meteorological factor — the ambient temperature. Focus on the design of the kernel ie. producing a kernel that relates to the function estimation problem at hand. The system is tested using standard load data from the ISO New England database.

The paper is structured as follows. In Section 2, a parametric model of the temperature-load relationship is described. Then, in Section 4, the kernel design method is presented. In Section **??**, the approximator method is described and the training procedure outlined. Finally, criteria used to assess the performance of the approximator are presented, the results are analysed and relevant conclusions are drawn.

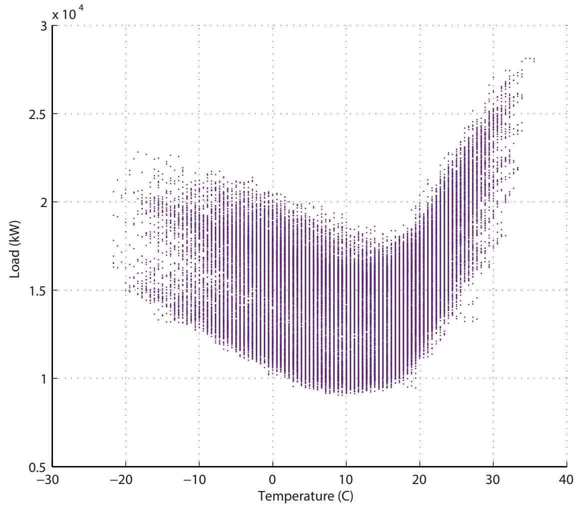

Figure 1: Figure showing the relationship between load and temperature (dry bulb) for the ISO New England data set.

2. The Explicit Load-Temperature Model

To derive a suitable kernel and function space we define a parametric model that describes the perceived trends in the data. For example, the load data displays a clear period trend with a period of 1 day. In Figure 2 it can be seen that the temperature shows a nearly quadratic relationship with the load, while the day type scales the load by some constant. A suitable parametric model, dervided by Charlton et al., is thus [8]

$$L = (a + bT + cT^2)(rD + k), \tag{1}$$

where L is the load value, a, b, c, r, k are regression coefficients or constants, T is the temperature and D is the type of day ie. $D \in 0, 1$.

The explicit parametric model that will be considered in this paper is

$$L = a + bT + cT^2, \tag{2}$$

which is Equation 1 with the day-type factor removed. The motivation for the removal of the day-type term is that in the current method, the interactions between the variables will be modelled by the multidimensional kernel (derived later) and not the terms themselves. Although these terms could be included, this unnecesarily complicates the design of the kernel.

3. The Nonparametric Approximator

It can be shown (see [21]) that any functional relationship can be modelled by the approximator

$$\tilde{F}(\cdot) = \sum_{l=0}^{M} a_l K(x_l, \cdot).$$

All that is required is a suitable kernel function, $K(x, y)$, and the set of kernel coefficients "a_i'' for the specific data which are found during training. This training involves minimizing the general cost function

$$\frac{1}{n} \sum_{i=1}^{n} ||\tilde{F}(\mathbf{x}_i) - y_i||_2 + \lambda J(f). \tag{3}$$

In this paper, the regularization term $J(f)$ is simply the functional norm and the training is carried out using a standard gradient descent procedure (see Appendix A).

4. Designing a Kernel based on the Explicit Model

One of several kernel functions is often chosen in the literature. The decision on which kernel to use is usually based on heuristics or simple trial and error methods. Examples of kernels are given in Table 4.

Although numerous kernels exist, the kernels applied to forecasting algorithms are very limited.

,,

The most popular kernel for SVR based methods is the exponetial or RBF kernel [9, 10, 11], while most ANN methods make use of the sigmoid kernel [12, 13, 14] (the standard activation function used for multi-layer perceptrons).

Table 1: List of general kernels to be found in the literature.

Name	$K(\mathbf{x}, \mathbf{y})$
Gaussian	$\exp\left(\frac{-\|\|\mathbf{x}-\mathbf{x}_i\|\|_2^2}{\sigma^2}\right)$
Exponential	$\exp\left(\frac{-\|\|\mathbf{x}-\mathbf{x}_i\|\|_2}{\sigma^2}\right)$
Laplacian	$\exp\left(\frac{-\|\|\mathbf{x}-\mathbf{x}_i\|\|_2}{\sigma}\right)$
ANOVA	$\sum_{k=1}^{n} \exp(-\sigma(x^k - y^k)^2)^d$
Quadratic	$1 - \frac{\|\|x-y\|\|^2}{\|\|x-y\|\|^2+c}$
Spherical	$1 - \frac{3}{2}\frac{\|\|x-y\|\|}{\sigma} + \frac{1}{2}\left(\frac{\|\|x-y\|\|}{\sigma}\right)^3$
Power	$-\|\|x-y\|\|^d$
Log	$-\log\left(\|\|x-y\|\|^d + 1\right)$
Cauchy	$\frac{1}{1+\frac{\|\|x-y\|\|^2}{\sigma^2}}$
Linear	$\langle \mathbf{x}, \mathbf{y} \rangle$
Polynomial	$(\langle \mathbf{x}, \mathbf{y} \rangle + 1)^q$
Sigmoid	$\tanh\left(a(\mathbf{x} \cdot \mathbf{y}) + b\right)$
Histogram	$\sum_{i=1}^{n} \min(x_i, y_i)$
T-Student	$\frac{1}{1+\|\|x-y\|\|^d}$
Wavelet	$\prod_{i=1}^{n} h\left(\frac{x_i-c}{a}\right) h\left(\frac{y_i-c}{a}\right)$
Chi-Square	$1 - \sum_{i=1}^{n} \frac{(x_i-y_i)^2}{\frac{1}{2}(x_i+y_i)}$

This section describes a procedure for deriving a kernel based on the trends that are observed in the data at hand. This procedure was derived by Heckman et al. in [19]. Heckman showed that a kernel can be found that penalizes the model on the basis of outliers (where different loss functions can be employed) as well as the expected parametric model of the data. The key insight is that by choosing the nullspace, certain desired functional forms not be penalized by the regularization term and will thus be "favoured" by the approximator.

This is the kernel derivation method that is considered in this paper. For more details on this method, the reader is referred to [19].

The kernel for parametric models of the form $1 + T + T^2$ is derived as follows.

1. Define a basis for the nullspace $\{u_1, u_2, \ldots, u_m\}$
2. Calculate the Wronskian using
$$W(t) = \begin{pmatrix} u_1 & u_2 & \ldots & u_m \\ u_1' & u_2' & \ldots & u_m' \\ \vdots & & & \\ u_1^{(m-1)} & u_2^{(m-1)} & \ldots & u_m^{(m-1)} \end{pmatrix} \tag{4}$$
3. Calculate the coefficient matrix C_{ij} using
$$C_{ij} = \left[(W(a)W'(a))^{-1}\right]_{ij} \tag{5}$$
4. Determine $K_0(x, x_i)$ from
$$K_0(x, x_i) = \sum_{i,j=1}^{m} C_{ij} u_i(x) u_j(x_i) \tag{6}$$
5. Find the Green's function corresponding to the basis using Equation
$$G(x, u) = \begin{cases} \sum_{i=1}^{m} u_i(x) u_i^*(u) & u \leq x \\ 0 & \text{else} \end{cases} \tag{7}$$
6. Determine $K_1(x, x_i)$

This procedure is now applied to the explicit parametric model described above. The basis of the null-space used here is

$$u_1(T) = 1, u_2(t) = T, u_2(t) = T^2$$

Here the Wronskian matrix is

$$W(T) = \begin{bmatrix} 1 & 0 & 0 \\ t & 1 & 0 \\ T^2 & 2T & 2 \end{bmatrix}$$

Which gives

$$(W(a)W'(a))^{-1} = \begin{bmatrix} \frac{a^3}{4} + a^2 + 1 & -a - \frac{a^3}{2} & \frac{a^2}{4} \\ -a - \frac{a^3}{2} & a^2 + 1 & -\frac{a}{2} \\ \frac{a^2}{4} & -\frac{a}{2} & \frac{1}{4} \end{bmatrix} \tag{8}$$

$$\begin{aligned} K_1(x, x_i) &= \int_0^1 G(x, u) G(x_i, u) du \qquad (9) \\ &= \int_0^{\min(x, x_i)} (x-u)^2 (x_i - u)^2 du \\ &= x^2 x_i^2 \min(x, x_i) - x^2 x_i \min(x, x_i)^2 \\ &+ \frac{x^3}{3} \min(x, x_i)^3 \\ &- x x_i^2 \min(x, x_i)^2 + \frac{4}{3} x x_i \min(x, x_i)^3 \\ &- \frac{1}{2} x \min(x, x_i)^4 + \frac{x^2}{3} \min(x, x_i)^3 \\ &- \frac{1}{2} x_i \min(x, x_i)^4 + \frac{1}{5} \min(x, x_i)^5. \end{aligned}$$

”

5. Method

An overview of the process followed to create the load forecasting approximator is presented in Figure 2. The figure shows the procedure from defining the univariate parametric models to combining the kernels (by means of the Grammian matrices) used to train the approximator. It should be noted that although the multivariate case is shown, only univariate approximators are addressed in this paper.

6. Numerical Results

To illustrate the universal approximation ability of the interpolator we apply Kernel 1 to the problem of approximating the function $f(x) = sinc(x)$ function using 10 points sampled on the domain $x = [-\pi, \pi]$. To do this, the kernel is used to calculate the Gram matrix $\mathbf{G}$ and then Equation **??** is iterated to find the optimal coefficients. After 500 iterations, the coefficit vector is obtained

$$\mathbf{c} = [-1.6775, 4.5917, -1.1885, -7.8102, 6.0844,\\ 6.0844, -7.8102, -1.1885, 4.5917, -1.6775]$$

The results from a range of approximators (with different regularisation parameters λ) are shown in Figure 3

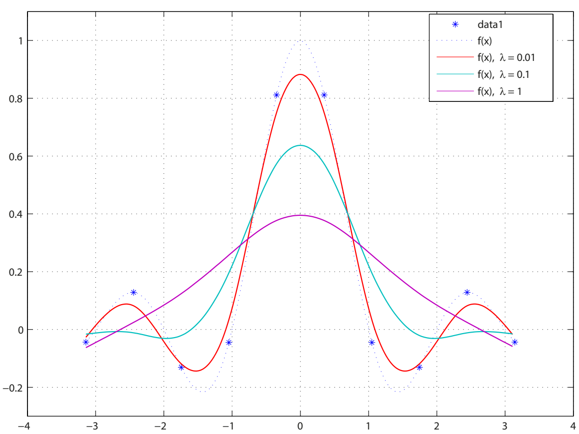

Figure 3: Figure showing approximators, sampled points and the true function

It is clear that as the regularisation parameter is decreased, the approximator tends toward an element of the null-space — in this case a constant. As the regularisation parameter is increased, the approximator more freely adapts to any functional form at the expense of greater ’non-linearity’. Because the samples are noise-free an therefore perfect representation of the function in this case, the regularisation actually decreases the performance of the approximator. However, if the data samples are subject to interference (as is usually the case) the regularisation becomes important to prevent overfitting and poor generalisation performance.

The ability of the exponential RBF kernel based approximator to model the relationship between temperature and load is shown in Figure 4. The first trend evident on this graph is that all the approximators tend to zero near the edges of the domain. This is expected as RBF functions (by definition) tend to zero as the distance from their center increases. Because the training data is sparse at the edges, and the γ vector has been initialised to zero, these points do not significantly affect the shape of the approximator in these regions and the approximators underestimate the load values. This can, however, easily be addressed by adding extra points in these regions. The γ vector could also be initialised with values other than zero, such as the mean of the training points, but the approximator will still remain inaccurate in regions where the training points are sparse.

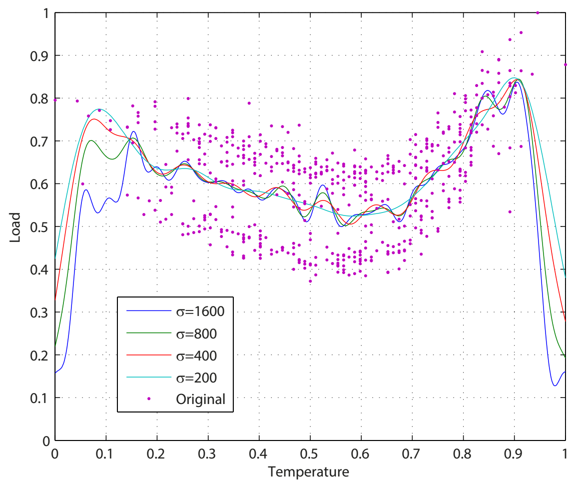

Figure 4: Approximators using the exponential kernel with different scale values. A scale that is too small results in over-fitting and poor generalisation performance.

The custom kernel is now utilised to train a one-dimensional approximator of the same temperature-load training data used for the RBF approximator. The result is shown in Figure 5. As the derived kernel has no variable parameters, only

,,

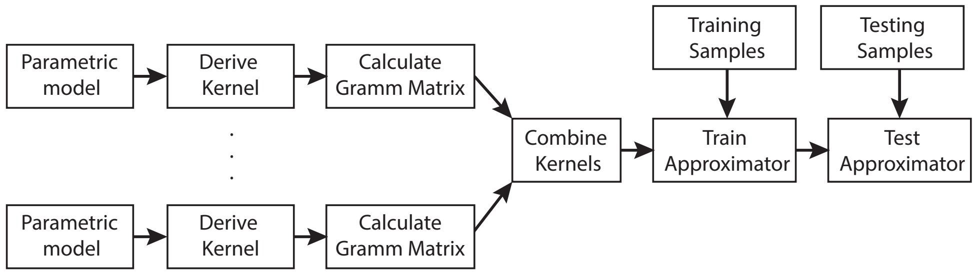

Figure 2: Overview of the method used to create thel approximator.

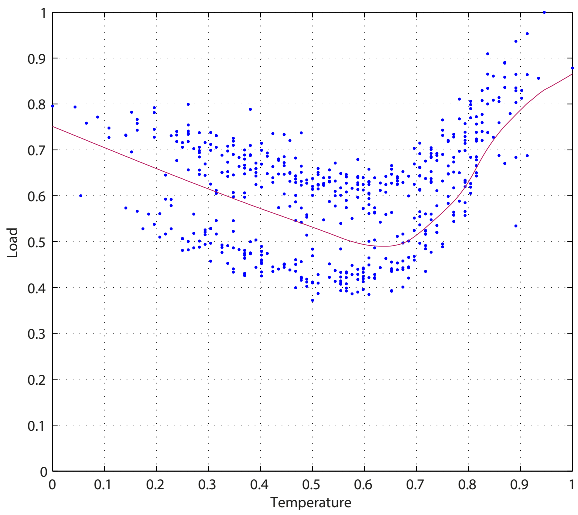

Figure 5: Approximator using the custom kernel derived for the expected temperature-load relationship ie. $1 + T + T^2$.

a single approximator has been plotted.

The approximator has a distinctly different form to the RBF kernel, although the same training data and number of training iterations have been used, with both approximators having near-identical final cost values. The approximator using the derived kernel provides a visually-satisfying fit and has a number of desirable characteristics - it is much less 'noisy' than the RBF interpolator and seems to capture a strong, general trend in the data. Its behaviour at the end points is also not as sensitive to the lack of training points, although the approximator does deviate slightly from a visually satisfying fit at the upper extreme.

To evaluate the performance of the kernels quantitatively, three tests were carried out using the popular exponential kernel (kernel 2) and the derived kernel (kernel 1). Each test made use of a different stopping criterion.The first test was fixed at a constant 5000 iterations, the second had a fixed final step size of 1×10^{-2} and the third test had a constant training time of 20s. The results obtained are given in Table 6. The training time is split into the time taken to set up the Grammian matrix and the total time spent performing the gradient descent. From the training times shown in Table 6, it is evident that neither of the kernels have a significant advantage in terms of computational effort required to train the approximator. The majority of the training time is spent on the gradient descent. As this process is not explicitly dependent on the evaluation of the kernel function (it only relies on the pre-computed Grammian matrix), no significant time difference is seen between the two kernels. There is a significant difference in the time taken to construct the Grammian matrix, as the function evaluations of the derived kernel are much more expensive than the exponential kernel. However, as mentioned, the time spent on this process is insignificant compared to the time required to perform the gradient descent.

A plot of the loss function during training is given in Figure 6. The figure shows that very fast convergence is achieved using both kernels. In this case the derived kernel is clearly superior as it shows faster convergence and converges to a lower final training error value. This is an indication that the derived kernel more easily "fits" the data compared to the arbitrarily selected exponential kernel.

Both kernels converge at around 2500 iterations and running the optimization for any longer does not significantly reduce the training error. At convergence, the training error of the derived kernel is 25.7% lower than that of the exponential kernel. Similar results are obtained on the testing set. In fact, as is shown in Table 6, by doubling the number of iterations from 5000 to ≈ 10000, the testing

''

Table 2: Results obtained by training the approximator to model the univariate load-temperature relationship.

	Final Step Size	Iterations	Time	Objective Function	Testing Error (RMS)
Kernel 1	0.2511	5000	9.17s + 66.1ms	3.176	0.0899
Kernel 2	0.3236	5000	9.21s + 3.4ms	3.994	0.0952
Kernel 1	0.15	4491	9.07s + 66.0ms	3.176	0.0899
Kernel 2	0.15	4400	9.01s + 3.9ms	3.994	0.0952
Kernel 1	0.1386	10910	20.00s	3.175	0.0899
Kernel 2	0.1418	10858	20.00s	3.994	0.0956

error of the exponential kernel increases. This is most likely due to over-fitting of the training data. The testing error obtained using the derived kernel remains the same, however negligible performance gain is achieved by increasing the number of iterations from 5000 to ≈ 10000. As with the training set, the RMS error of the derived kernel on the testing set is less than that of the exponential kernel — in this case 5.89% lower.

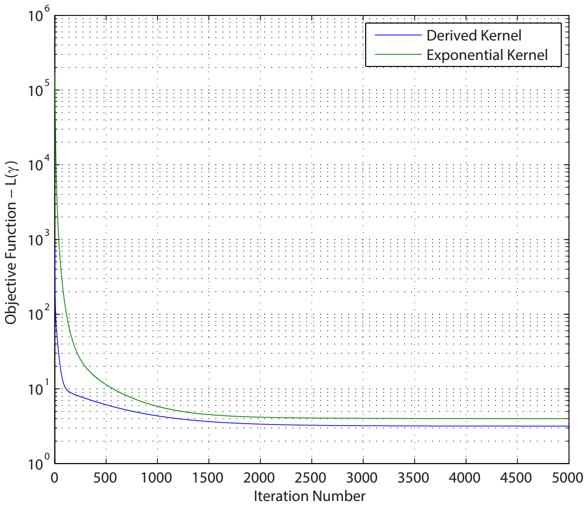

Figure 6: Plot of the error function during training of the two kernels.

To create the actual multidimensional interpolator to be used for forecasting, the procedure presented in Section 5 is followed.

7. Conclusion and Future Work

The kernel design method evaluated in this paper is essentially a non-parametric regression model that extends the simple linear and quadratic regression models to handle more intricate non-linearities as well as the interactions between variables. The designed kernel was demonstrated using a simple univariate load-forecast that learns the relationship between the temperature and load demand. The advantages of the derived kernel can be summarised as follows:

- The specific choice of the kernel is easier to justify than choosing an arbitrary kernel. That is, the kernel derivation is based on characteristics of the problem at hand - compare this to selecting a generic kernel for the SVR method based on heuristics or trial and error.
- As the kernel is more closely related to the underlying relationships in the data, the convergence is faster than an arbitrarily selected kernel
- The training error at convergence is lower than that of the test kernel
- The general kernel design procedure outlined here can be used for any type of general parametric model

The model was trained using a gradient descent procedure which provides the following advantages:

- The method allows for on-line training and can therefore cope with non-stationarity of the underlying relationships in the data
- As training can be performed on-line, the method is suitable for handling dynamic data sets

The interpolator-based load prediction presented here has a number of shortcomings. The most significant of which is that only a univariate kernel was considered. As practical load forecasting often include multiple factors to increase the accuracy of the forecast, future investigations should therefore focus on designing multivariate kernels (possibly using the methods suggested in this paper).

,,

8. A note on Composite Kernels

The material presented thus far has only been concerned with the one-dimensional case ie. the derived kernel function operates on pairs of one-dimensional elements drawn from the set X. In general, elements in the domain of the approximator will have dimension > 1. A number of difficulties arise. For example, the linear differential operator specifying the regularisation term now becomes a partial differential operator with its null space defined by a corresponding partial differential equation. Thus, the null-space is highly unlikely to be spanned by a finite dimensional basis. Even if an arbitrary basis is chosen, the calculation of the Wronskian and Green's function also become increasingly more complex as the number of variables rises.

However, it is obvious that the demand depends on all these variables simultaneously and/or the interactions between these variables. A simple method to include these dependencies in the interpolator-based prediction algorithm is to create a multi-dimensional kernel which is a combination of the individual, simple kernels.

There are many different options for combining kernels to form new ones. For example, one possible method for combining kernels is simply the product of the univariate [24] as shown in Equation 10.

$$K(\mathbf{x}, \mathbf{y}) = \prod K(x_i, y_i). \tag{10}$$

References

[1] P. Zhu, B. Chen, J. Principe, Learning nonlinear generative models of time series with a kalman filter in rkhs, Signal Processing, IEEE Transactions on 62 (1) (2013) 141–155.

[2] G. feng Pan, P. He, Y.-T. Zhou, J.-H. Li, Constructing a wavelet-based rkhs and its associated scaling kernel for support vector approximation, in: Wavelet Analysis and Pattern Recognition, 2007. ICWAPR '07. International Conference on, Vol. 3, 2007, pp. 1403–1407.

[3] A. Tanaka, H. Imai, M. Kudo, M. Miyakoshi, Theoretical analyses on a class of nested rkhs's, in: Acoustics, Speech and Signal Processing (ICASSP), 2011 IEEE International Conference on, 2011, pp. 2072–2075.

[4] M. Van Wyk, T. Durrani, B. Van Wyk, A rkhs interpolator-based graph matching algorithm, Pattern Analysis and Machine Intelligence, IEEE Transactions on 24 (7) (2002) 988–995.

[5] N. Aronszajn, Theory of reproducing kernels, Am. Math. Soc. Trans 69 (1950) 337–404.

[6] G. Wahba, Spline models for observational data, SIAM.

[7] R. T. Hastie T., J. H. Friedman, The elements of statistical learning, Am. Math. Soc. Trans.

[8] N. Charlton, C. Singleton, A refined parametric model for short term load forecasting, International Journal of Forecasting-doi:http://dx.doi.org/10.1016/j.ijforecast.2013.07.003.

[9] W.-C. Hong, C.-Y. Lai, W.-M. Hung, Y. Dong, Electric load forecasting by svr with chaotic ant swarm optimization, in: Cybernetics and Intelligent Systems (CIS), 2010 IEEE Conference on, 2010, pp. 102–107.

[10] Z. Zhang, S. Ye, Long term load forecasting and recommendations for china based on support vector regression, in: Information Management, Innovation Management and Industrial Engineering (ICIII), 2011 International Conference on, Vol. 3, 2011, pp. 597–602.

[11] Z. Zhang, S. Ye, Long term load forecasting and recommendations for china based on support vector regression, in: Information Management, Innovation Management and Industrial Engineering (ICIII), 2011 International Conference on, Vol. 3, 2011, pp. 597–602.

[12] J.-C. Lu, D. xiao Niu, Z.-Y. Jia, A study of short-term load forecasting based on arima-ann, in: Machine Learning and Cybernetics, 2004. Proceedings of 2004 International Conference on, Vol. 5, 2004, pp. 3183–3187 vol.5.

[13] K. Solaiman, M. Elkateb, Y. Al-Turki, Applied medium term weather dependent electric load forecast using ann and other techniques ldquo;case study of jeddah area rdquo;, in: Power Engineering Society Summer Meeting, 2000. IEEE, Vol. 3, 2000, pp. 1791–1795.

[14] Y. ShangDong, L. Xiang, A new ann optimized by improved pso algorithm combined with chaos and its application in short-term load forecasting, in: Computational Intelligence and Security, 2006 International Conference on, Vol. 2, 2006, pp. 945–948.

[15] H. Moustafa, An ann decision support for optimal judgment of egyptian power system load forecasting, in: Universities Power Engineering Conference, 2004. UPEC 2004. 39th International, Vol. 1, 2004, pp. 412–416.

[16] I. Borlea, A. Buta, B. Lustrea, Some aspects concerning mid term monthly load forecasting using ann, in: Computer as a Tool, 2005. EUROCON 2005.The International Conference on, Vol. 1, 2005, pp. 253–256.

[17] I. Drezga, S. Rahman, Input variable selection for ann-based short-term load forecasting, Power Systems, IEEE Transactions on 13 (4) (1998) 1238–1244.

[18] H. Mori, A. Yuihara, Deterministic annealing clustering for ann-based short-term load forecasting, Power Systems, IEEE Transactions on 16 (3) (2001) 545–551.

[19] N. Heckman, The theory and application of penalized methods, Statistics Surveys 6 (1) (2012) 113–141.

[20] E. Kreyszig, Introductory Functional Analysis With Applications, John Wiley & Sons, 1978.

[21] M. Van Wyk, T. Durrani, A framework for multiscale and hybrid rkhs-based approximators, Signal Processing, IEEE Transactions on 48 (12) (2000) 3559–3568.

[22] A. Nosedal-Sanchez, C. B. Storlie, T. C. Lee, R. Christensen, Reproducing kernel hilbert spaces for penalized regression: A tutorial, The American Statistician 66 (1) (2012) 50–60.

[23] Y. Chen, Y. Gu, A. O. Hero, Regularized least-mean-square algorithms, arXiv preprint arXiv:1012.5066.

[24] M. O. Stitson, A. Gammerman, V. Vapnik, V. Vovk, C. Watkins, J. Weston, Support vector regression with anova decomposition kernels, Tech. rep., University of London (1997).

Bibliography

[1] R. Luna-Rubio, M. Trejo-Perea, D. Vargas-Vzquez, and G.J. Ros-Moreno. Optimal sizing of renewable hybrids energy systems: A review of methodologies. *Solar Energy*, 86(4):1077 – 1088, 2012. {ISRES} 2010.

[2] R.K. Akikur, R. Saidur, H.W. Ping, and K.R. Ullah. Comparative study of stand-alone and hybrid solar energy systems suitable for off-grid rural electrification: A review. *Renewable and Sustainable Energy Reviews*, 27(0):738 – 752, 2013.

[3] Franco F. Yanine and Enzo E. Sauma. Review of grid-tie micro-generation systems without energy storage: Towards a new approach to sustainable hybrid energy systems linked to energy efficiency. *Renewable and Sustainable Energy Reviews*, 26 (0):60 – 95, 2013.

[4] Aviel Verbruggen and Volkmar Lauber. Basic concepts for designing renewable electricity support aiming at a full-scale transition by 2050. *Energy Policy*, 37(12): 5732 – 5743, 2009.

[5] Hanane Dagdougui, Riccardo Minciardi, Ahmed Ouammi, Michela Robba, and Roberto Sacile. Modeling and optimization of a hybrid system for the energy supply of a green building. *Energy Conversion and Management*, 64(0):351 – 363, 2012.

[6] Gabriele Seeling-Hochmuth. *Optimisation of hybrid energy systems sizing and operation control*. Kassel University Press, 1998.

[7] Tariffs and charges 2013/2014, April 2013. URL http://www.eskom.co.za/CustomerCare/TariffsAndCharges/Documents/Website_PDF.pdf.

[8] CD Barley, CB Winn, L Flowers, and HJ Green. Optimal control of remote hybrid power systems. part 1: Simplified model. Technical report, National Renewable Energy Lab., Golden, CO (United States), 1995.

[9] Matthew P. Johnson, Amotz Bar-Noy, Ou Liu, and Yi Feng. Energy peak shaving with local storage. *Sustainable Computing: Informatics and Systems*, 1(3):177 – 188, 2011.

[10] G. Dupont and P. Baltus. Dimensioning and grid integration of mega battery energy storage system for system load leveling. In *PowerTech, 2009 IEEE Bucharest*, pages 1–6, 2009.

[11] E. Palomino, J. Stevens, and J. Wiles. A control system for improved battery utilization in a pv-powered peak-shaving system. In *Photovoltaic Specialists Conference, 1996., Conference Record of the Twenty Fifth IEEE*, pages 1525–1528, 1996.

[12] E. Tsoi and K.P. Wong. Artificial intelligence algorithms for short term scheduling of thermal generators and pumped-storage. *Generation, Transmission and Distribution, IEEE Proceedings-*, 144(2):193–200, Mar 1997.

[13] Tsung-Ying Lee. Operating schedule of battery energy storage system in a time-of-use rate industrial user with wind turbine generators: A multipass iteration particle swarm optimization approach. *Energy Conversion, IEEE Transactions on*, 22(3): 774–782, Sept 2007.

[14] Yoash Levron and Doron Shmilovitz. Power systems optimal peak-shaving applying secondary storage. *Electric Power Systems Research*, 89(0):80 – 84, 2012.

[15] N. Gast, D.-C. Tomozei, and J.-Y. Le Boudec. Optimal generation and storage scheduling in the presence of renewable forecast uncertainties. *Smart Grid, IEEE Transactions on*, 5(3):1328–1339, May 2014.

[16] A. Nottrott, J. Kleissl, and B. Washom. Energy dispatch schedule optimization and cost benefit analysis for a grid-connected, photovoltaic-battery storage systems. *Renewable Energy*, 55(0):230 – 240, 2013.

[17] Chih-Chiang Hua and Meng-Yu Lin. A study of charging control of lead-acid battery for electric vehicles. In *Industrial Electronics, 2000. ISIE 2000. Proceedings of the 2000 IEEE International Symposium on*, volume 1, pages 135–140, 2000.

[18] A. Ota, H. Taniguchi, T. Nakajima, K.M. Liyanage, K. Shimizu, T. Masuta, J. Baba, and A. Yokoyama. Effect of autonomous distributed vehicle-to-grid for ubiquitous power grid and its effect as a spinning reserve. *J. Int. Council Electr. Eng.*, 1, 2011.

[19] J. R. Pillai and B. Bak-Jensen. Integration of vehicle-to-grid in the western danish power system. *IEEE Trans. Sustainable Energy*, 1, 2011.

[20] J. Matsuki Y. Hanai, K. Yoshimura and Y. Hayashi. Load management using heat-pump water heater and electric vehicle battery charger in distribution system with pv. *J. Int. Council Electr. Eng.*, 1, 2011.

[21] J.A. Taylor, D.S. Callaway, and K. Poolla. Competitive energy storage in the presence of renewables. *Power Systems, IEEE Transactions on*, 28(2):985–996, May 2013.

[22] M. Giuntoli and D. Poli. Optimized thermal and electrical scheduling of a large scale virtual power plant in the presence of energy storages. *Smart Grid, IEEE Transactions on*, 4(2):942–955, June 2013.

[23] Lin-Her Jeng, Yuan-Yih Hsu, B.S. Chang, and K.-K. Chen. A linear programming method for the scheduling of pumped-storage units with oscillatory stability constraints. *Power Systems, IEEE Transactions on*, 11(4):1705–1710, Nov 1996.

[24] A.G. Bakirtzis and P.S. Dokopoulos. Short term generation scheduling in a small autonomous system with unconventional energy sources. *Power Systems, IEEE Transactions on*, 3(3):1230–1236, Aug 1988.

[25] C Dennis Barley and C Byron Winn. Optimal dispatch strategy in remote hybrid power systems. *Solar Energy*, 58(4):165–179, 1996.

[26] Tamer Khatib, Azah Mohamed, and K. Sopian. A review of photovoltaic systems size optimization techniques. *Renewable and Sustainable Energy Reviews*, 22(0): 454 – 465, 2013.

[27] Gabriele Seeling-Hochmuth. *Optimisation of Hybrid Energy Systems Sizing and Control*. PhD thesis, University of Kassel, 1998.

[28] E.I. Vrettos and S.A. Papathanassiou. Operating policy and optimal sizing of a high penetration res-bess system for small isolated grids. *Energy Conversion, IEEE Transactions on*, 26(3):744–756, 2011. ISSN 0885-8969. doi: 10.1109/TEC.2011.2129571.

[29] G. Carpinelli, G. Celli, S. Mocci, F. Mottola, F. Pilo, and D. Proto. Optimal integration of distributed energy storage devices in smart grids. *Smart Grid, IEEE Transactions on*, 4(2):985–995, 2013. ISSN 1949-3053. doi: 10.1109/TSG.2012.2231100.

[30] Ronald L Rardin and Reha Uzsoy. Experimental evaluation of heuristic optimization algorithms: A tutorial. *Journal of Heuristics*, 7(3):261–304, 2001.

[31] Y. del Valle, G.K. Venayagamoorthy, S. Mohagheghi, J.-C. Hernandez, and R.G. Harley. Particle swarm optimization: Basic concepts, variants and applications in power systems. *IEEE Transactions on Evolutionary Computation*, 12(2):171–195, 2008.

[32] Zuo Li-yun and Zuo Li-feng. An ant colony optimization algorithm based on automatic dynamic updating. In *Computer Science and Automation Engineering (CSAE), 2012 IEEE International Conference on*, volume 1, pages 111–116, 2012.

[33] Zhenzhen Dai, Aimin Zhou, Guixu Zhang, and Sanyi Jiang. A differential evolution with an orthogonal local search. In *Evolutionary Computation (CEC), 2013 IEEE Congress on*, pages 2329–2336, 2013.

[34] Haitham Hindi. A tutorial on convex optimization. In *American Control Conference*, 2004.

[35] Ying-Yi Hong and Ruo-Chen Lian. Optimal sizing of hybrid wind/pv/diesel generation in a stand-alone power system using markov-based genetic algorithm. *Power Delivery, IEEE Transactions on*, 27(2):640–647, 2012. ISSN 0885-8977. doi: 10.1109/TPWRD.2011.2177102.

[36] Y.M. Atwa, E. F. El-Saadany, M. M A Salama, and R. Seethapathy. Optimal renewable resources mix for distribution system energy loss minimization. *Power Systems, IEEE Transactions on*, 25(1):360–370, 2010. ISSN 0885-8950. doi: 10.1109/TPWRS.2009.2030276.

[37] A. G. Ter-Gazarian and N. Kagan. Design model for electrical distribution systems considering renewable, conventional and energy storage units. *Generation, Transmission and Distribution, IEE Proceedings C*, 139(6):499–504, 1992. ISSN 0143-7046.

[38] S. Boyd, C. Baratt, and S. Norman. Linear controller design: limits of performance via convex optimization. *Proceedings of the IEEE*, 78(3):529–574, 1990.

[39] B. Behmardi and R. Raich. Convex optimization for exact rank recovery in topic models. In *Machine Learning for Signal Processing (MLSP), 2011 IEEE International Workshop on*, pages 1–6, 2011.

[40] A. Aggarwal and T.H. Meng. Minimizing the peak-to-average power ratio of OFDM signals using convex optimization. *IEEE Transactions on Signal Processing*, 54(8): 3099–3110, 2006.

[41] S. Boyd and L. Vandenberghe. CRCd program: convex optimization for engineering analysis and design. In *American Control Conference, Proceedings of the 1995*, volume 2, pages 1069–1071, 1995.

[42] Stephen P Boyd and Lieven Vandenberghe. *Convex optimization*. Cambridge university press, 2004.

[43] Jean-Baptiste Hiriart-Urruty and Claude Lemaréchal. *Fundamentals of convex analysis*. Springer, 2001.

[44] Inc. CVX Research. CVX: Matlab software for disciplined convex programming, version 2.0. http://cvxr.com/cvx, 2012.

[45] Y. Labit and D. Peaucelle, D. ; Henrion. Sedumi interface 1.02: a tool for solving lmi problems with sedumi. In *Proceedings, IEEE International Symposium on Computer Aided Control System Design.*, pages 272–277, 2002.

[46] Kim-Chuan Toh, Michael J Todd, and Reha H Tütüncü. On the implementation and usage of sdpt3–a matlab software package for semidefinite-quadratic-linear programming, version 4.0. In *Handbook on semidefinite, conic and polynomial optimization*, pages 715–754. Springer, 2012.

[47] Thermodynamic analysis of pumped thermal electricity storage. *Applied Thermal Engineering*, 53(2):291 – 298, 2013.

[48] T. Lambert, P. Gilman, and P. Lilienthal. *Micropower System Modeling with HOMER*. John Wiley & Sons, Inc., 2006.